Spatio-temporal investigation and quantitative analysis of the BMP signaling pathway

Raum-Zeitliche Untersuchung und quantitative Analyse des BMP-Signaltransduktionsweges

Doctoral thesis for a doctoral degree
at the Graduate School of Life Sciences,
Julius-Maximilians-Universität Würzburg,
Section Biomedicine

submitted by

Daniela Schul

from

Hohenroda

Würzburg**……..**

Year of Thesis Submission

Submitted on:

……..……..

Office stamp

Members of the *Promotionskomitee*:

Chairperson: Prof. Dr. Manfred Gessler

Primary Supervisor: Prof. Dr. Dr. Manfred Schartl

Supervisor (Second): Prof. Dr. Thomas Müller

Supervisor (Third): Prof. Dr. Christoph Winkler

Supervisor (Fourth): Dr. Toni Wagner

Date of Public Defence: ……..…..

Date of Receipt of Certificates: ……

Table of contents

1. Summary

Bone Morphogenetic Proteins (BMPs) are key regulators for a lot of diverse cellular processes. During embryonic development these proteins act as morphogens and play a crucial role particularly in organogenesis. BMPs have a direct impact on distinct cellular fates by means of concentration-gradients in the developing embryos. Using the diverse signaling input information within the embryo due to the gradient, the cells transduce the varying extracellular information into distinct gene expression profiles and cell fate decisions. Furthermore, BMP proteins bear important functions in adult organisms like tissue homeostasis or regeneration. In contrast to TGF-ß signaling, currently only little is known about how cells decode and quantify incoming BMP signals. There is poor knowledge about the quantitative relationships between signal input, transducing molecules, their states and location, and finally their ability to incorporate graded systemic inputs and produce qualitative responses. A key requirement for efficient pathway modulation is the complete comprehension of this signaling network on a quantitative level as the BMP signaling pathway, just like many other signaling pathways, is a major target for medicative interference. I therefore at first studied the subcellular distribution of Smad1, which is the main signal transducing protein of the BMP signaling pathway, in a quantitative manner and in response to various types and levels of stimuli in murine c2c12 cells. Results indicate that the subcellular localization of Smad1 is not dependent on the initial BMP input. Surprisingly, only the phospho-Smad1 level is proportionally associated to ligand concentration. Furthermore, the activated transducer proteins were entirely located in the nucleus. Besides the subcellular localization of Smad1, I have analyzed the gene expression profile induced by BMP signaling. Therefore, I examined two endogenous immediate early BMP targets as well as the expression of the stably transgenic Gaussia Luciferase. Interestingly, the results of these independent experimental setups and read-outs suggest oscillating target gene expression. The amplitudes of the oscillations showed a precise concentration-dependence for continuous and transient stimulation. Additionally, even short-time stimulation of 15’ activates oscillating gene-expression pulses that are detectable for at least 30h post-stimulation. Only treatment with a BMP type I receptor kinase inhibitor leads to the complete abolishment of the target gene expression. This indicated that target gene expression oscillations depend directly on BMP type I receptor kinase activity.

2. Zusammenfassung

Bone Morphogenetic Proteins (BMPs) stellen wichtige Regulatoren für eine Vielzahl von verschiedenen zellulären Prozessen dar. Während der Embryonalentwicklung agieren diese Proteine als Morphogene und spielen daher eine entscheidende Rolle für diesen Prozess, vor allem in der Organogenese. Durch Konzentrationsgradienten üben BMPs einen direkten Einfluss auf verschiedene zelluläre Schicksale im entwickelnden Embryo aus. Aufgrund dieser Gradienten gelangen vielfältige Signalinformationen zu den verschiedenen Zellen, welche die extrazelluläre Information in verschiedene Genexpressionsprofile und Zellschicksalsentscheidungen umwandeln. Darüber hinaus tragen BMPs wichtige Funktionen im erwachsenen Organismus, wie z.B. Gewebshomöostase oder -regeneration. Im Gegensatz zu dem verwandten TGF-ß Signaltransduktionsweg ist derzeit nur wenig über die zelluläre Übersetzung und Quantifizierung eingehender BMP-Signale bekannt. Es gibt wenige Kenntnisse über die quantitative Beziehung zwischen Signaleingang, Überträgerproteinen, ihren Zuständen sowie intrazellulären Positionen, und schließlich ihre Fähigkeit Signaleingänge systemisch zu integrieren und qualitative Antworten der Zelle zu produzieren. Eine wesentliche Voraussetzung für die effiziente Signaltransduktions-modulierung ist das vollständige Verständnis des Signalnetzwerkes auf einer quantitativen Ebene, da der BMP-Signalweg, wie auch viele andere Signalwege, ein wichtiges Ziel für medizinische Anwendungen und Medikamentenentwicklung ist. Daher untersuchte ich zunächst die subzelluläre Verteilung der wichtigsten Signalweiterleitungsproteine des BMP-Signalweges, der Smad1-Proteine, auf quantitativer Ebene und deren Reaktion auf verschiedene Stimulierungsarten und BMP-Konzentrationsstufen in murinen c2c12-Zellen. Die Ergebnisse zeigen, dass die subzelluläre Lokalisation von Smad1 unabhängig von der BMP-Konzentration ist und nur das phospho-Smad1 Level proportional zur Konzentration des Liganden steigt. Darüber hinaus befanden sich die aktiven Überträgerproteine nach Stimulierung vollständig im Zellkern. Neben der subzellulären Lokalisation von Smad1, habe ich das Genexpressionsprofil von BMP-Zielgenen analysiert. Ich untersuchte zwei endogene und frühe BMP-Zielgene sowie die Expression der stabil transgenen Gaussia Luciferase. Interessanterweise deuten die Ergebnisse dieser zwei unabhängigen Versuchsaufbauten und Detektionsmethoden auf eine oszillierende Expression der Zielgene hin. Die Amplituden der Schwingungen zeigten eine deutliche Konzentrationsabhängigkeit bei kontinuierlicher und transienter Stimulation. Außerdem aktiviert eine Kurzzeitstimulierung von 15 Minuten ebenfalls ein oszillierendes Genexpressionsprofil, welches für mindestens 30 Stunden nach der Stimulierung nachweisbar ist. Nur die Behandlung mit einem BMP Typ-I-Rezeptorkinaseinhibitor

führt zur vollständigen Aufhebung der Zielgenexpression. Infolgedessen sind die Oszillationen der Zielgenexpression direkt von der Aktivität der BMP Typ-I-Rezeptorkinase abhängig.

3. Introduction

3.1 Bone Morphogenetic Proteins

Bone Morphogenetic Proteins (BMPs) are secreted growth factors that belong to the TGF-ß superfamily. BMPs were originally identified as proteins bearing the ability to cause bone and cartilage differentiation in the 1960s [1]. However, this name has become misleading because its various functions that have been revealed [12]. Today, about 20 members of the BMP family have been identified and characterized. The main biological functions of BMPs are predominantly related to bone and cartilage formation [2]. This includes BMP2 to BMP9 for bone formation and BMP11 to BMP14 for cartilage formation. However, there are several BMPs that do not have known roles in the range of bone and cartilage. These proteins play a role in spermatogenesis, heart morphogenesis, ovary physiology and embryonic patterning. BMP1 is a misidentified protein with chordinase and procollagen proteinase activities and thus not a member of the BMP family of growth factors [3].

BMPs are secreted growth factors and posttranslational processing is important for the secretion of a biologically active molecule. These proteins are expressed as large precursor polypeptide chains composed of a signal peptide, a prodomain and a mature domain with a highly conserved C-terminal region. A distinguishing structural feature of the TGF-ß superfamily is the presence of seven conserved cysteines, which are involved in folding the molecule into a three-dimensional structure, the cysteine knot [4]. This immortile cystine-knot structure is necessary to stabilize the entire BMP2 protein dimer. Furthermore another conserved cysteine residue is accountable for single disulfide bridges between two subunits. This results in the formation of a covalently linked homo- or heteromeric biologically active protein dimer [5]. Some heterodimers, for example BMP2/BMP7 and BMP4/BMP7 show a higher biological activity than the corresponding homodimeric proteins [6].

BMPs are known to be implicated in a variety of functions. Besides their ability to induce bone and cartilage formation, they also play a role in non-osteogenic processes like embryonic patterning [7] and organogenesis of other tissues. During early embryogenesis, Bone Morphogenetic Proteins are involved in dorso-ventral patterning and induction of head and tail formation [8]. Later during embryo development, a BMP gradient in signaling directs cells into forming organs such as bone, cartilage, kidney [9], heart [10] or reproductive organs [11].

3.2 BMP receptors

3.2.1 Subtypes, structure and function

For about 20 BMP ligands a comparably small number of specific receptors are known. BMPs bind to heteromeric receptor complexes composed of two major types of serine/threonine kinase receptors, the type I and type II receptors. There are three distinct BMP type II receptors: activin type IIA and IIB receptors (ActRIIA and ActRIIB) and BMP type II receptor (BRII). These receptors bind to three type I receptors, named Activin receptor-like kinase (ALK): Activin type Ia receptor (ActRIa), BMP type Ia receptor (BRIa or ALK3) and BMP type Ib receptor (BRIb or ALK6) [13]. Both receptor subtypes consist of a relatively short extracellular domain, a single transmembrane region and an intracellular part, containing the serine/threonine kinases. The ligands bind to the extracellular region of the type I receptor in the absence of type II receptor. When both receptor subtypes are present, their binding affinity increases dramatically [14]. The kinase domains of type II receptors are constitutively active and phosphorylate the type I receptor kinase upon ligand binding.

BRII is expressed in two splice variants, the short form (BRII-SF) and the long form (BRII-SF). The long form subtype has a long cytoplasmic tail followed by the kinase [14,15]. This cytoplasmic tail is more widely expressed [16] and thought to determine BMP signaling specificity, complexity and intensity by allowing interactions with multiple adaptor proteins [17].

In case of ligand stimulation, the type I receptor undergoes a very fast phosphorylation mediated by the type II receptor [18]. Target for this phosphorylation is the GS-box, the glycine- and serine-rich N-terminally located domain of the type I receptor kinase. This domain is an important regulatory structure for signaling of the whole TGF-ß superfamily. The kinase of the constitutively active type II receptor phosphorylates multiple serine and threonine residues of the cytoplasmic GS region of the type I receptor and therefore leads to its activation [19]. Signaling can be inhibited by the immunophilin FKBP12 by binding to unphosphorylated GS-boxes and lock the catalytic center in an inhibited conformation [20].

Most of the cytoplasmic parts of the BMP type I receptor are functionally exchangeable. Feng and Derynck (1997) observed that the specificity of TGF-ß signaling is dependent on the L45 region of the kinase domain. The L45 loop of the type I receptor is a short amino acid sequence between ß-sheet VI and V of the kinase domain. It is exposed in the kinases 3D structure, invariant among the type I receptors and therefore responsible for distinct signaling ability [21]. Furthermore this loop specifically interacts with the R-Smads, the major signal transducer of BMP signaling.

3.2.2 Ligand binding and activation of BMP signaling

After getting activated, the type I receptor kinase in turn phosphorylates cytoplasmically located signal transducers, the Smad proteins. The Smad family comprises eight proteins classified into three subgroups: receptor-activated Smads (R-Smads), the common Smad (Smad4) and the inhibitory Smads (I-Smads). Among the R-Smads, Smad2 and 3 are thought to be specific for TGF-ß signaling whereas Smad1, 5 and 8 transduce BMP signals. The R-Smads become phosphorylated on an SSXS-motif at their C-termini and this modification leads to the activation of these signal transducer proteins. Upon phosphorylation, the Smad proteins form homomeric or heteromeric triplexes with Smad4, translocate into the nucleus and subsequently regulate Smad-complexes target gene transcription through direct binding to DNA, interaction with other DNA-binding proteins and recruitment of transcriptional co-activators or co-repressors.

A lot of studies have been done to examine the structure of ligand-receptor complexes. Kirsch observed in 2000 the crystal structure of human dimeric BMP2 in complex with two high affinity BMP type Ia receptor extracellular domains [22]. The receptor binds to distinct epitopes from both BMP2 monomers [22]. The large epitope 1 (wrist epitope) is a high-affinity binding site for BMP type Ia receptor and a smaller juxtaposed epitope 2 (knuckle epitope) acts as a low-affinity binding site for BMP type II receptor [23]. The wrist epitope comprises residues from both BMP2 subunits and the homomeric BMP2 shows a symmetry resulting in two pairs of both epitopes (Figure 3.1). No contact exists between the extracellular domains of the two receptor subtypes [22,24].

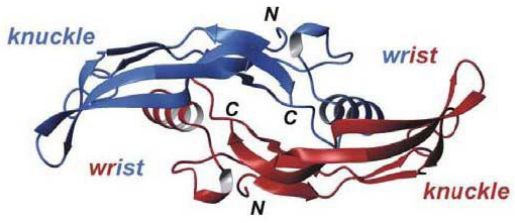

Figure 3.1: Ribbon-model of a BMP2 dimer along the two-fold axis [23]**.** The figure shows the location of the wrist and knuckle epitopes as BMPs binding interfaces. The two BMP2 monomers are colored in blue and red.

Ten hydrogen bonds are formed in one BMP2/type Ia receptor complex. One of these bonds is a hotspot in ligand/receptor recognition and invariant within the BMP family. Hence, this residue is thought to play an important role in the type I receptor specificity [25]. Allendorph and coworkers claimed that specific signaling output is largely determined by two variables, the ligand/receptor pair identity and the mode of

cooperative assembly of relevant receptors governed by the ligand flexibility in a membrane-restricted manner [24].

Receptor oligomerization and signal induction of the related BMP-ligand receptors differs. The oligomerization pattern of BMP type I and type II receptors is flexible and can be influenced and modulated by ligand binding [26]. It has also been shown that a low but measureable level of BMP receptors is already complexed at the cell surface prior to ligand binding, the preformed hetero-oligomeric complexes (PFCs). But the major amounts of receptor complexes are formed after ligand binding to the high-affinity type I receptor, the BMP-induced signaling complexes (BISCs). It has been shown in 2002 that binding of BMP2 to PFCs activate the canonical Smad pathway, whereas BISC activate non-Smad signaling with the induction of alkaline phosphatase activity via p38 MAPK (Figure 3.2) [27].

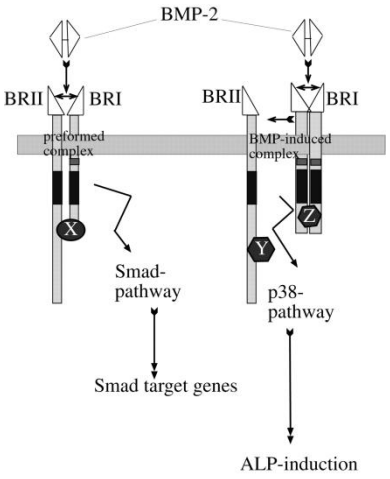

Figure 3.2: Model of signaling through PFCs versus BISCs [27]**.** Upon BMP2 binding to preformed complexes (left side) the canonical Smad pathway gets activated, whereas BMP induced signaling complexes activate non-Smad signaling with the induction of alkaline phosphatase activity via p38 MAPK.

3.2.3 Dorsomorphin

During *in vivo* screening assays BMP antagonists were found to lead to substantial and reproducible dorsalization in developing zebrafish embryos. Dorsomorphin (6-[4-(2-Piperidin-1-yl-ethoxy)phenyl]-3-pyridin-4-yl-pyrazolo[1,5-a]pyrimidine), also known as compound C, is a small molecule inhibitor of the BMP pathway. This compound selectively inhibits the BMP type I receptor serine-threonine kinase and blocks BMP mediated Smad1/5/8 phosphorylation in a dose dependent manner, while having no effect on TGF-ß or Activin induced Smad activation as well as BMP induced p38 activation [28]. The heterocyclic structure of Dorsomorphin binds with different affinities the ATP binding site of the kinase domain of the type I receptors and thus inhibits their kinase activity [28,29]. Since BMP mediated signaling induces osteoblast differentiation

of c2c12 cells, it was shown that Dorsomorphin is able to completely abolish the osteogenic direction in multipotent mesenchyme-derived cells without cytotoxicity [28]. This small molecule inhibitor is also potentially effective for some clinical disorders. Yu and colleagues have shown with a mouse model of Fibrodysplasia ossificans progressiva (FOP) expressing a constitutively active form of the ALK-2 receptor, that a Dorsomorphin derivate inhibited the Smad phosphorylation through the caALK-2 leading to a reduction in ectopic ossification and functional impairment in mice [30]. Futhermore, Hao et al. reported that this compound induces stem cell differentiation into cardiomyocytic lineage when the treatment is limited to the initial stages of embryonic stem cell differentiation. This indicates that BMP type I receptor kinase inhibitors could also be used as a tool for the research in regenerative medicine [31].

3.3 BMP signal transduction via Smad proteins

Upon binding of BMPs to their corresponding receptor complexes, two major downstream pathways may be triggered. PFCs activate the Smad-signaling route and BMP-induced signaling complexes induce the non-Smad pathways, which goes primarily via MAPKs.

3.3.1 Smad proteins

Mammalian Smad proteins are named by their orthologues that were found in *Drosophila* (MAD proteins) and *C.elegans* (Sma proteins). These proteins are the major signal transducers for the TGF-ß family signaling cascade [32]. Eight different Smad-proteins have been identified in mammals that are classified into three subgroups. As previously described, the first group are the R-Smads or receptor-mediated Smads and comprise Smad1, 2, 3, 5 and 8 which are intracellular messenger molecules. In general, Smad1, 5 and 8 are BMP signaling transducers and Smad2 and 3 are TGF-ß specific transducer proteins [19,33]. Smad1, Smad5 and Smad8 are structurally highly similar to each other and their primary structure is about 465aa. Furthermore they have highly conserved N- and C-terminal regions, which are known as Mad homology (MH) 1 and MH2 domains. These domains are linked by a region with a highly variable structure. The MH1 domain is responsible for DNA-binding, protein-interaction, nuclear translocation and repression of the MH2 domain function. The Smad-proteins bind DNA through a hairpin loop of 11 amino acids, which protrudes from the surface of the molecule [34]. The structure of this loop is conserved in R-Smads as well as the co-Smad protein in mammals.

The MH2 domain is responsible for the Smad's interaction with receptors, other Smads and distinct DNA-binding proteins as well as the activation of target gene transcription. The responsiveness to BMP signaling is achieved by the L3 loop. This is a short amino acid sequence protruding from the molecule and interacting with the L45 loop of the type I receptor kinase [35]. Two amino acid-residues of Smad1 and 5, His 425 and Asp 428, are critical for R-Smad specificity and recognition of the receptor type I kinases L45 loop and thus for discrimination between BMP and TGF-ß specific signals [35,36].
The crystal structure of non-phosphorylated Smad1 illustrates the high flexibility of the protein [37]. After phosphorylation of the protein on its SSXS motif, the MH2 domain undergoes conformational changes [37]. The phosphorylated SSXS domain of one Smad-molecule gets in contact with a basic phosphoserine binding pocket in the MH2 domain of another Smad protein [37]. Here is an important distinction to the TGF-ß activated Smads. Their MH2 domains are conformational stable upon phosphorylation [38,39]. Once they got phosphorylated, the R-Smad molecules form homomeric or heteromeric complexes. Heteromerization with Smad4, the only common-mediator Smad, exhibit strong electrostatic interactions whereas these complexes are more often [40,41]. This model of heterotrimers is supported by the fact that Smad complex induced transcription requires the presence of Smad4 [42]. Furthermore, it was shown that the Smad complex formation happens in a promoter-specific manner [43].
When inactive, the R-Smads are blocked by autoinhibition through intramolecular interaction of the MH2 with the MH1 domain [44]. The linker region between the two MH domains varies among the Smad proteins and comprises multiple phosphorylation sites which allow crosstalk to other signaling pathways.

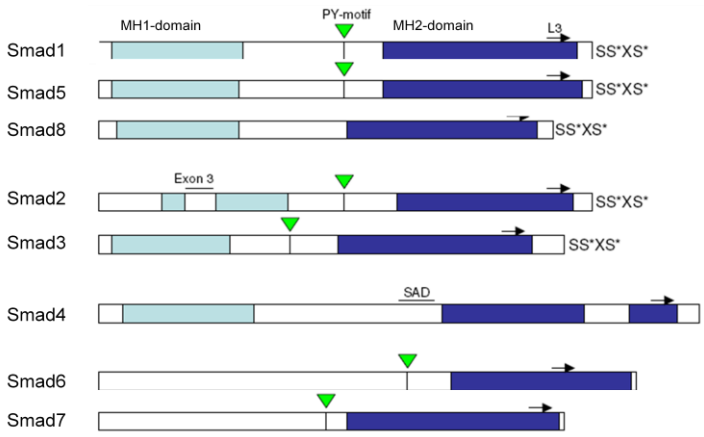

Figure 3.3: Schematic structure of all Smad proteins (modified from [45]**).**

Besides, this linker region contains a PY motif. This motif is a proline-rich conserved sequence recognized by the E3 ubiquitin ligase family members, like Smad ubiquitin regulatory factor 1 (Smurf1), specifically interacting with BMP-mediated Smad proteins

[46] and leading to their degradation. A comparison of the schematic structures of all Smad proteins is shown in Figure 3.3.

Smad4 is the only member of the second functional group, the common-mediator Smad or co-Smad. This proetin is the central mediator of the Smad function since it does not bind to the receptors but the R-Smads [47]. Structurally, Smad4 is highly homologue to the R-Smads and comprises both MH domains connected by the linker-region. Compared to the R-Smads, Smad4 lacks the SSXS- and PY-motifs [48]. The MH2 domain of Smad4 has two different functions. Firstly, it is required for the heterotrimeric complex formation with R-Smads and secondly, it is necessary for the full transcriptional response [49]. A proline-rich sequence of the MH2 domain, the Smad activation domain (SAD), has been shown to tighten the structural core and the surfaces of the MH2 domains for interaction with transcription partners [50]. It has also been shown, that Smad4 is ubiquitinated and degraded following complex formation with Smurf mediated by R-Smads or I-Smads [51]. Tumorigenic Smad4 mutants are also polyubiquitinated and degraded by the proteasome [52,53]. But Morén and coworkers also observed that mono- or oligoubiquitination of Smad4 can lead to the enhancement of signaling and hence the positive regulation of Smad4 function [52]. Furthermore, Smad4 gets sumoylated by SUMO-1. This protects Smad4 from ubiquitin-mediated degradation and consequently enhances transcriptional responses of Smad4 [54].

The third functional group of Smad proteins are the inhibitory Smads (I-Smads). The group members, Smad6 and Smad7, lead to the downregulation of BMP signaling. Both inhibitory Smads are direct target genes of the BMP and TGF-ß ligands, resulting in a negative feedback loop [55,56]. The N-terminal domain of these proteins differs from the MH1 domain of the R-Smads and the co-Smad but they even contain the MH2 domain with high homology to the other Smad proteins. Additionally, they lack the SSXS motif comparable to Smad4 [19]. The N-terminal domain regulates the specificity and the subcellular distribution of the protein, whereas the MH2 domain is responsible for the inhibitory effect [57]. The inhibitory mechanisms of the I-Smads will be further discussed in section 1.4.3.

3.3.2 Smad nucleocytoplasmic shuttling

Upon active signaling, the Smads form complexes and translocate into the nucleus and regulate gene transcription. Most of the work regarding nucleocytoplasmic shuttling has been done on the TGF-ß/Smad2, 3 pathway, hence the TGF-ß pathway will also be discussed here.

The first evidence for nucleocytoplasmic shuttling has been shown in studies with Smad4. In the absence of ligand, Smad4 is ubiquituously distributed in the cell. But treatment with the specific exportin 1 inhibitor Leptomycin B (LMB) [58], led to nuclear accumulation of Smad4 [59]. This study indicated that Smad4 must be shuttling continuously between the nucleus and the cytoplasm of a cell.

The transport of proteins through the nuclear envelope occurs by the nuclear core complex (NPC) that forms a hydrophobic channel. Small molecules with a size of about 20-30 kDa are able to diffuse through the NPC, but larger proteins have to be transported actively by transport proteins. These transport proteins are karyopherins and can be subdivided in two different groups, the importins and the exportins [60]. The importins bind the cargo proteins on their nuclear localization sequences (NLS), which is a short lysine- and arginine-rich sequence. In the nucleus, the transported protein is released by binding of the GTPase Ran-GTP to the importin. For the export, the cargo proteins bind to leucine- or isoleucine-rich nuclear export sequences (NES) of the exportins. The cargo protein is released upon GTP hydrolysis in the cytoplasm.

R-Smad proteins are known to possess a basal shuttling activity [61,62]. In a non-stimulated case, they are predominantly located in the cytoplasm in consequence of a faster nuclear export to import rate. Due to a decrease in the export rate and a constant import rate upon stimulation, Smad2 accumulates in the nucleus [63]. As a result of R-Smad dephosphorylation, R-Smad/Smad4 complexes activated by TGF-ß signals dissociate in the nucleus and the monomeric Smads are exported to the cytoplasm separately by distinct mechanisms [64]. When the receptors are still active, the R-Smads get rephosphorylated, form complexes and return to the nucleus. When the receptors are unactive, the Smads will be located predominantely in the cytoplasm [64]. Smad2 and 3 are imported via two different mechanisms: due to the NLS in their MH1 domain and are imported by importin ß and importin-7 and -8 [65,66], furthermore they underlie karyopherin-independent import mediated by the MH2 domain and other nucleoporins [67]. The export of Smad2 and Smad3 has been shown to be Leptomycin B insensitive, thus exportin 1 is not involved in their export mechanism [59]. Smad3 nuclear export is mediated by exportin 4 and Ran [66].

Smad1 contains a NLS-motif in its MH1 domain [62] and gets imported via importins 7 and 8 [68]. For the nuclear export, Smad1 has two NES. The first sequence, NES1, is located in the MH2 domain and the second one, NES2, is located in the linker region adjacent to the MH1 domain. NES2 partly overlaps with the functional NES of Smad4. Experiments with mutant versions of NES1 and NES2 have shown that the nuclear enrichment was more prominent with the mutated NES2 than with the NES1 mutant version. The Smad1 NES1 mutant showed good ligand responsiveness and

moderately decreased transcriptional activity compared to wild type Smad1. In contrast, the Smad1 NES2 mutant shows a severe disruption in reporter gene activation. Furthermore, it has been observed that only NES2 is included in exportin 1 transport [69].

The subcellular distribution of the inhibitory Smads differs between the two members. In the unstimulated situation, Smad7 is predominantely located in the nucleus whereas Smad6 is distributed ubiquituously [70,71]. Both inhibitory Smads translocate to the cytoplasm in association with Smurf proteins upon ligand stimulation [72,73].

3.3.3 Smad transcriptional complexes

Upon phosphorylation, the Smad-complexes translocate into the nucleus and act as transcriptional mediators. Several genes are well known to be direct BMP targets like *id1* [74], *smad6* [75]*, tlx-2* [76] and *ventx1, 2 and 3* [77]**.** Due to the MH1 domain on their N-terminus, the R-Smads and co-Smad are able to bind DNA in a sequence specific manner and in conjunction with other transcription factors. The MH1 domain of the Smad proteins create a ß-hairpin structure and recognize the Smad-binding element (SBE) in the major groove of the DNA, which is composed of the nucleotide sequence 5' – GTCT – 3' [34]. Since the ß-hairpin structure is present in all R-Smad proteins, this Smad-DNA contact is not able to provide selectivity in target gene selection. However, the most occurring splice version of Smad2 lacks DNA-binding activity [34]. The reason for this interesting fact still remains unclear.

The SBE has been shown to exist as mono- or multimers in several target gene promoters [78,79]. But *in vivo* the affinity to one single Smad-binding element is very low. Since Smad complexes comprised multiple Smad proteins, the presence of SBE-multimers enables a tighter contact of Smad-complex and DNA [80]. However, natural Smad promoter regions rarely contain SBE-multimers, thus high-affinity binding to DNA is thought to be due to other DNA-binding factors within the Smad-complexes. These cofactors of the transcription machinery also recognize the SBE sequence with low affinity, but they are able to bind with high affinity to a further cognate sequence (XBE) [48]. The SBE and XBE act as transcriptional enhancers and are located upstream of the TATA box, where the transcription machinery is assembled (Figure 3.4). Besides, this machinery includes other coactivators or corepressors for additional determination and selectivity of gene expression response.

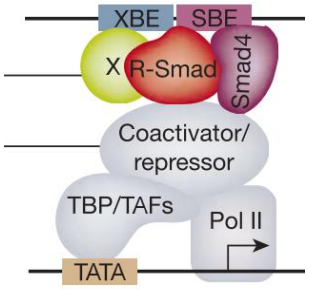

Figure 3.4: Structure of Smad transcription factor complex [48]**.**

Further promoters with GC-rich sequences are known to recognize Smad-complexes. The *smad6* promoter contains a BMP-responsive element with four overlapping GC-rich motifs [55]. Some years later it has been shown that both, the SBE and the GC-rich elements, are required for BMP-mediated induction of *id1* [81]. To date, no crystal structure of Smad binding to GC-rich motifs has been identified.

3.4 Regulatory system of BMP signaling

Since signaling pathways consist of many single steps and the interaction with a lot of different cellular components, it gets obvious that this networking has to be tightly controlled. The following chapter discusses all regulators causing signaling fine-tuning. The BMP pathway can be regulated at several signaling stages: a) the inhibition of ligand-receptor interaction by BMP antagonists, b) the presence of pseudoreceptors, c) the blocking of BMP signaling by I-Smads, d) the inhibition of BMP signaling by intracellular proteins and e) proteasomal degradation of Smad proteins.

3.4.1 Antagonists

Antagonists are proteins interfering the binding of BMP ligands to the receptor. They block the receptor epitopes of BMP and inhibit the ligand-receptor oligomerization. The structure of these antagonists is very similar to the BMP structure, as the antagonists are homodimerc peptides stabilized by a cysteine-knot motif. Based on this motif, three different BMP antagonist families are classified: the Chordin/Noggin family (ten-cysteine knot motif), the twisted gastrulation family (nine-membered knot motif) and the DAN/Cerebrus family (eight-membered cysteine ring) [82].

Chrodin and Noggin are the best characterized BMP antagonists. Noggin binds to several BMP ligands, but with very high affinity to BMP2 and BMP4 [83]. The crystal structure of Noggin/BMP7 showed that Noggin inhibits signaling by blocking both binding epitopes for receptor binding [84]. Since Noggin expression is induced by BMP2, 4 and 7, it generates a negative feedback loop of BMP signaling [84]. Chordin

also specifically binds to BMP2 and 4 and consequently blocks BMP binding to the receptor.

3.4.2 Co-receptors and Pseudoreceptors

Although type I and type II receptors are sufficient for BMP signaling transduction, the binding efficiency and signaling activity of certain ligands is regulated by co-receptors. Three members of the repulsive guidance molecule (RGM) family have been shown to play a role during BMP signaling [85,86]. These Glycosylphosphatidylinositol (GPI)-anchored proteins are co-receptors for BMP2 and BMP-4 (RGMa, DRAGON (or RGMb) and hemojuvelin (or RGMc)), associate them with BMP type I and type II receptors and specifically enhance BMP signaling but not the TGF-ß pathway [85,87].

Endoglin (CD105) is a transmembrane protein that binds to various ligands like TGF-ß1/3, activin-A and BMP2/7. It has been found, that ectopic expression of endoglin results in inhibition of TGF-ß induced responses, but enhances BMP-7 induced Smad1/5 signaling [88].

Furthermore Betaglycan, also named TGF-ß type III receptor, interacts with BMP2, 4 and 7 and facilitates the binding efficiency of BMP2 to the receptor [89].

There are also some receptor associated proteins that negatively regulate BMP signaling. The pseudoreceptor BMP and Activin membrane-bound inhibitor (BAMBI) is structurally very similar to the TGF-ß type I receptors and consequently competes with type I receptors for heterodimerization with type II receptors. But this receptor lacks the kinase domain and thus fails to activate R-Smads after ligand binding [90]. Two other pseudoreceptors are known. The tyrosin kinase receptor Ror2 binds to the BMP type I receptor and creates a BMP independent receptor complex [91] and TrkC directly binds the type II receptor and suppresses BMP induced Smad1 phosphorylation [92].

3.4.3 Intracellular regulatory proteins

Besides the extracellular interactions of the BMP receptors, there are a lot of intracellular components acting as signal transducers or regulators. As the inhibitory Smads6 and 7 have a negative regulator function, their inhibition mechanisms are reviewed here. Smad6 is a specific inhibitor for the BMP pathway since it competes with Smad4 for binding to the receptor-activated Smads [93]. In cooperation with Smurf1, Smad6 additionally mediates BMP type I receptor degradation [94]. Furthermore, Smad6 acts as a nuclear repressor of BMP-dependent transcription [95,96]. Smad7 affects both, the BMP and the TGF-ß pathway [97], and undergoes polyubiquitynation leading to amplification of BMP and TGF-ß signaling [98].

When phosphorylated, Smad1/5/8 hetero-oligomerizes with Smad4, translocates into the nucleus and mediates target gene transcription in conjunction with co-activators and -repressors. Ski and SnoN are oncoprotein homologoues and important TGF-ß negative regulators. Both proteins interact with the R-Smads (mainly Smad2/3) and Smad4 and thus block the ability to activate target gene transcription. Ski is furthermore able to bind and repress the activity of Smad1 and Smad5 [99]. To date, three different inhibition mechanisms of Ski are known: a) blocking of newly activated Smads by stabilizing Smad complexes on DNA, b) interference of Smad binding to transcriptional activator proteins and c) recruitment of nuclear co-repressors and histone deacetylase complex (HDAC) [100].

Another intracellular repressor for BMP signaling is the Tob protein. This protein is a member of the antiproliferative proteins and decreases signaling outcome by associating with the BMP-signaling relevant Smad proteins and inhibit target gene transcription [101]. Furthermore, Tob interacts with Smad6 by supporting the binding of Smad6 with BMP type I receptors and thus mediating downregulation of BMP signaling [102].

BMP signaling is also regulated by the ubiquitin-mediated proteasomal system. The ubiquitin-proteasome proteolytic pathway is critical for biological processes including gene transcription and signal transduction. Smad-ubiquitination regulatory factor (Smurf) 1 and Smurf 2 are Smad specific E3 ubiquitin ligases, specifically interacting with Smad 1, 5, 6 and 7 and targeting these proteins for degradation [103]. Smurf 1 is located in the nucleus and gets exported to the cell membrane and cytoplasm to induce the proteasomal degradation of type I receptors and Smads [13]. Furthermore Smurf 1 represses BMP signaling by enhancing the interaction of I-Smads with type I receptors [94].

3.5 BMPs in embryonic development

Originally isolated because of their competence to promote bone and cartilage formation [1], it could be shown that the BMP genes are expressed in many embryonic organs and tissues and are crucial for morphogenesis and differentiation at different embryonic stages. These observations were mostly done by genetic screens and knock out experiments in mice.

Several publications claim that the genes for the BMP ligands, their receptors and the Smad proteins are expressed in early mouse embryos before and during gastrulation, germ cell fate determination and mesoderm formation [104–108].

For a long time, only little was known about the function of BMPs during left-right asymmetry establishment in mammals, because null-mutants show embryonic lethality before the left-right patterning [109]. Some years ago it has been shown that *smad5* mutant mice have defects in heart-looping and embryonic turning, which are first indications of left-right asymmetry in mice [110]. Furthermore BMP4 influences left-right asymmetry, since it mediates the expression of left-right determinants like *lefty2* and *nodal* [111].

Multiple experiments in animal models showed, that BMP signaling is also implicated in neural development. In Xenopus, enhanced BMP signaling drives neuronal cell fate into epidermal fate, while reduced signaling results in increased neural tissue [112]. In mouse embryonic stem cells it has also been shown, that BMP4 has negative effects on neuronal differentiation during several stages [113]. Most *bmp4* knockout mice die during gastrulation, but few mice that reached stage E9.5 – E10.5 failed to induce lens formation due to lacking BMP4 expression [114].

Since BMPs got their name because of their ability to cause bone and cartilage formation they have several functions in skeleton and limb development. *bmp7* mutant mice have skeletal defects in addition to eye and kidney defects [115]. Defects in anterior-posterior patterning of axis skeleton are caused by mutations in the *bmp11* gene and *bmp3* mutants surprisingly show increased bone density with the hint that BMP3 acts as an antagonist to osteogenic BMPs [116]. *bmp4* heterozygotes and *bmp7* homozygotes additionally show pre-axial polydactyly of the hindlimb, implying a role of BMP signaling in the anterior-posterior axis formation of the limb [115].

Furthermore, BMP signaling is known to be crucial for different organs such as heart and kidney. *bmp2* homozygous mutants show a roughly abnormal heart development. BMP5, 6 and 7 are also detectably expressed within the surrounding of the heart and it has been observed that single mutations do not show any defects. But double mutants show severe defects in heart formation and septation as well as delayed heart development, indicating compensatory effects of these proteins [117].

Among the BMP family, several members are expressed in the reproductive organs. The testis expresses BMP2, 4, 7, 8a and 8b and the maturing oocytes BMP6 and 15. In the testis, it has been shown that targeted disruption of *bmp4* or bmp*8b* results in failure of primoridal germ cell (PGC) formation [118,119] and BMP2 inactivation reduces germ cell numbers significantly [120]. Females with null mutations in the *bmp15* gene are infertile with arrested follicle development at the primary stage [121].

3.6 Diseases dependent on impaired BMP signaling

As described in the former chapters, BMP signaling is highly regulated and fine-tuned. Since it plays a crucial role during developmental processes, several diseases are related to mutations of BMP signaling components.

Fibrodysplasia ossificans progressiva (FOP) is a disease with progressive ossification of extraskeletal tissue in addition to severe skeletal malformations of the body [122]. This rare medical condition is autosomal dominant inheritable, but in most cases the disease arises as a result of a spontaneous new mutation. The phenotype is affected by genetic, as well as environmental factors. Several studies provided evidence for an impaired BMP-regulation of FOP patients and a genome-wide analysis identified *actrIa (alk2)* as the responsible gene. An identical heterozygous missense mutation in the GS-box of the receptor was identified [123], resulting in a constitutively active receptor isoform. Furthermore, this disease has been found to be associated to mutated versions of the BMP antagonist Noggin [124,125].

Pulmonary arterial hypertension (PAH) is a rare disorder, characterized by abnormal vascular cell proliferation and constriction of the pulmonary artery. Affected people suffer from enhanced blood pressure in the pulmonary artery and right ventricular failure. In severe cases, this leads to an impaired blood circulation and subsequent death [126,127]. PAH has been shown to be caused by heterozygous germline mutations of the BRII gene in familial as well as idiopathic cases [128–130]. These mutations are supposed to cause nonsense, missense or frame-shift mutations and thus lead to the loss of correct BRII-function. Studies in transgenic mice expressing a dominant-negative BRII in smooth muscle cells showed that this mutation is sufficient to produce the pulmonary arterial hypertension phenotype [131]. Recent studies revealed that the pro-proliferative and anti-apoptotic effects of the SMCs are caused by the Smad-independent MAPK-activation via TGFß-associated kinase 1 (TAK1). This discovery could be a new potential therapeutic target in PAH [132].

Hereditary hemorrhagic telangiectasia (HHT; also known as Osler-Weber-Rendu syndrome) is an inherited autosomal disease and characterized by the presence of multiple arteriovenous malformations resulting in direct connections between arteries and veins [133]. Most patients suffer from mild symptoms like nosebleeds and telangiectasia, but about 30% of the HHT-patients have chronic anemia with gastrointestinal bleeding and common complications include stroke and brain abscess [134,135]. Three genes are known to be related to HHT; each of these proteins is involved in the TGF-ß superfamily signaling. Besides the receptor subtype ALK1 [136,137], the co-receptor Endoglin [138], and Smad4 [139] have been found in mutated versions in HHT-patients.

The juvenile polyposis syndrome is autosomal dominant inherited and is characterized by gastrointestinal hamartomatous polpys and a risk for gastrointestinal cancers [140]. BRIa and Smad4 are known to be mutated in these patients. Furthermore, impaired BMP signaling contributes to several cancer types as BMPs regulate proliferation negatively and thus presumably is a potential tumor growth modulator [141]. The following cancertypes have been shown to be associated with impaired BMP-signaling: malignant and metastatic bone tumors [142], breast cancer [143], colon cancer [144,145], gastric cancer [146], malignant gliomas [147], hair follicle tumors [148], medulloblastomas [149], malignant prostate cancer [150], pancreatic cancer [151] and malignant skin tumors [148,152].

3.7 Bone Morphogenetic Proteins in clinical applications

Natural bone healing and formation involves several mechanical and biological factors and is a complex regulated process. Approximately 1/10 of all bone fractures experience difficulties with healing, resulting in sequelaes, pain and physiological stress [153]. BMPs play an important role in regulating osteoplastic differentiation and bone formation and most clinically relevant drugs are based on the concept of altering signaling events. When combined with biocompatible carriers, recombinant BMP2/4 and 7 are able to heal critical bone defects [154] and their potential has been shown in animal models [155]. Currently, collagen-based BMP2 and BMP7 are approved to be used for clinical applications. These products are applied for the treatment of long bone defects, spinal fusion, dental and periodontal tissue engineering craniofacial defects, fracture repair, the improvement of osteointegration with metallic implants and musculoskeletal reconstructive surgery [156]. Application of BMP7 in joint fusions for example, resulted in healing rates of 90% and satisfactory functional outcome in 70% of all cases [157]. BMP-7 is also thought to be a strong candidate for the treatment of chronic kidney disease, as it prevents the development of adynamic bone disease in a preclinical model of chronic kidney failure [158]. Another new approach at the initial trial stage of development is the adhesion of short BMP peptides onto polyethylene terephthatalate surfaces. These biomaterials should enhance osteogenic differentiation and mineralization of pro-osteoblastic cells [159].

3.8 Aim of the project

The mechanism of how cells decode extracellular stimuli intracellular and convert the information into specific responses is generally still unclear. There is poor knowledge

about the quantitative relationship between signal input, signaling transducers, their subcellular localization and their ability to integrate graded inputs and generate correlating responses. Understanding the signaling network and mechanisms on a quantitative level should be considered a prerequisite for efficient pathway modulation.

The aim of this project is to construct the first quantitative connection between BMP signaling input, Smad1 modification, Smad1 spatio-temporal subcellular localization and target gene transcription dynamics. The BMP pathway was chosen for several reasons. There is enough basic knowledge as well as mechanistic understanding and quantitative data will be feasible. Secondly, it can serve as a typical model for signaling pathways with latent transcription factors as signal transducers. Furthermore, BMP signaling plays a major role in embryonic development as well as a series of severe diseases, clinical trials and drug development.

Several questions concerning BMP signaling modulation should be addressed during this study:

- Which levels of BMP ligand can be discriminated by cells?
- Is there a link between the Smad1 mobility as well as subcellular localization and the ligand exposure?
- What is the quantitative correlation between varying BMP stimuli and the transcriptional output?
- How do cells respond to bursted signal inputs?
- Which impact has the BMP type I receptor kinase for the signaling

4. Materials and Methods

4.1 Oligonucleotide Sequences

Oligo Name	5'- Sequence -3'
2xBRE_f01	CGTTACATCGATCTCAGACCGTTAGACGCCAGGACGGGCTGTC AGGCTGGCGCCGCTCAGACCGTTAGACGCCAGGACGGGCTGT CAGGCTGGCGCCGGGATCCCGTTAC
2xBRE_r01	GTAACGGGATCCCGGCGCCAGCCTGACAGCCCGTCCTGGCGT CTAACGGTCTGAGCGGCGCCAGCCTGACAGCCCGTCCTGGCG TCTAACGGTCTGAGATCGATGTAACG
EGFP-r01	CGGTGAACAGCTCCTCGCCCTT
loxP-cmv_f04	GTAACGAAGCTTATAACTTCGTATAGCATACATTATACGAAGTTA TCCGTATTACCGCCATGCAT
loxP-pA_r05	CGTTACAAGCTTATAACTTCGTATAATGTATGCTATACGAAGTTA TGGACAAACCACAACTAGAATGCA
mCherry_screen_r01	GATGATGGCCATGTTATC
MLP_f01	CGTTACGGATCCTGAAGGGGGGCTATAAAAGGGGGTGGGGGC GCGTTCGTCCTCACTCTCTTCCGAATTCCGTTAC
MLP_r01	GTAACGGAATTCGGAAGAGAGTGAGGACGAACGCGCCCCCAC CCCCTTTTATAGCCCCCCTTCAGGATCCGTAACG
mSmad6_f02	CAAGATCGGTTTTGGCATACTG
mSmad6_r02	GTCGGGGAGTTGACGAAGAT
mus-ef1a_f02	TCAGGAGGAGACCACACCTT
mus-ef1a_r03	ATATCCACAGGCAGCAAACA
mus-ID1_f06	AGAACCGCAAAGTGAGCAAG
mus-ID1_r6	GTGGTCCCGACTTCAGACTC

pMTC_screen_rev	GTTCTTGAGGCTGGTTTAGTGG
pt109LucFor2	CACGCGTCACCTTAATATGC
pt109LucRev	CCCCCTGAACCTGAAACATA
S1-screen_r01	TCTCTTCACAGCTGGACTTGT
Smad1-screen_f01	TCAACAATCGTGTGGGTGAA
Smad1-screen_f02	TACTTCCTCCTGTGCTGGTT
Smad1-screen_r01	AAACGGGTGGCTGTTG
Sp6Promoter	ATTTAGGTGACACTATAG
TKprom_f01	TCTAGAGGATCCGGCCCCGCCC
TKprom-end_r01	GTAACGGAATTCTTTACCAACAGTACCGGAA
tol2-5_f01	TTGCGCTGATGCCCAGTTTA

4.2 Antibodies

Primary antibody	**Manufacturer**	**Catalog Number**
Smad1 (A4)	Santa Cruz Biotechnology	sc-7965
pSmad1/5/8	Cell Signaling Technology	9511

Secondary Antibody	**Manufacturer**	**Catalog Number**
Alexa Fluor 488 anti-rabbit	Invitrogen	A21441
Alexa Fluor 488 anti-mouse	Invitrogen	A11001
Alexa Fluor 594 anti-mouse	Invitrogen	A11032

4.3 Special technical devices and software

used for	Device	Manufacturer
(gradient-)PCR	TPersonal Thermocycler	Biometra
Confocal microscopy	Microscope SP5 and software	Leica
Confocal microscopy	Microscope C1 and software	Nikon
Confocal Stacks analysis	Volocity® 3D Image Analysis Software	Improvision
DNA/RNA quantifiaction	NanoDrop 1000	Thermo Scientific
Fluorescent microscopy	Microscope M205FA and software LAS V3.4.0	Leica
Luciferase measurements	GloMax® 96 Microplate Luminometer	Promega
Real-time PCR	Realplex^2 Mastercycler and software	Eppendorf

4.4 Kits

Kit	Manufacturer	Catalog Number
peqGOLD TriFast	PEQLAB	30210
RevertAid™ First Strand cDNA Kit	Fermentas	K1622
GenElute™ HP Plasmid Miniprep Kit	Sigma-Aldrich	NA0160-1KT
GenElute™ PCR Clean-Up Kit	Sigma-Aldrich	NA1020-1KT
PureYield Plasmid Miniprep System	Promega	A2495
PureYield Plasmid Midiprep System	Promega	A1223
Wizzard SV Gel&PCR Clean-Up Kit	Promega	A9282

4.5 Fluorescent dyes

Dye	Manufacturer	Catalog number
Hoechst33342	Invitrogen	H3570
CellMask Orange	Invitrogen	C10045

4.6 Chemicals

Chemical	Manufacturer	Catalog number
BMP-2	Walter Sebald, Würzburg	-
hBMP-4	PeproTech	120-05 ET
Coelenterazine	Synchem OHG	s053
Dorsomorphin	Sigma Aldrich	P5499
Leptomycin B	Sigma Aldrich	L2913

4.7 c2c12 cell line

c2c12 is a mouse myoblast progenitor cell line. The cells were originally isolated by David Yaffe and Ora Saxel in 1977 from a mouse muscle after a crush injury. Since these cells are progenitors, they are a useful tool to study the differentiation into myoblasts and osteoblasts and the investigation of the involved pathways [160].

4.8 Cell culture

4.8.1 Cell cultivation

The mouse myoblast cell line c2c12 and the derived c2c12_BRE-Luc cell line were cultured in D10 medium, consisting of DMEM supplemented with 10% FCS (PAA) and 1% Penicillin/Streptomycin (Sigma), at 37°C in a humidified atmosphere of 5% CO_2 in air. Ongoing adherent cell culture for both cell lines was done by detaching cells with 0.5x Trypsin/EDTA (PAA) in 1x PBS for 2-3 min at 37°C. Then the solution was withdrawn and the cells were resuspended in D10 medium. Generally, the cells were passaged every 2-3 days and splitted 1:10 - 1:20.

To examine the cellular response of the cells to BMP2-stimulation, the cells of both cell lines were starved over night in pure DMEM with antibiotics.

4.8.2 Cryo-conservation

Cryo-conservation of both cell lines was carried out by detaching cells with Trypsin/EDTA, centrifuging at 1000rpm for 5 min, resuspending thoroughly in D10/10% DMSO v/v and immediate freezing at -80°C over night. For long-term conservation cell were preserved in liquid nitrogen at -196°C.

4.8.3 Transfection

Transfections were performed using the Fugene HD transfection reagent (Roche) or the X-tremeGene HP DNA transfection reagent (Roche) following the manufacturer's instructions in a 3:1 ratio.

4.8.4 Generation of stable c2c12_BRE-Luc cell line

For generation of the c2c12_BRE-Luc cell line, the miniTol2 transposase system [161] was used. c2c12 wildtype cells were cotransfected with a construct containing the coding sequence of the transposase under control of the CMV promoter and the miniTol2_5'-MLP-BRE_GLuc-CMV_mCherryZeo-miniTol2_3' reporter construct in a 2:1 ratio and subsequently selected with 1.5mg/ml Zeocin in D10 culture medium for two weeks. Single colonies were picked utilizing the fluorescence microscope, expanded and then checked for correct function of the BRE-Luc construct.

4.8.5 Cell treatment for the gene expression experiments

The c2c12_BRE-Luc cells were seeded out in a density of 15000cells/cm^2 in 6cm dishes and starved over night. On the following day, cells were stimulated with 0nM (control), 0.1nM or 1nM BMP2 in hunger medium. Then the three different cell treatments followed:

(1) The cells were permanently stimulated with BMP2 (continuous treatment),

(2) The cells were stimulated for 15 min, then the BMP signaling pathway was inhibited by the administration of Dorsomorphin or

(3) The cells were stimulated for 15 min, then the stimulation medium was removed, the cells were washed three times with hunger medium and then fresh hunger medium was given to the cells for the rest of the experiment (wash-away treatment).

The cells were harvested after different stimulation time-points, by removing the stimulation medium and lysing the cells by adding the Trizol containing RNA Isolation Reagent. The lysates were stored at -80°C until the RNA isolation procedure.

4.8.6 Cell treatment for the transient Luciferase experiments

c2c12 wildtype cells were seeded out in 6-well plates at the evening. On the next day, the cells were transfected with the BRE-Luciferase reporter construct using the Fugene HD transfection reagent:

150µl DMEM pure
500ng vector DNA → mix
2µl Fugene HD transfection reagent → mix

15-20’ incubation at RT

The transfection mix was added dropwise to the cells and incubated for at least 4h. Then the cells were starved over night in DMEM with antibiotics. For the different experiments, the cells were stimulated with different BMP-concentrations alone, or with BMP and the pathway inhibitor Dorsomorphin in DMEM with antibiotics. 50µl medium were removed from every well of the stimulated cells and stored at 4°C until the measurement. An equal volume of fresh hunger medium was added to the cells to keep a constant medium volume. The Luciferase activity of the samples was measured with the GloMax® 96 Microplate Luminometer and Coelenterazine (Synchem OHG) as substrate.

Luciferase reaction mix: 100µl buffer (10mM Tris, 1mM EDTA, 0.6M NaCl, pH7.8)
20µM Coelenterazine
25µl culture medium (containing the Gaussia Luciferase)

4.8.7 Cell treatment for the Luciferase experiments

The c2c12_BRE-Luc cells were seeded out in a density of 15000cells/cm^2 in 6-well plates and starved over night. On the next day, 50µl medium of all wells were withdrawn hourly for four hours to generate the baseline and ensure that the cells in each well are on the same level. Then the cells were stimulated with 0nM (control), 0.1nM, 1nM or 10nM BMP2 in hunger medium (three wells for sample-taking and three wells for medium refill). Then three different cell treatments followed:

(1) The cells became permanently stimulated with BMP2 (continuous stimulation),
(2) The cells became stimulated for 15 min, then the pathway was inhibited by the administration of 10µM final concentration of Dorsomorphin (BMP receptor type I kinase inhibitor) or
(3) The cells became stimulated for 15 min, then the stimulation medium was removed, the cells were washed three times with hunger medium and fresh hunger medium was given to the cells (wash-away treatment).

Then every hour 50µl medium were removed from every well of the stimulated cells for 30h after stimulation and stored at 4°C until the measurement. An equal volume of conditioned medium or fresh hunger medium was added to the cells to keep a constant

medium volume over the whole time of the experiment. The Luciferase activity of all culture media samples were measured with the GloMax® 96 Microplate Luminometer, the Luciferase substrate Coelenterazine (Synchem OHG) and a specific buffer at the same day.

Luciferase reaction mix: 100µl buffer (10mM Tris, 1mM EDTA, 0.6M NaCl, pH7.8)
20µM Coelenterazine
25µl culture medium (containing the Gaussia Luciferase)

4.8.8 Cell treatment for the Smad1 live-shuttling experiments and confocal imaging

A meGFP-Smad1 fusion protein was cloned in front of a CMV-promoter (please see section 2.13.2). This vector was cotransfected with a H2B-mCherry fusion construct in a 2:1 ratio into c2c12 wildtype cells and starved over night. On the next day, cells were treated with 0nM BMP2, 0nM BMP2 with 10ng/ml Leptomycin B, 1nM BMP2 or 1nM BMP2 with 10ng/ml Leptomycin B (Sigma-Aldrich) in starvation medium. Then the cells were incubated at 37°C and imaged for 1h with the Nikon Eclipse Ti confocal microscope. The resulting data were processed using Volocity 3D Image Analysis Software (Improvision).

4.8.9 Cell treatment for the immunofluorescence stainings and observation of the Smad1 subcellular localization

c2c12 wildtype cells were seeded out on glass coverslips and starved over night. Then, the cells were stimulated with 0nM, 0.1nM or 1nM BMP2 for indicated time points. Immunofluorescent staining was performed (please see section 2.18) using anti-Smad1 antibody (Santa Cruz, sc-9765**),** Alexa Fluor 488 secondary antibody (Invitrogen), Hoechst 33258 (Molecular probes) for DNA staining and CellMask Orange (Invitrogen) for cell membrane staining. Confocal stacks were taken at room temperature using a Nikon Eclipse Ti confocal microscope and data were processed using Volocity 3D Image Analysis Software (Improvision).

4.9 PCR

Polymerase chain reaction was used for bacterial colony screens and for the amplification of templates for DNA cloning.

Standard PCR reaction mix	100ng Template-DNA
	1x ReproFast reaction buffer
	400µM each dNTP
	0.3µM each primer
	1U His-Taq DNA polymerase
	Ad 20µl with dH_2O

Standard PCR cycler program		5 min, 95°C
	30-35 cycles	30 sec, 95°C (denaturation)
		30 sec, specific temperature for oligos (annealing)
		1min/kb DNA, 72°C (elongation)
		10min, 72°C

4.10 Endonuclease digestion

Endonuclease digestion was used for bacterial colony screens and the preparation of plasmids and DNA-fragments for DNA ligation.

Standard reaction mix	3µg vector DNA or PCR product
	1x specific enzyme reaction buffer
	1U restriction enzyme
	Ad 50µl with dH_2O
	Incubation at 37°C for 1h

The restriction enzymes with the specific buffers were obtained from Fermentas, New England Biolabs or Promega. The clean-up of the digested DNA-fragments was usually performed utilizing the kits from section 2.4.

4.11 Ligation

Ligations were performed to insert enzyme digested DNA-fragments into target vectors.

Standard reaction mix	1µl Vector-DNA (from 2.9)
	1µl Insert-DNA (from 2.9)
	1x Ligation-buffer
	5U T4-DNA Ligase
	Ad 10µl with dH_2O
	Incubation at RT for 1h

The concentration of vector and insert were estimated using agarose gels and adjusted to the same molarities for the ligation reaction.

4.12 Heat-shock transformation of DNA into chemically competent bacteria

This method was used to transform ligated DNA into bacteria or to get new plasmid glycerine-stocks.

Standard reaction procedure

(1) Thaw chemically competent bacteria on ice
(2) Add 50µl of the bacteria to the ligation/DNA mix
(3) Keep this mix on ice for 20-30 min
(4) Heat-shock at 42°C for 1-1.5 min
(5) Put reaction mix on ice for 2 min
(6) Add 1ml fresh LB medium
(7) Shake for 1h at 37°C
(8) Slowly centrifuge at 2000rpm for 5 min
(9) Remove 80% of the supernatant and resuspend bacteria in the remaining liquid
(10) Plate out on agar plates with the appropriate antibiotic

4.13 Cloning

4.13.1 BRE-Luc reporter construct

The BRE-Luciferase reporter construct contains a dimer of a published BMP responsive element[81] in front of a MLP-minimal promoter and the Gaussia Luciferase gene as well as an independent mCherry-Zeocin fusion under control of the CMV-

promoter. Both genes are flanked by a tol2 recognition site for generation of a stable cell line including both reporters.

4.13.2 meGFP-Smad1 expression construct

The meGFP-Smad1 fusion protein was cloned using a cut-and-paste cloning procedure without an amplification step to ensure the right function of both proteins. The donor plasmid was kindly provided by Qiang Gan (Rudolf-Virchow-Centre, Würzburg) and incorporates the meGFP-Smad1 fusion protein, a blue fluorescent protein located in the cell nucleus and a red fluorescent protein located at the cell membrane. The meGFP-Smad1 protein was cut out utilizing BamHI and XbaI (both Fermentas) and ligated into the pMTC-loxP-GFPZeo-mCherry-loxP vector (#184). The resulting vector contains the meGFP-Smad1 fusion protein under control of a CMV-promoter, Xenopus beta-globin UTRs and miniTol2 recognition sites, enabling the generation of a stable cell line.

4.14 Plasmid preparation

For isolation and purification of the plasmid DNA from bacterial residuals, kits from Promega or Sigma-Aldrich (section 2.4) were used according to the manufacturer's instructions in the manuals.

4.15 total RNA isolation

The total RNA was isolated from all cell culture samples using the peqGOLD TriFast (PEQLAB) reagent and subsequent Phenol/Chloroform extraction.

Standard protocol

(1) Incubate for 5 min at RT
(2) Add 200µl Chloroform and invert for 15 sec
(3) Incubate 5 min at 4°C
(4) Centrifuge for 20 min at 4°C and maximum speed
(5) Remove upper phase and transfer it into a fresh Eppendorf tube
(6) Add 1µl Glycogen and 600µl ice-cold Isopropanol (100%)
(7) Incubate 20 min at -20°C
(8) Centrifuge for 20 min at 4°C and maximum speed
(9) Wash pellet with 1ml 70% ice-cold Ethanol

(10) Centrifuge 5 min at 4°C and maximum speed
(11) Remove and waste supernatant
(12) Dry pellet for 5 min at RT
(13) Dilute pellet in 20µl DEPC-treated water
(14) Incubate 10 min at 50-60°C
(15) Store at -70°C until use

4.16 In-vitro cDNA transcription

1-2µg total RNA were subjected to cDNA synthesis using the RevertAid™ First Strand cDNA synthesis kit (Fermentas) and random hexamer primers, according to the manufacturer's instructions. All samples were digested with DNAseI (Fermentas) for 1h to exclude gDNA contamination prior to cDNA synthesis reaction.

4.17 real-time PCR

Real-time PCR was performed on 25ng cDNA using primer pairs for EF1a, ID1, Smad6 and GLuc in single reactions using SYBR Green reagent (Cambrex Bioscience Rockland, Inc.). A standardized PCR was carried out using the following protocol:

Standard PCR reaction mix		2µl cDNA
		1x ReproFast reaction buffer
		400µM each dNTP
		0.15x SYBR green
		0.3µM each primer
		1.5U His-Taq DNA polymerase
		ad 25µl with dH_2O
Standard PCR cycler program		5 min, 95°C
	40 cycles	30 sec, 95°C (denaturation)
		30 sec, 55°C (annealing)
		20 sec, 72°C (elongation)
		10min, 72°C

The PCR products of the single primer pairs are of approximately the same size and have a similar melting point, enabling direct comparison of the amount of all examined transcripts. PCR values for each sample were determined from triplicates. For the quantification, the data were analyzed using the $2^{-\Delta\Delta ct}$ method. The fold change for the target genes were normalized to the housekeeping gene EF1a, and calculated relative to expression of the target genes in untreated cells. The results are averages from four independent experiments. Data were evaluated using Student's t-test.

4.18 Fluorescent staining of c2c12 cells

4.18.1 Immunofluorescence staining

The cells were seeded out on cover slips, treated as described in section 2.8.5 and subjected to the standard Immunofluorescence procedure.

Standard procedure

(1) Wash the cells twice with 1x PBS for 5 min
(2) Fix the cells with 4% PFA/1xPBS for 10 min at RT
(3) Wash the cells twice with 1x PBS for 5 min
(4) Block the cells for 10 min with 0.1M Glycin/1xPBS at RT
(5) Wash the cells with 1x PBS for 5 min
(6) Permeabilize the cells with 0.1% TritonX-100/1x PBS for 10 min at RT
(7) Wash the cells with 1x PBS for 5 min
(8) Block the cells with 5% BSA/1x PBS for 10 min at RT
(9) Wash the cells with 1x PBS for 5 min
(10) Add primary antibody and incubate for 1h at RT or over night at 4°C
(11) Wash twice with 1x PBS for 5 min
(12) Block the cells with 5% BSA/1x PBS for 10 min at RT
(13) Add appropriate secondary antibody and incubate for 1h at RT
(14) Wash twice with 1x PBS for 5 min
(15) Prepare a slide with Mowiol
(16) Drop the cover slip on the Mowiol, keep dark and let dry
(17) Store at 4°C until use

4.18.2 Cell membrane staining

The cell membranes were stained using the following protocol:

(1) Cells were fixed like described in section 2.18.1
(2) Add 1:5000 CellMask Orange/1x PBS (1µg/ml final) and incubate for 10 min at RT
(3) Wash at least five times with 1x PBS for 5 min to reduce background signal
(4) Prepare a slide with Mowiol
(5) Drop the cover slip on the Mowiol, keep dark and let dry
(6) Store at 4°C until use

This approach is also applicable after the Immunofluorescence procedure.

4.18.3 DNA staining with Hoechst 33342

The nuclei were stained according to the following protocol:

(1) Cells were fixed like described in section 2.18.1
(2) Add 1:10000 Hoechst33342/1x PBS and incubate for 5 min at RT
(3) Wash twice with 1x PBS for 5 min to reduce background signal
(4) Prepare a slide with Mowiol
(5) Drop the cover slip on the Mowiol, keep dark and let dry
(6) Store at 4°C until use

This procedure is also applicable after the Immunofluorescence technique.

4.19 Mathematical Analysis

The results from the Luciferase experiments were entered to the MATLAB software and transformed using the fft algorithm.

5. Results

5.1 Generation of the stable c2c12_BRE-Luc cell line

Luciferase enzymes are commonly used as reporter to assess the transcriptional activity of a special promoter of interest [162]. The Luciferase genes can be introduced transiently or stably into cell lines or organisms and the observation of biological processes can be conducted with luminometers or modified optical microscopes. For investigating the transcriptional activity of the BMP-signaling pathway, the gene of the secreted Gaussia Luciferase (GLuc) was cloned behind a published BMP-responsive element (BRE) [163]. This construct also contained an independent mCherry-Zeocin fusion protein for optical and chemical selection of stably transgenic cells. Both genes were flanked by miniTol2 recognition sites enabling the generation of a stable cell line by the Tol2 technology (Figure 5.1).

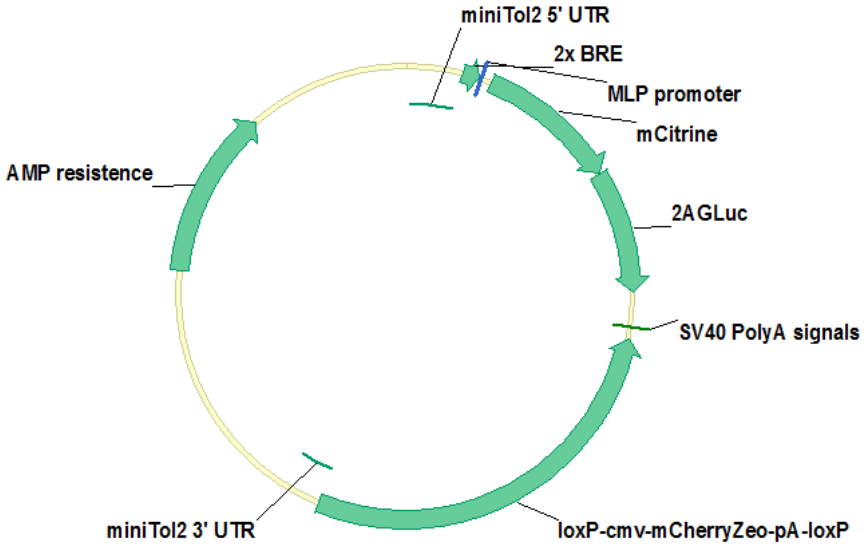

Fig. 5.1 Vector map of the reporter construct. The Gaussia Luciferase gene was cloned behind a BMP responsive element and the MLP promoter. Furthermore, it contains an independent mCherry-Zeocin fusion protein under control of a CMV-promoter. Both genes are flanked by miniTol2 recognition sites.

Four clones have been tested for the right function. Cells from every clone were stimulated with either 1nM BMP2 or without BMP2 as negative control and medium-samples were taken hourly for a time period over 8h. All four tested clones showed a similar pattern of the total Luciferase activity (Figure 5.2A) for the non-stimulated and stimulated situation. The black lines depict the non-stimulated control cells whereas the red lines show the stimulated cells. The Luciferase activity increased over time in both

cases, whereas the raw data for the stimulated cells are sharply higher. Clone A5 and clone A8 showed noticeable higher Luciferase activities than clones A1 and A2. Every clone has been found to be positive for the insert and this approach is applicable for assessing the transcriptional activity of the BMP-pathway.

Clone A5 and clone A8 were chosen for further test experiments over a longer time period and with a broader concentration range. Cells of both clones were seeded, stimulated with 0nM, 0.1nM, 1nM or 10nM BMP2 and medium samples were taken over 50h experiment time. Figure 5.2B shows the total Luciferase activities of both clones on the left, and the activity fold changes of the stimulated cells relative to the non-stimulated cells on the right side. The total data show an increase of the Luciferase activity for every stimulation concentration. Furthermore, it became apparent that after stimulation with 10nM BMP2 the Luciferase activity clearly increased compared to the other stimulation concentrations. The relative fold change data underlined this result.

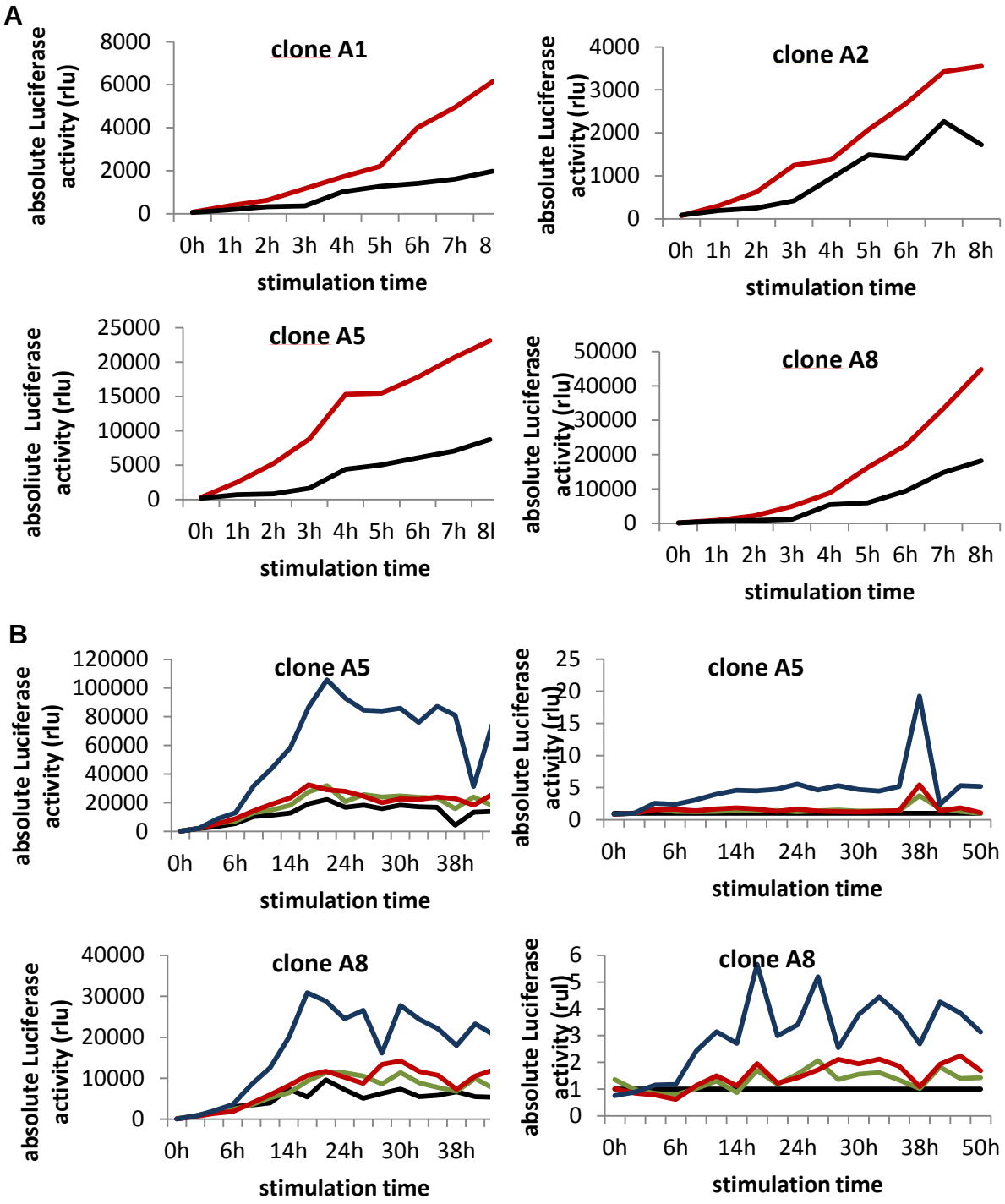

Fig. 5.2 Functional testing of individual clones. (A) Four clones were picked, expanded and tested for the correct Luciferase function. The cells were seeded, stimulated with 0nM (black lines) or 1nM BMP2 (red lines) and medium samples were taken hourly over 8h. The samples were measured utilizing a Luminometer and Coelenterazine as Luciferase substrate. (B) Two clones were seeded out and stimulated with 0nM (black), 0.1nM (green), 1nM (red) and 10nM (blue) BMP2. Medium samples were taken over 50h with two or four hourly intervals and measured using the Coelenterazine substrate. The left graphs depict the absolute Luciferase activity data for both clones and the right graphs show the fold changes, relative to the non-stimulated control cells.

The activity of the Gaussia Luciferase enzyme decreased to a baseline level, when incubated at 37°C for 1h [164]. This feature provided a fast response to stimulation and repression and yields an accurate kinetic and BMP2 concentration-dependent response. To ensure this property for the applied Luciferase during these experiments, it has been tested in a pilot experiment (Figure 5.3). In both cases, the non-stimulated and the stimulated situation, the samples incubated at 37°C for another hour (grey line and light blue line) were sharply lower and decreased to a background level compared to the samples that were immediately stored at 4°C (black line and dark blue line). This experiment proved this feature. Thus clone A8 of this stably transgenic cell line was decided to be used for gene expression experiments.

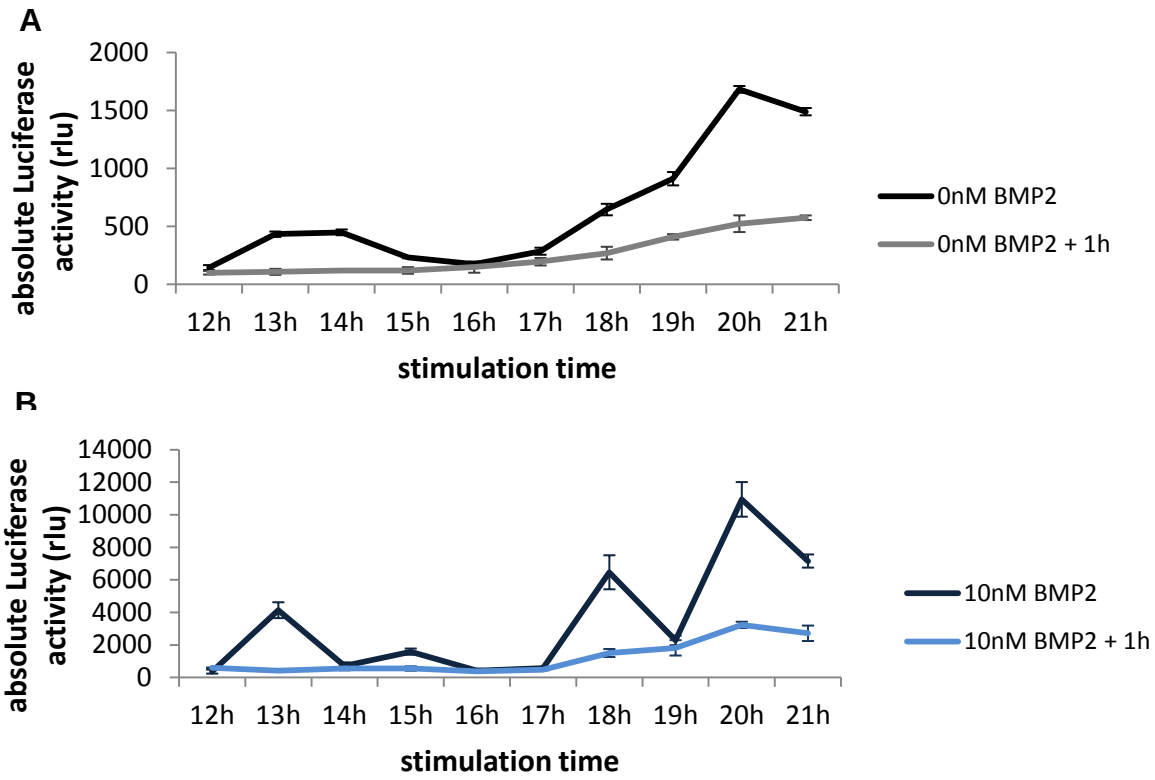

Fig. 5.3 Testing of the Luciferase activity decrease. The c2c12_BRE-Luc cells of clone A8 were seeded out and stimulated with (A) 0nM or (B) 10nM BMP2. After 12h stimulation time, 50µl from every well were removed twice every hour. One sample was stored at 4°C (black and dark blue lines) until the measurement and the other sample was incubated for one additional hour at 37°C (grey and light blue line) and then stored at 4°C until the measurement. All samples were measured on the same day with the same Coelenterazine-solution. The assigned values represent averages from independent triplets out of one experiment. (Figure modified from Schul et al. [172])

5.2 Gene expression analysis upon sustained stimulation with BMP2

In order to analyze the target gene expression induced by continuous stimulation with BMP2, two independent approaches with different read-outs were conducted. First, the

stably transgenic c2c12_BRE-Luc cell line was used to track the Luciferase's activity in every well and in real time as exact as possible. To verify the results of these experiments, qRT-PCR analyses were performed on well known BMP target genes.

5.2.1 Expression analysis utilizing the stable c2c12_BRE-Luc cells

The expression of the secreted Gaussia Luciferase was investigated for different BMP2-concentrations and over 4h prior to and 30h after stimulation. The transgenic cells were seeded, starved over night and stimulated with 0nM, 0.1nM, 1nM or 10nM BMP2. As expected, the absolute Luciferase activity showed an obvious dependency from the used concentrations (Figure 5.4). This result provided clear evidence for an efficient read-out system. The latency period at the beginning could possibly be attributed to the different molecular steps required until the Luciferase reaches the culture medium (RNA transcription, protein translation, secretion and folding).

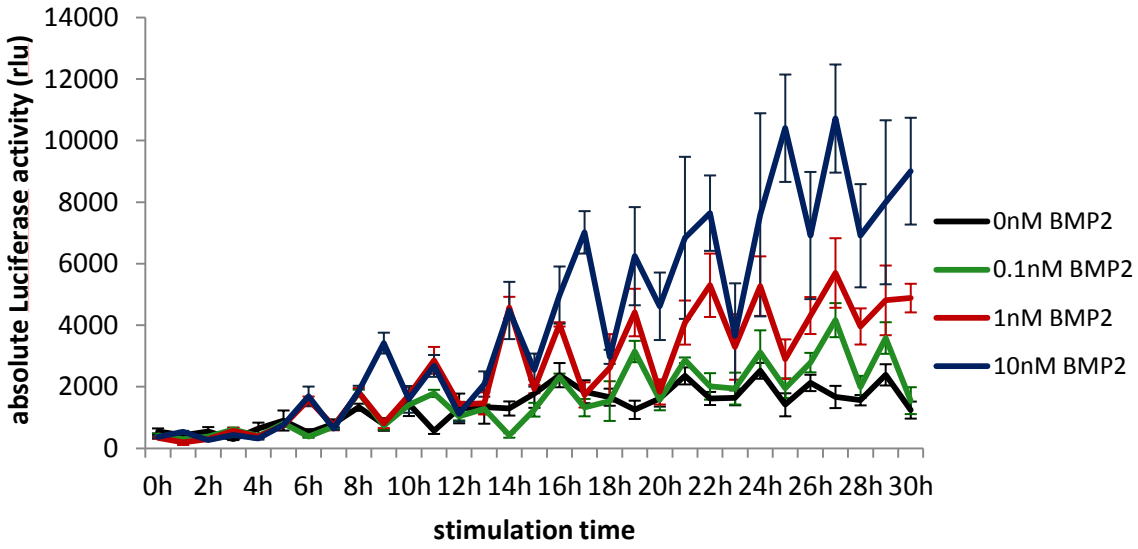

Fig. 5.4 Absolute Gaussia Luciferase activity as a result of continuous stimulation with different concentrations of BMP2. Cells of the stable c2c12_BRE-Luc cell line were seeded in 6-well plates and starved over night. On the following day, the cells were stimulated with 0nM (black), 0.1nM (green), 1nM (red) or 10nM (blue) BMP2. 50µl medium from every well were removed hourly and stored at 4°C until the measurement. All samples were measured on the same day with the same Coelenterazine-solution. The assigned values represent averages from independent triplet wells out of one experiment. (Figure modified from Schul et al. [172])

Enabling a better comparison between the different BMP2 concentrations and independent experiments, the activity fold change of the stimulated to the non-stimulated cells was calculated. Three independent 30h experiments were conducted and the results are depicted in Figure 5.5.

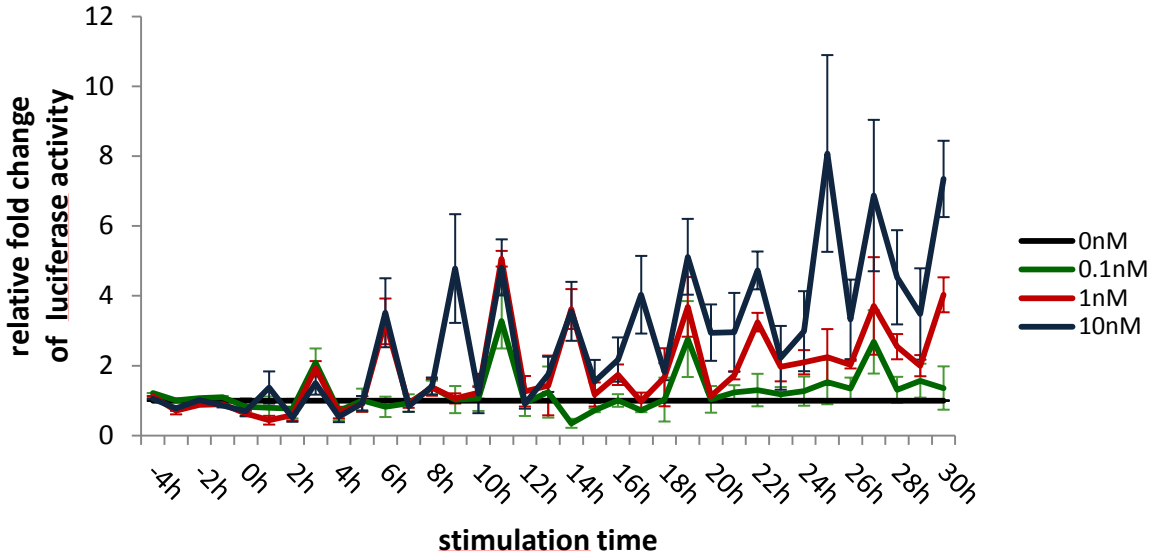
relative fold change of luciferase activity
12
10
8
6
4
2
0
-4h
-2h
0h
2h
4h
6h
8h
10h
12h
14h
16h
18h
20h
22h
24h
26h
28h
30h
stimulation time
0nM
0.1nM
1nM
10nM

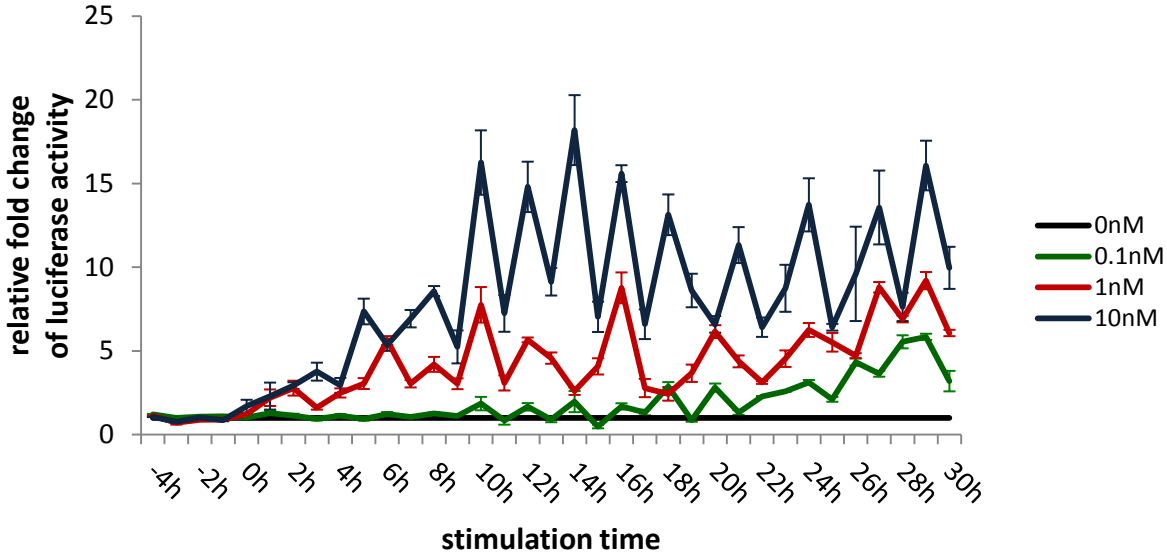
relative fold change of luciferase activity
25
20
15
10
5
0
-4h
-2h
0h
2h
4h
6h
8h
10h
12h
14h
16h
18h
20h
22h
24h
26h
28h
30h
stimulation time
0nM
0.1nM
1nM
10nM

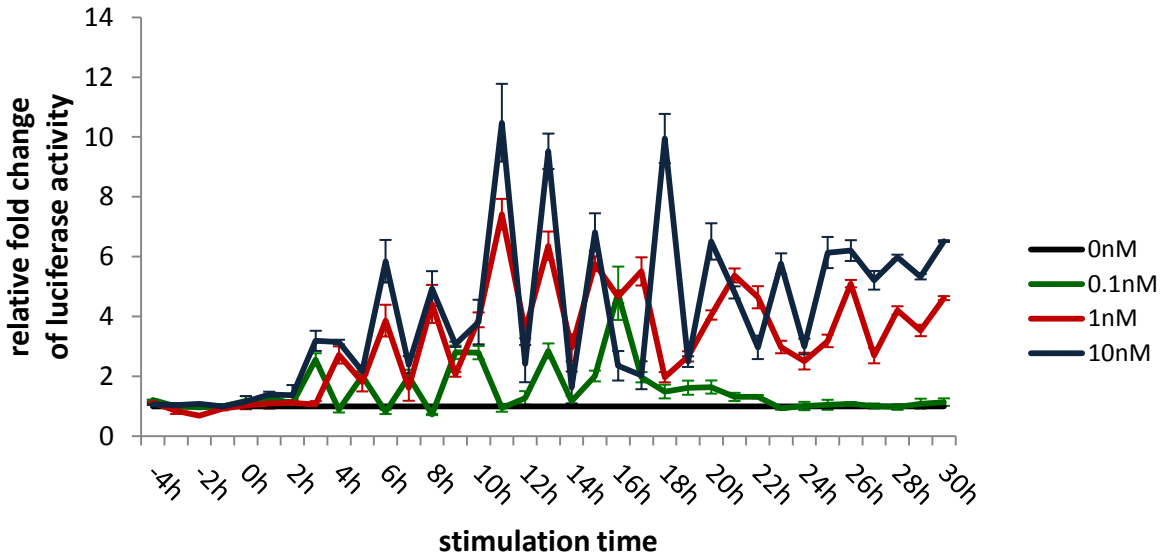
relative fold change of luciferase activity
14
12
10
8
6
4
2
0
-4h
-2h
0h
2h
4h
6h
8h
10h
12h
14h
16h
18h
20h
22h
24h
26h
28h
30h
stimulation time
0nM
0.1nM
1nM
10nM

Fig. 5.5 Three independent Gaussia Luciferase gene expression experiments. Results of three independent experiments over 30h experiment time and using the stable c2c12_BRE-Luc cell line. The cells were stimulated with 0nM (black), 0.1nM (green), 1nM (red) or 10nM (blue) BMP2, 50µl medium were removed every hour and the Luciferase activity was measured. The relative fold change to the non-stimulated control was calculated and assigned. (Figure modified from Schul et al. [172])

The data from the three biological independent experiments indicated a clear dependence of the cellular BMP-signaling response on the stimulation-concentration; the higher the concentration, the higher is the resulting Luciferase activity or the gene expression, respectively. Furthermore, significant oscillating progressions suggested gene expression pulses every second hour during continuous stimulation with BMP2, indicating a stimulation-time dependence. Interestingly, the frequencies of the activity bursts were similar for all tested ligand concentrations, however, the amplitudes showed a clear correlation with the corresponding BMP2-concentration used for stimulation.

5.2.2 Quantification of BMP target gene expression upon sustained stimulation

To verify the results from the Luciferase experiments with an independent experimental setup, qRT-PCR analyses were conducted on the well known BMP target genes *id1* and *smad6* as well as the housekeeping gene *ef1a*. Therefore, c2c12_BRE-Luc cells were seeded and stimulated with 0nM, 0.1nM or 1nM BMP2. The cells were harvested after different time points.

The results for *id1* showed an oscillating expression profile with a significant mRNA maximum after 1h for stimulation with 0.1nM and 1nM BMP2 and a subsequent significant decrease after 2h and 3h (Figure 5.6A). After 4h stimulation time, the *id1* mRNA level re-increased for both concentrations, but only the increase for 0.1nM BMP2 turned out to be significant. At later time points after stimulation, the mRNA expression pulses decreased gradually to a lower level of oscillations. The fold change maxima at later time points were still about 15 or 6, respectively.

The expression profile for *smad6* showed a similar oscillating expression pattern with a maximum at 2h stimulation time for 0.1nM and 1nM BMP2 (Figure 5.6B). Only 0.1nM BMP2 caused a significant increase of the mRNA amount. After 3h the *smad6* mRNA levels decreased significantly with both BMP2 concentrations and as previously observed for *id1*, the oscillation amplitudes decreased over time to a lower level.

Both endogenous targets were expressed over the whole time of the experiment, whereas the fold changes of *smad6* were generally lower than the expression levels of

id1. The fold changes of the non-stimulated controls, as expected, did not vary over time for both concentrations, suggesting that this read-out works successfully.

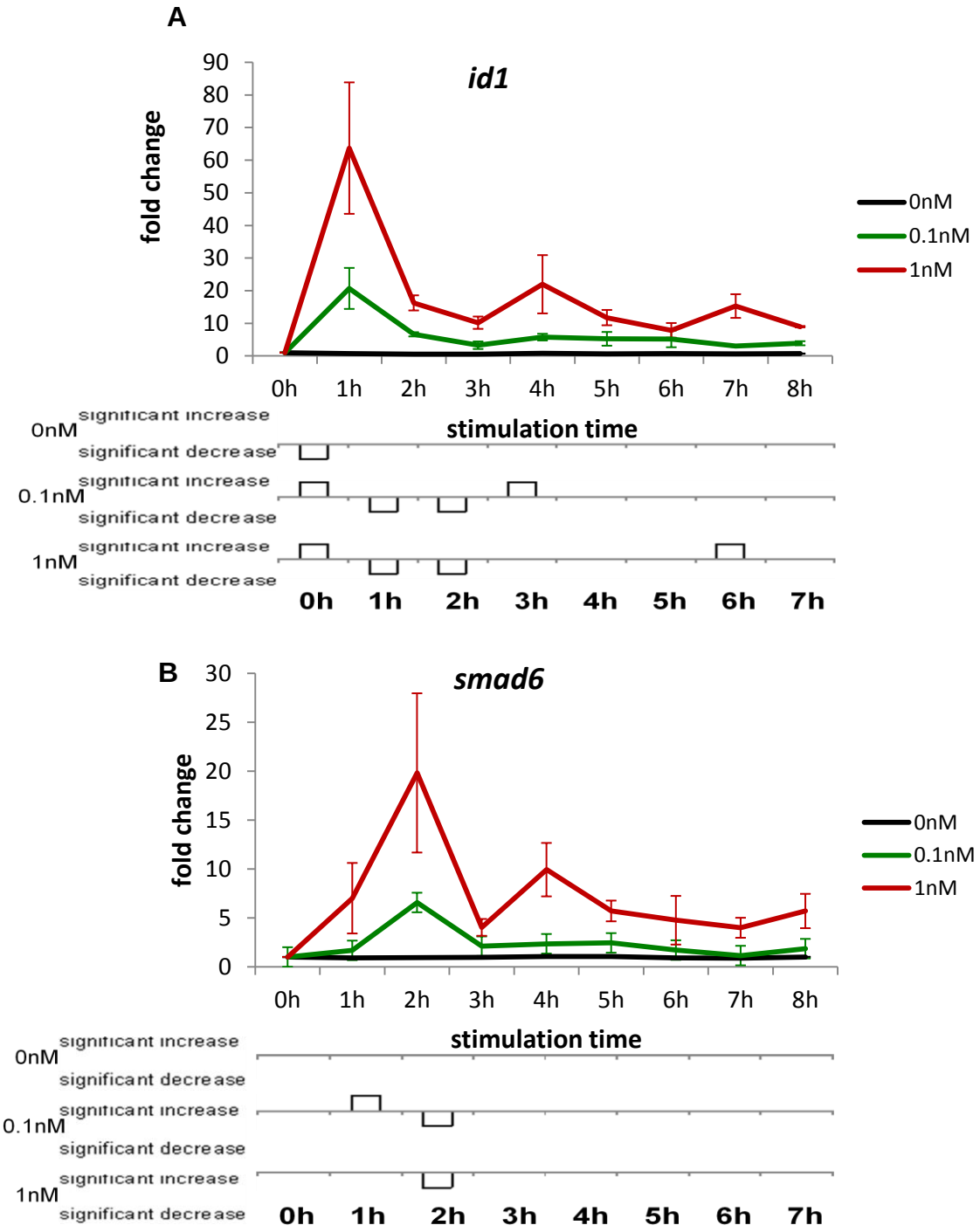

Fig. 5.6 Target gene expression after stimulation with different concentrations of BMP2. The cells were stimulated with 0nM (black), 0.1nM (green) or 1nM (red) BMP2 and every hour one sample was lysed and frozen at -80°C until the further processing. Quantitative real-time PCR was performed on the BMP target genes (A) *id1* and (B) *smad6* as well as the housekeeping gene *ef1a*. The relative fold change to the housekeeping gene was calculated and depicted. The PCR values were determined in triplicates for every cDNA. The depicted values are averages from four independent experiments. (Figure modified from Schul et al. [172])

To ensure that the maximum peaks at 1h or 2h, respectively, were indeed the highest mRNA levels after continuous stimulation with BMP2, the experiment was repeated at higher temporal resolution.

The cells were stimulated with either 0nM or 1nM BMP2 and every half hour one sample of both treatments were harvested over 4h experiment time. qPCR reactions were performed on *id1*, *smad6* and *ef1a* and the relative fold change of the target genes was assigned. Figure 5.7 shows the results of the higher temporal resolution experiment and confirmed that the maximum peaks of *id1* (A) and *smad6* (B) were indeed after 1h or 2h stimulation with 1nM BMP2. Furthermore, this experiment showed that the expression level of *id1* re-increases after 2.5h stimulation and not after 3h, as expected from the preceding lower resolute experiment and the *smad6* mRNA transcription re-increases after 3.5h and not after 3h stimulation time.

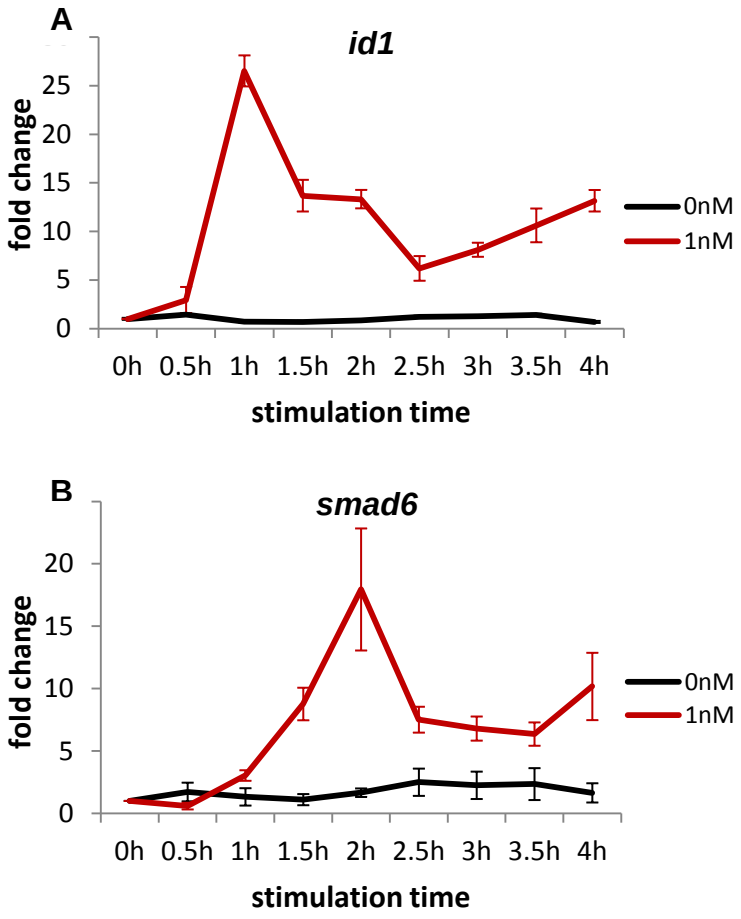

Fig. 5.7 Higher temporal resolution of the target gene curve progression. c2c12_BRE-Luc cells were seeded out and starved over night. Then the cells were stimulated with 0nM (black) or 1nM (red) BMP2 and harvested at the indicated time points after stimulation. qRT-PCR analysis of the BMP target genes (A) *id1* and (B) *smad6* as well as the housekeeping gene *ef1a* followed. The relative fold change to the housekeeping gene was calculated and depicted. This figure represents the average of two independent experiments. (Figure modified from Schul et al. [172])

In order to investigate the long-term gene expression, qPCR analysis was performed after 25h to 30h upon sustained stimulation. Figure 5.8 points out that the expression of both target genes was detectable until 30h after stimulation for every stimulation concentration. The gene expression patterns of both target genes revealed further oscillating progressions after 25h. The oscillation amplitudes of *id1* and *smad6* after 25h were comparable to the amplitudes after 4h stimulation. Additionally, the *id1* and *smad6* mRNA levels of the non-stimulated controls showed elevated levels after 25h to 30h compared to the mRNA levels for 0h until 8h stimulation time. This observation suggested a slight basal expression of both target genes.

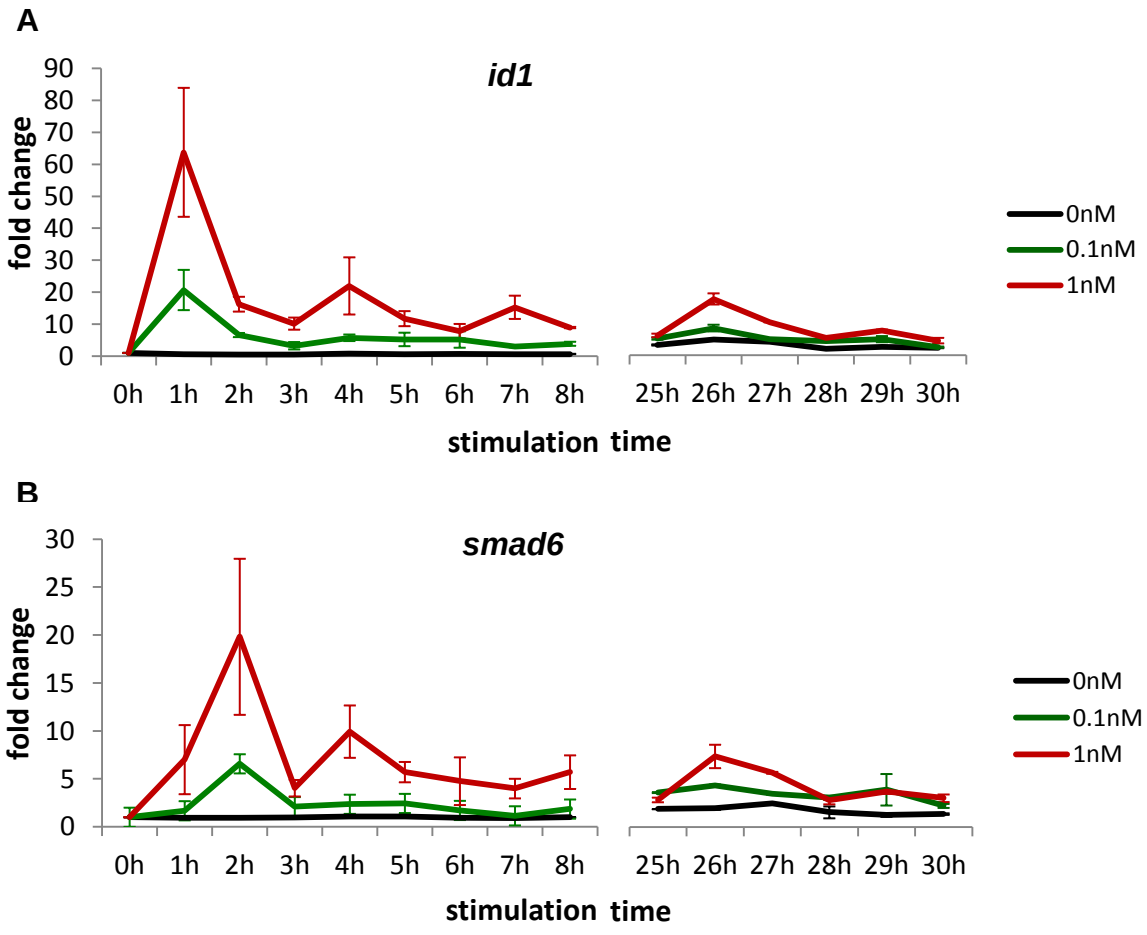

Fig. 5.8 Long-term analysis of BMP target gene transcription. c2c12_BRE-Luc cells were seeded stimulated with 0nM (black), 0.1nM (green) or 1nM (red) BMP2 and harvested at the indicated time points after stimulation. The qPCR anaylsis of the BMP target genes (A) *id1*, (B) *smad6* and the housekeeping gene *ef1a* followed. The relative fold change to the housekeeping gene was calculated and depicted. This figure represents the average of two independent experiments. (Figure modified from Schul et al. [172])

Table 5.1 Raw data out of two independent qRT-PCR experiments. (A) Triplet of ct-values from one experiment analyzing *ef1a* and *id1* after stimulation with 1nM BMP2. (B) Triplet of ct-values from one experiment analyzing *ef1a* and *smad6* after stimulation with 0.1nM BMP2. (Figure modified from Schul et al. [172])

A

	EF1a						ID1						
Sample	ct- value_1	ct- value_2	ct- value_3	standard deviation	average ct-value	D Ct_{EF1a} ctr.-sample	ct- value_1	ct- value_2	ct- value_3	standard deviation	Average ct-value	D Ct_{ID1} ctr.-sample	rel Ex act ($2^{D\ CtID1}$: $2^{D\ CtEF1a}$)
0h	24,04	24,20	24,03	0,10	24,09	0,00	23,55	23,59	23,51	0,04	23,55	0,00	**1,00**
1h	24,11	24,20	23,92	0,14	24,08	0,01	18,33	18,43	18,54	0,11	18,43	5,12	**34,38**
2h	24,73	24,47	24,62	0,13	24,61	-0,52	20,19	19,99	20,05	0,10	20,08	3,47	**15,89**
3h	24,85	24,89	24,73	0,08	24,82	-0,73	21,52	21,55	21,41	0,07	21,49	2,06	**6,92**
4h	24,41	24,56	24,53	0,08	24,50	-0,41	20,56	20,59	20,52	0,04	20,56	2,99	**10,58**
5h	24,02	23,98	23,95	0,04	23,98	0,11	20,40	20,29	20,24	0,08	20,31	3,24	**8,77**
6h	24,74	24,64	24,85	0,11	24,74	-0,65	22,00	22,12	22,06	0,06	22,06	1,49	**4,42**
7h	24,23	24,69	24,62	0,25	24,51	-0,42	20,73	20,81	20,79	0,04	20,78	2,77	**9,17**
8h	24,99	24,88	24,74	0,13	24,87	-0,78	21,17	21,13	21,04	0,07	21,11	2,44	**9,30**

B

	EF1a						Smad6						
Sample	ct- value_1	ct- value_2	ct- value_3	standard deviation	average ct-value	D Ct_{EF1a} ctr.-sample	ct- value_1	ct- value_2	ct- value_3	standard deviation	Average ct-value	D Ct_{smad6} ctr.-sample	rel Ex act ($2^{D\ Ct\ smad6.}$: $2^{D\ CtEF1a}$)
0h	23,91	24,02	23,93	0,06	23,95	0,00	29,33	29,78	29,99	0,34	29,70	0,00	**1,00**
1h	24,30	24,30	24,29	0,01	24,30	-0,34	29,44	29,32	29,24	0,10	29,33	0,37	**1,64**
2h	24,10	24,14	23,97	0,09	24,07	-0,12	27,76	27,34	27,40	0,23	27,50	2,20	**4,98**
3h	24,16	23,87	24,08	0,15	24,04	-0,08	29,34	28,88	29,07	0,23	29,10	0,60	**1,61**
4h	24,18	24,01	24,43	0,21	24,21	-0,25	28,14	28,50	28,91	0,39	28,52	1,18	**2,71**
5h	24,78	24,53	24,42	0,18	24,58	-1,62	27,82	28,90	28,70	0,57	28,47	0,23	**3,61**
6h	24,60	24,90	23,58	0,69	24,36	-0,41	30,01	28,56	28,84	0,77	29,14	0,56	**1,96**
7h	24,47	24,53	24,15	0,20	24,38	-0,43	29,57	29,55	29,29	0,16	29,47	0,23	**1,58**
8h	25,04	25,28	25,11	0,12	25,14	-1,19	29,71	29,66	29,88	0,12	29,75	-0,05	**2,20**

Table 5.1 points out, that the expression level oscillations directly reflected changes of the target gene levels, not changes of the used associated housekeeping gene levels. The depicted tables contain the raw data of two single and independent qPCR experiments for analyzing the expression levels of *id1* after stimulation with 1nM BMP2 and *smad6* after stimulation with 0.1nM BMP2. The columns colored in blue show the ct-value triplicates of the housekeeping gene *ef1a*, whereas the red colored columns

include the ct-triplicates of the target genes. The ct-values of *ef1a* are around 24 for every time point and the standard deviation of the triplicates is 0.25 at most, with one exception. These data emphasized the claim that the oscillating patterns are attributed to a real oscillating target gene expression.

5.3 Gene expression experiments after short time stimulation with BMP2

The preceding experiments indicated that sustained stimulation with BMP2 leads to continuous and oscillatory gene expression profiles of the immediate target genes *id1* and *smad6*. A recent study revealed that the duration of stimulation is critical for the cellular response [165]. To better understand the signaling dynamics and the critical parameters, I analyzed the cellular response to a short time receptor stimulus of only 15 minutes. Instead of keeping the stimulation medium on the cells until the end of the experiment, it has been replaced with basal DMEM medium after 15 minutes stimulation time (wash-away treatment).

5.3.1 c2c12_BRE-Luc cellular response to short-time receptor stimulus

As described previously, the stably transgenic cells were seeded, starved over night and stimulated with 0nM, 0.1nM, 1nM or 10nM BMP2. After 15 minutes, the stimulation medium was removed and the cells were washed using a series of PBS and DMEM medium washes. Then fresh DMEM was given to the cells and medium samples, containing the secreted Gaussia Luciferase, were taken hourly over a time period of 4h prior to and 30h after stimulation.

Figure 5.9 illustrates that the Luciferase activity induced by 0.1nM, 1nM and 10nM BMP2 in case of the short-time stimulation led to an activity pattern similar to that seen during the continuous treatment. As observed in the continuous stimulation experiments, the relative Luciferase activity showed a clear positive correlation to the BMP2 concentration as well as time dependence. Furthermore, the fold change of the Gaussia Luciferase activity depicted an oscillating curve progression with fast and significant increasing and decreasing trends almost every second hour. As seen before for the sustained stimulation, the short-term stimulation resulted in equal oscillation frequencies for the different BMP2 concentrations. However, the fold changes of the Luciferase activities were lower for 15 minutes stimulation than for continuous treatment.

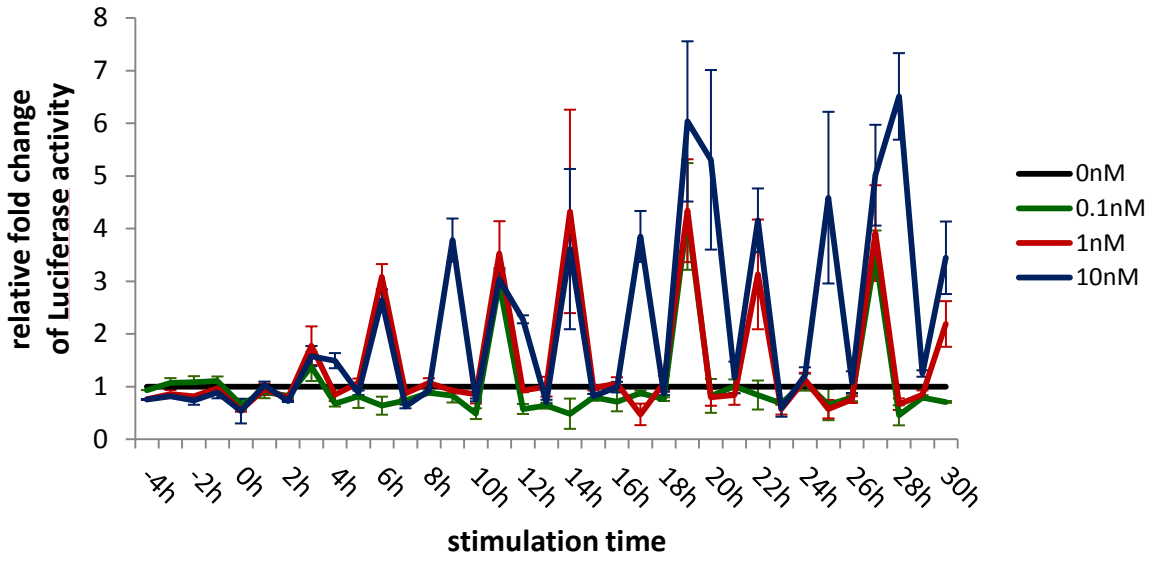
relative fold change of Luciferase activity
0
1
2
3
4
5
6
7
8
-4h
-2h
0h
2h
4h
6h
8h
10h
12h
14h
16h
18h
20h
22h
24h
26h
28h
30h
stimulation time
0nM
0.1nM
1nM
10nM

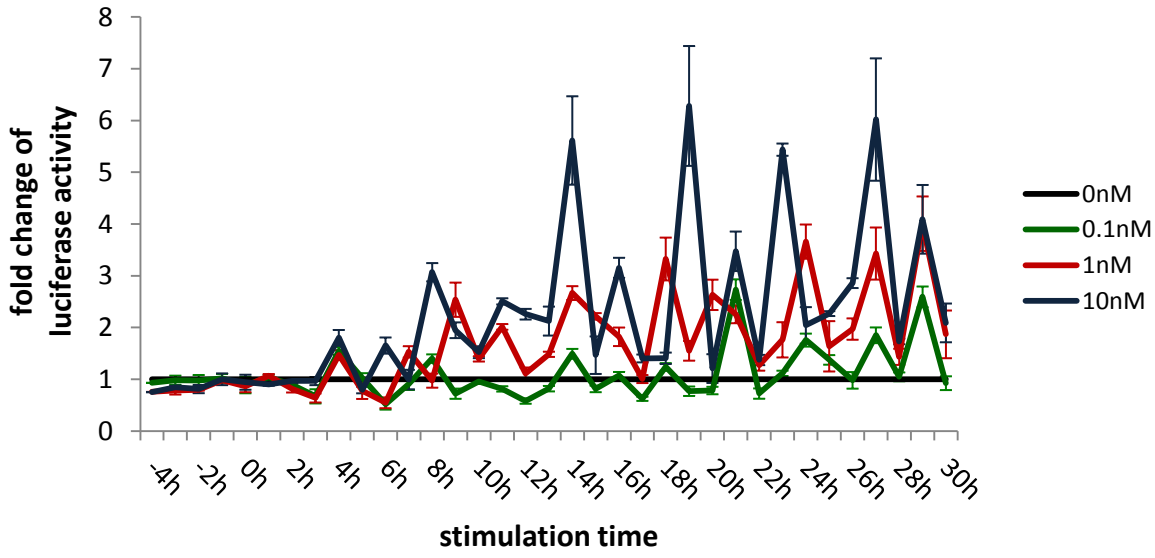
fold change of luciferase activity
0
1
2
3
4
5
6
7
8
-4h
-2h
0h
2h
4h
6h
8h
10h
12h
14h
16h
18h
20h
22h
24h
26h
28h
30h
stimulation time
0nM
0.1nM
1nM
10nM

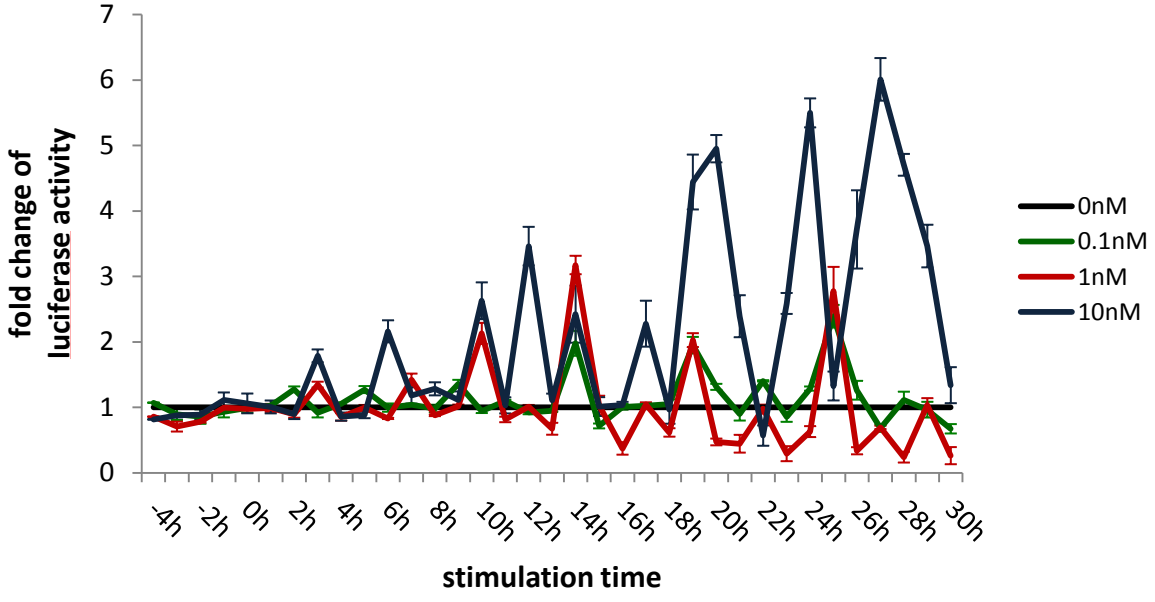
fold change of luciferase activity
0
1
2
3
4
5
6
7
-4h
-2h
0h
2h
4h
6h
8h
10h
12h
14h
16h
18h
20h
22h
24h
26h
28h
30h
stimulation time
0nM
0.1nM
1nM
10nM

Fig. 5.9 Three independent Gaussia Luciferase gene expression experiments after short-time receptor stimulation. Results of three independent experiments over 30h time and using the stable c2c12_BRE-Luc cell line. The cells were stimulated with 0nM (black), 0.1nM (green), 1nM (red) or 10nM (blue) BMP2 and after 15 minutes stimulation time, the medium containing BMP2 was removed, the cells were washed thoroughly, twice with PBS and twice with fresh medium, and then pure DMEM was given to the cells until the end of the experiment. 50µl medium were removed every hour and the Luciferase activity was measured. The relative fold change to the non-stimulated control was calculated and assigned. (Figure modified from Schul et al. [172])

5.3.2 Target gene expression analysis upon short-time receptor stimulation

The results of the Luciferase experiments were verified by qRT-PCR analyses of the BMP target genes *id1* and *smad6* as well as the housekeeping gene *ef1a*. The stably transgenic c2c12_BRE-Luc cells were seeded out and stimulated with 0nM, 0.1nM or 1nM BMP2 for 15 minutes and the stimulation medium was exchanged for fresh DMEM. The cells were harvested hourly for the following procedures.

Figure 5.10 depicts the results of these experiments and clearly demonstrates that 15 minutes receptor activation is sufficient to drive target gene expression for at least 8h and for 0.1nM and 1nM BMP2. As found for the continuous treatment, an oscillating transcription pattern also emerged for the short-time stimulation. The oscillation frequencies were equal for both BMP2 concentrations; however, the amplitudes were dependent on the stimulation concentration.

The significant maximum peaks for *id1* were exactly the same as for the sustained stimulation with both concentrations, even the significant decreases were at accurately the same time points. Solely the fold changes were at lower levels as against the sustained treatment. The same applied for the comparison for the *smad6* mRNA levels between the two treatments.

In conclusion, the Luciferase experiment and the endogenous target gene analysis underlined that short-time receptor stimulation of 15 minutes with BMP2, independent of the ligand concentration, is sufficient to drive gene expression in the same fashion as the continuous stimulation, except for the lower expression level.

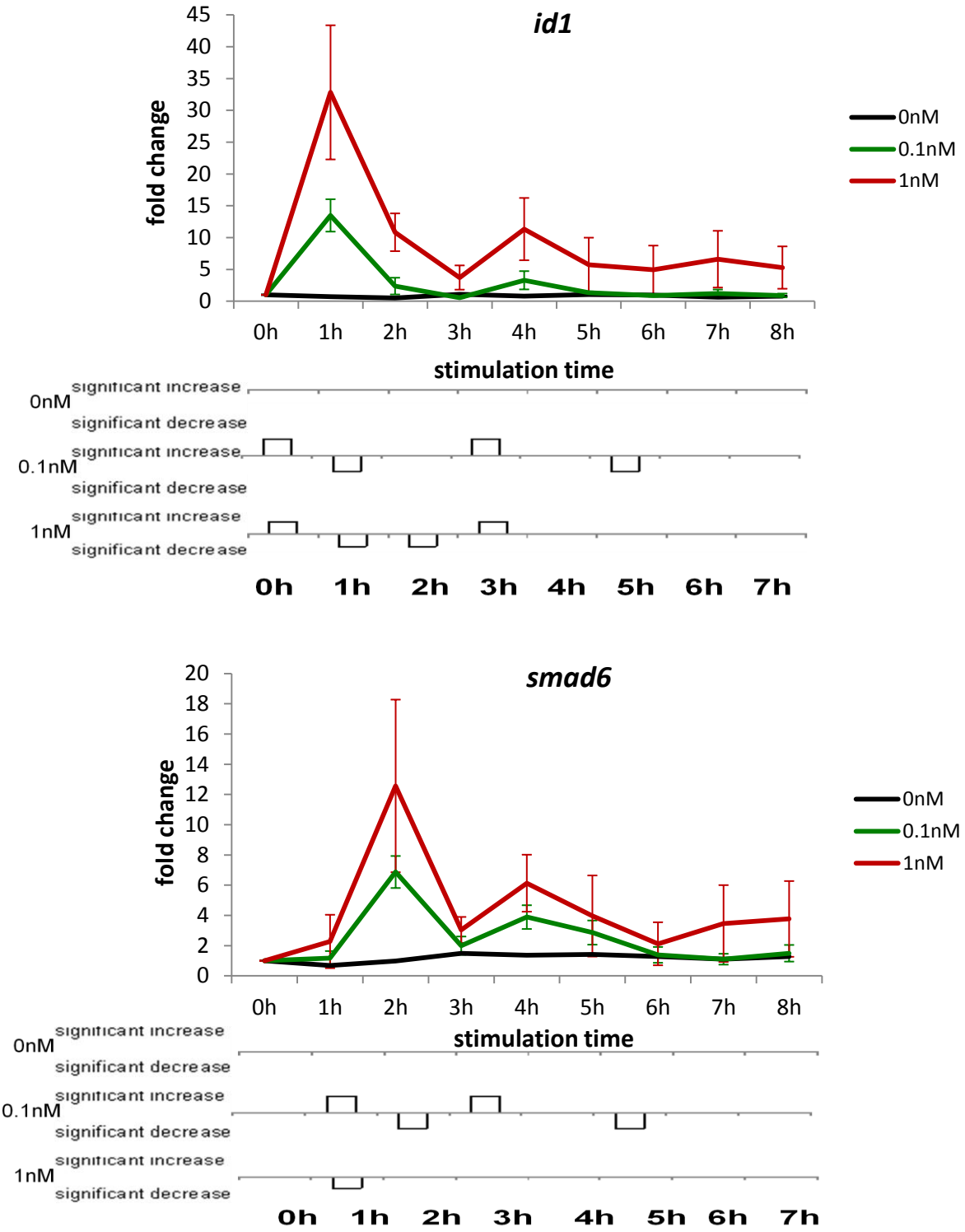

Fig. 5.10 Target gene expression analysis after short-time stimulation with different BMP2-concentrations. The cells were stimulated with 0nM (black), 0.1nM (green) or 1nM (red) BMP2 and after 15 minutes the stimulation medium was removed. Every hour one sample for every concentration was lysed and frozen at -80°C until the further processing. Quantitative real-time PCR was performed on the BMP target genes (A) *id1* and (B) *smad6* as well as the housekeeping gene *ef1a*. The relative fold change to the housekeeping gene was calculated and depicted. The PCR values were determined in triplicates for every cDNA. The depicted values are averages from four independent experiments. (Figure modified from Schul et al. [172])

5.4 Gene expression after short-time Smad phosphorylation

Short-time receptor stimulation was sufficient to activate target gene expression for as long as continuous stimulation. To examine the influence of the receptor kinase on this mechanism, I next examined how the gene expression profile changed when the receptor kinase was inhibited and no further Smad-proteins could be activated. The Luciferase experiments as well as the qRT-PCR experiment were repeated as previously described and modified by adding the BMP receptor type I kinase inhibitor Dorsomorphin directly to the cell culture medium after 15 minutes stimulation time.

5.4.1 c2c12_BRE-Luc response to 15 minute Smad-activation

The stably transgenic cells were stimulated with BMP2, Dorsomorphin was administrated to the cells 15 minutes post stimulation and the 30h Luciferase assay was performed.

The relative Luciferase activities out of the three biologically independent experiments are depicted in Figure 5.11. Compared to the two other cell treatments, these experiments again show an oscillatory pattern, but decreased activity fold changes. The activity fold changes of the other treatments were at least 10fold or 6fold, respectively, whereas after the Dorsomorphin treatment the activities were 4fold on an average. Furthermore, the clear concentration-dependence could not be detected any more. The fold changes for the 1nM and 10nM stimulation were approximately the same in all experiments, but stimulation with 0.1nM BMP2 again led to a lower activity fold change than 1nM or 10nM.

During the continuous and the wash-away treatment, stimulation with BMP2 led to a measurable Luciferase activity for the whole 30h experiment time. In contrast, the Dorsomorphin treatment led to a complete termination of the Luciferase activity after 12h stimulation time in the three independent experiments.

In summary, the inhibition of the receptor kinase led to decreased Luciferase activity levels and its complete breakdown. Interestingly, the oscillating progression could be observed until 12h post-stimulation although Smad-phosphorylation was inhibited after 15’ stimulation time. Furthermore, the Luciferase activity suddenly broke off instead of getting down regulated.

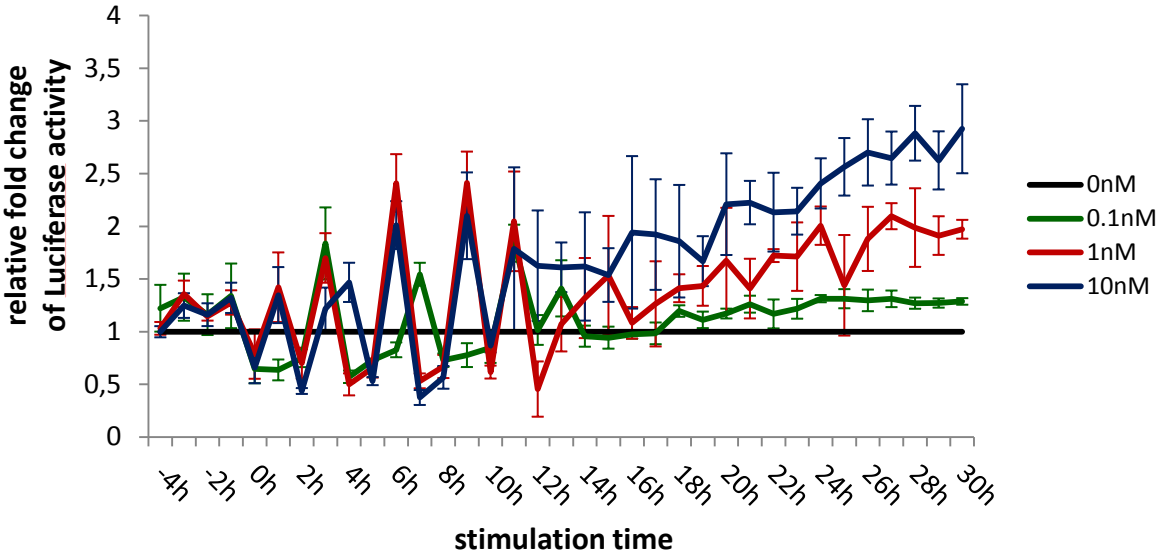
relative fold change of Luciferase activity
4
3,5
3
2,5
2
1,5
1
0,5
0
-4h
-2h
0h
2h
4h
6h
8h
10h
12h
14h
16h
18h
20h
22h
24h
26h
28h
30h
stimulation time
0nM
0.1nM
1nM
10nM

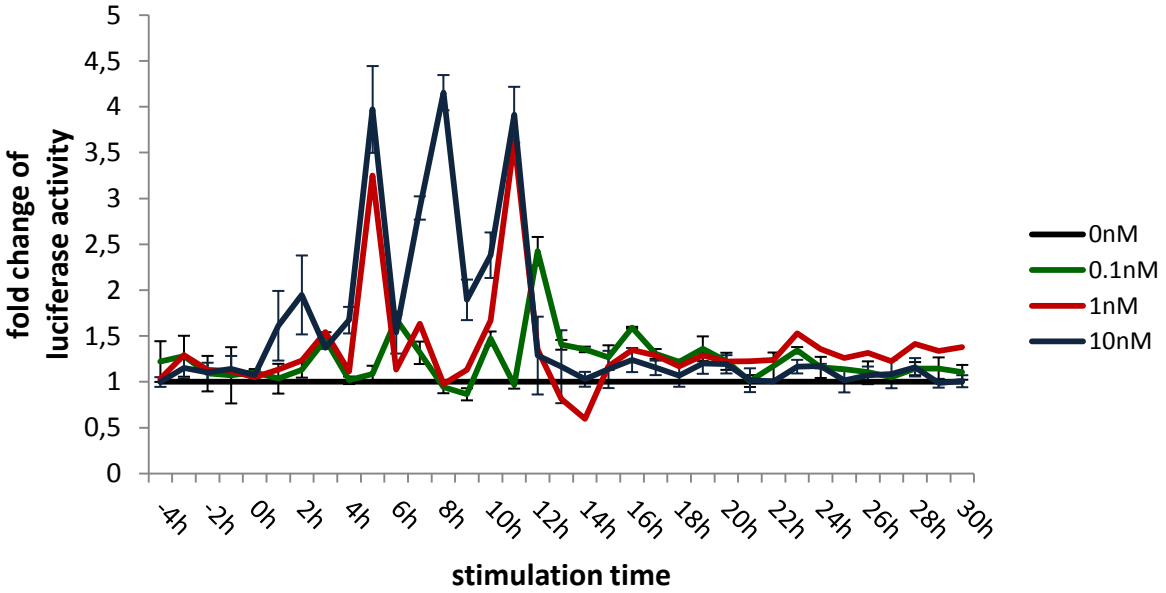
fold change of luciferase activity
5
4,5
4
3,5
3
2,5
2
1,5
1
0,5
0
-4h
-2h
0h
2h
4h
6h
8h
10h
12h
14h
16h
18h
20h
22h
24h
26h
28h
30h
stimulation time
0nM
0.1nM
1nM
10nM

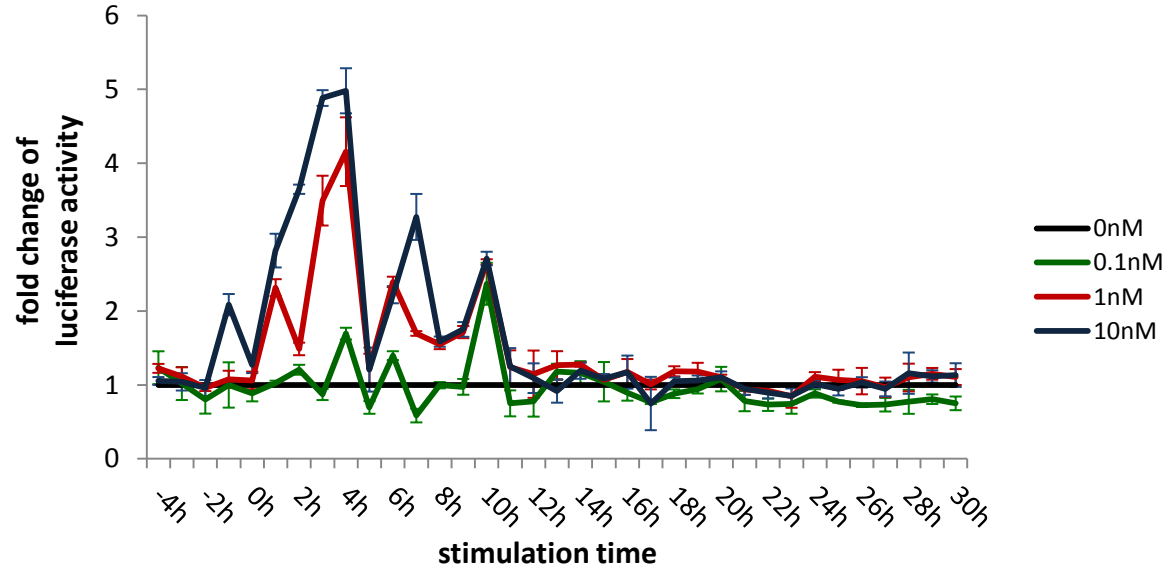
fold change of luciferase activity
6
5
4
3
2
1
0
-4h
-2h
0h
2h
4h
6h
8h
10h
12h
14h
16h
18h
20h
22h
24h
26h
28h
30h
stimulation time
0nM
0.1nM
1nM
10nM

Fig. 5.11 Three independent Gaussia Luciferase gene expression experiments after 15 minute Smad-activation. Results of three independent experiments over 30h and using the stable c2c12_BRE-Luc cell line. The cells were stimulated with 0nM (black), 0.1nM (green), 1nM (red) or 10nM (blue) BMP2 and after 15 minutes stimulation time, 10µM Dorsomorphin were added to the cell culture medium. 50µl medium were removed every hour and the Luciferase activity of all samples were measured on the same day and using the same Coelenterazine solution. The relative fold change to the non-stimulated control was calculated and depicted. (Figure modified from Schul et al. [172])

5.4.2 Real-time analysis of *id1* and *smad6* expression after short term Smad-activation

The corresponding quantitative PCR experiments also suggested reduced levels as well as the total breakdown of gene expression after treatment with Dorsomorphin.

For the endogenous expression of *id1*, Figure 5.12 shows that target gene expression is significantly upregulated after 1h stimulation-time with 1nM BMP2, but already 2h after stimulation it was significantly downregulated to a level beneath the basal level. In contrast, cells stimulated with 0.1nM BMP2 and the control cells showed an immediate and significant downregulation of *id1* expression after 1h. This result strengthened the fact for the concentration-dependence of the cellular response.

The *smad6* expression level was significantly downregulated for every tested ligand concentration after 1h.

These data indicated that the half-life time of the receptor-kinase activity is 0.5h. Furthermore they suggest a basal target gene transcription level or Smad phosphorylation activity, respectively, that also gets abandoned by the Dorsomorphin treatment.

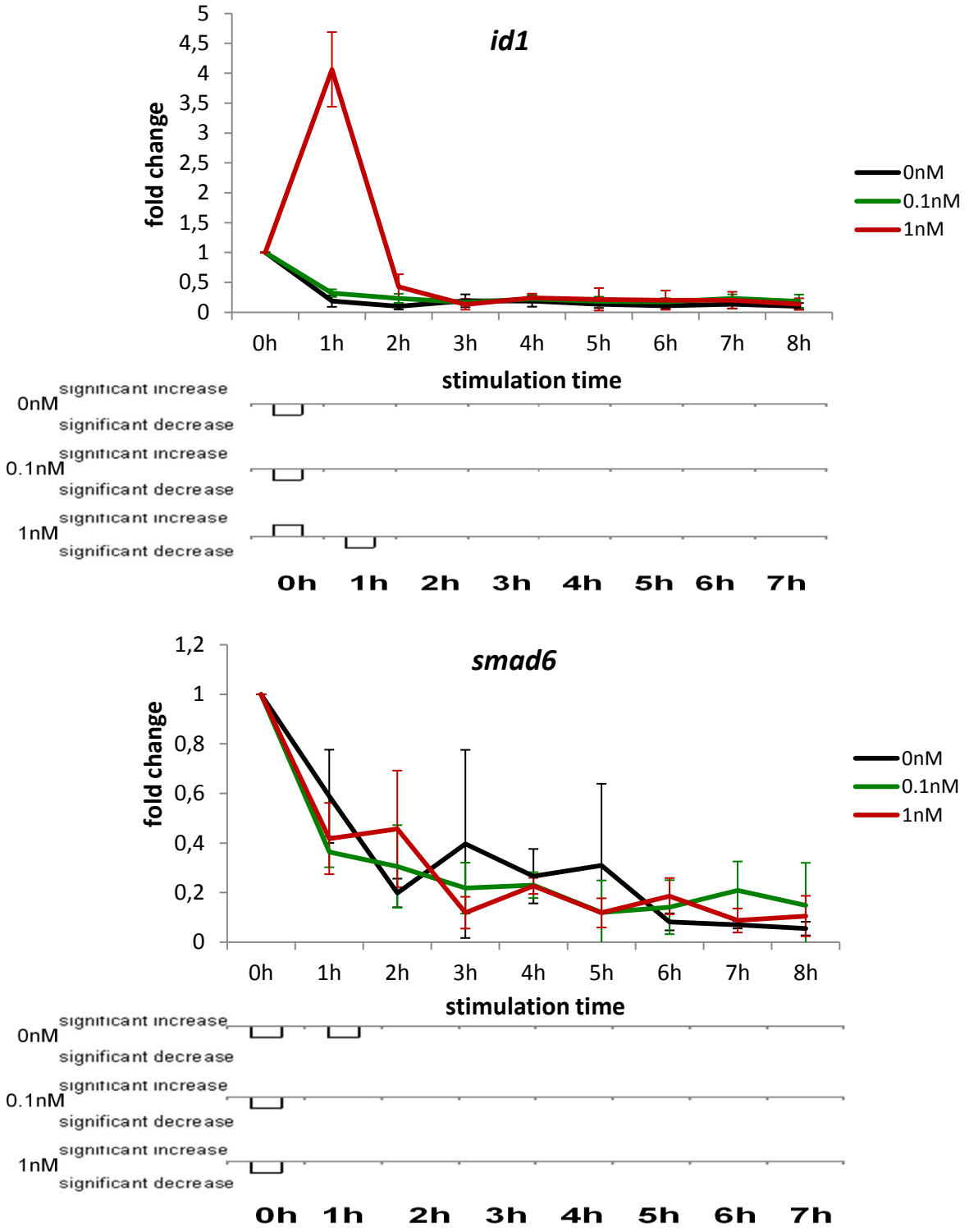

Fig. 5.12 Target gene expression analysis after 15 minutes Smad-activation. The cells were stimulated with 0nM (black), 0.1nM (green) or 1nM (red) BMP2 and after 15 minutes stimulation time, 10µM Dorsomorphin was administrated to the cell culture medium. Every hour samples for both concentrations were lysed and frozen at -80°C. After mRNA isolation and cDNA synthesis quantitative real-time PCR was performed on the BMP target genes (A) *id1* and (B) *smad6* as well as the housekeeping gene *ef1a*. The relative fold change to the housekeeping gene was calculated and depicted. The PCR values were determined in triplicates for every cDNA. The depicted values are averages from four independent experiments. (Figure modified from Schul et al. [172])

5.5 Fast Fourier Transformation

The gene expression experiments revealed that continuous as well as short-time receptor stimulation results in sustainable and oscillating cellular responses, whereas short-time Smad activation leads to abbreviated and decreased responses.

Next, I focused on identifying components of the detected oscillation patterns of the three treatments. Therefore, the absolute activity results of the Luciferase experiments were studied with a mathematical method. Figure 5.13 shows the results of a Fast Fourier Transformations (FFT) of the absolute Luciferase activities of the three different cell treatments. Interestingly, the plots of the continuous and the short-term receptor stimulus treatments showed the same prominent oscillation components (Fig. 5.13A and B). Both share the same slow oscillation with a 31 h frequency which appeared to be concentration dependent, as the amplitudes riseed with higher ligand concentrations. Moreover, at about 16 h/cycle was an oscillation progression that increased in proportion to the ligand amount in the case of the continuous stimulation, but it was inversely proportional with the short-time treatment. Two more curves at about 10.5 and 2.8 h/cycle were in proportion to the BMP2 concentration in both cases. Finally, another interesting wave can be seen at 2.5 h/cycle, which is proportional to the ligand concentration for the continuous stimulation and for the short receptor stimulus treatment. On the contrary to these two treatments is the treatment with the receptor kinase inhibitor (Fig. 5.13C). Here only one distinctive oscillation at 31 h/cycle could be identified, suggesting that different components of the signaling pathway contribute to the overall oscillatory behaviour.

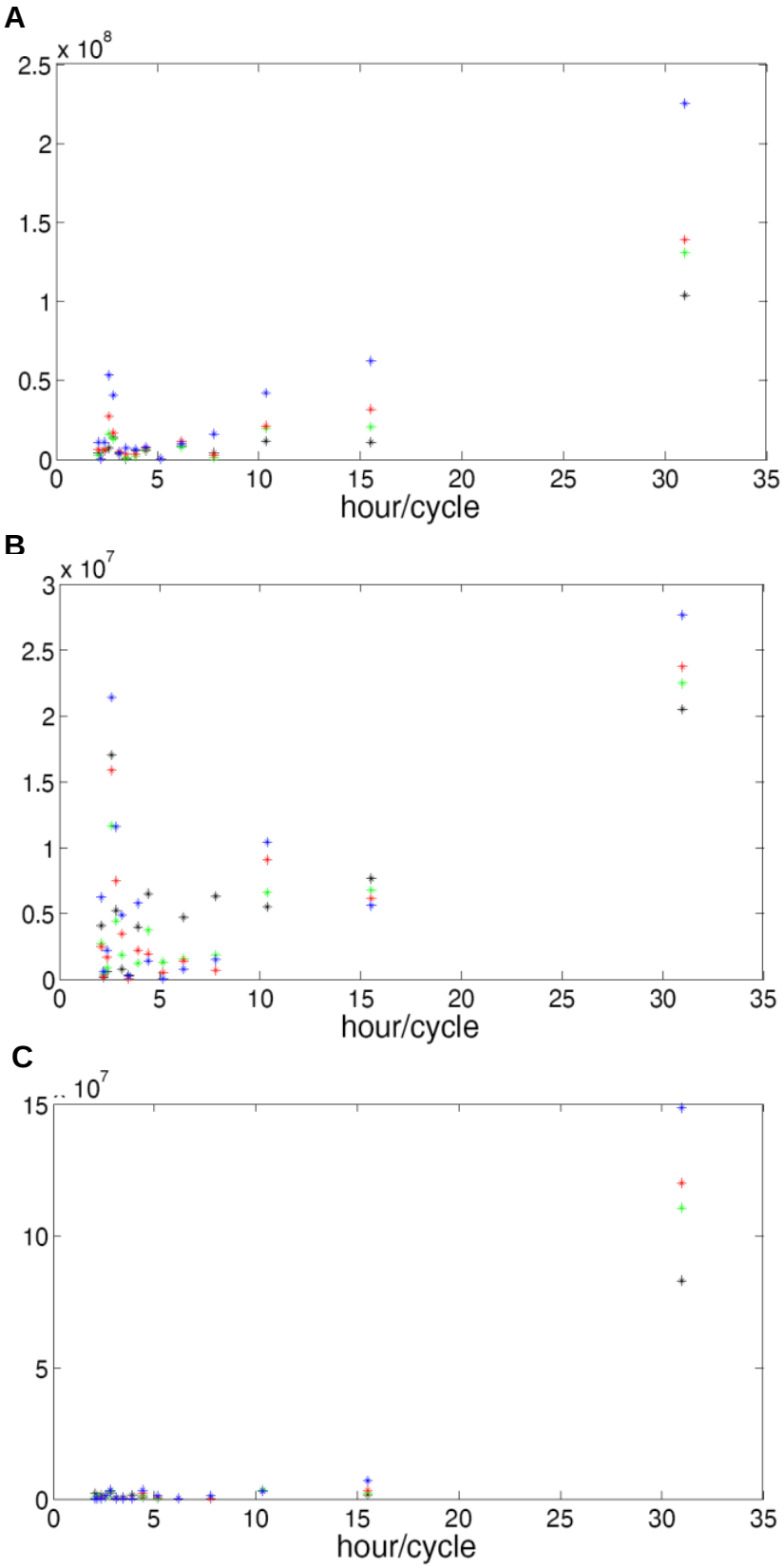

Fig. 5.13 Fast Fourier Transformation (FFT) of the absolute Luciferase data. The absolute values of one representative Gaussia Luciferase experiment triplet were entered to the MATLAB software and transformed utilizing the “fft” comand. During the experimental approach, the cells were stimulated with 0nM (black), 0.1nM (green), 1nM (red) and 10nM (blue). (A) FFT of the continuous stimulation experiment. (B) FFT of the 15 minute receptor stimulation. (C) FFT of 15 minute Smad-activation. (Figure modified from Schul et al. [172])

5.6 Spatio-temporal investigation of Smad1 after stimulation with BMP2

5.6.1 Anaylsis of Smad1 subcellular distribution using immunofluorescence

To identify the subcellular localization of Smad1 under non-stimulated and stimulated conditions, c2c12 wildtype cells were seeded and stimulated with 0nM, 0.1nM or 1nM BMP2 and fixed after the indicated time points. After that, indirect immunofluorescence staining using primary anti-Smad1 and secondary Alexa488 antibodies was performed. For the determination of the Smad1 amounts in the nucleus and the cytoplasm respectively, the cell membranes and the nuclei were further stained with specific dyes.
Figure 5.14C shows the immunofluorescent staining of the non-stimulated control cells. After 0min, 30min and 1h Smad1 was predominantly located in the cytoplasm. But after 1.5h and 2h the Smad1 protein seemed to be equally distributed within the whole cell.
For the stimulation with 0.1nM (B) and 1nM BMP2 (A) the Smad1 location was similar to the control cells for all time points. One exception seemed to appear for 0.1nM and 1nM BMP2 and for 1.5h stimulation time. For these two cases, Smad1 was predominantly located in the nuclei.
In order to confirm this visual observation, the nuclear/cytoplasmic ratio of Smad1 was calculated and illustrated. Therefore, a 3D-Analysis of the confocal stacks was conducted using the Volocity 3D image analysis software. Figure 5.15 supports the optically received results. There is no obvious and statistically significant difference between the non-stimulated and the stimulated cells concerning the subcellular Smad1 distribution. But this graphic is also a hint for a basal Smad1 shuttling between the nucleus and the cytoplasm.
Confocal stacks and optical analysis of these stainings hypothesized nuclear accumulation of Smad1 after 1.5h stimulation with 0.1 and 1nM BMP. But statistical analysis of the raw data revealed no significant difference in Smad1 subcellular localization upon ligand stimulation with neither 0.1nM nor 1nM BMP2 over 2h (Figs. 5.14 and 5.15). Instead both, the non-stimulated as well as the stimulated cells showed a nucleocytoplasmic shuttling behavior of Smad1.

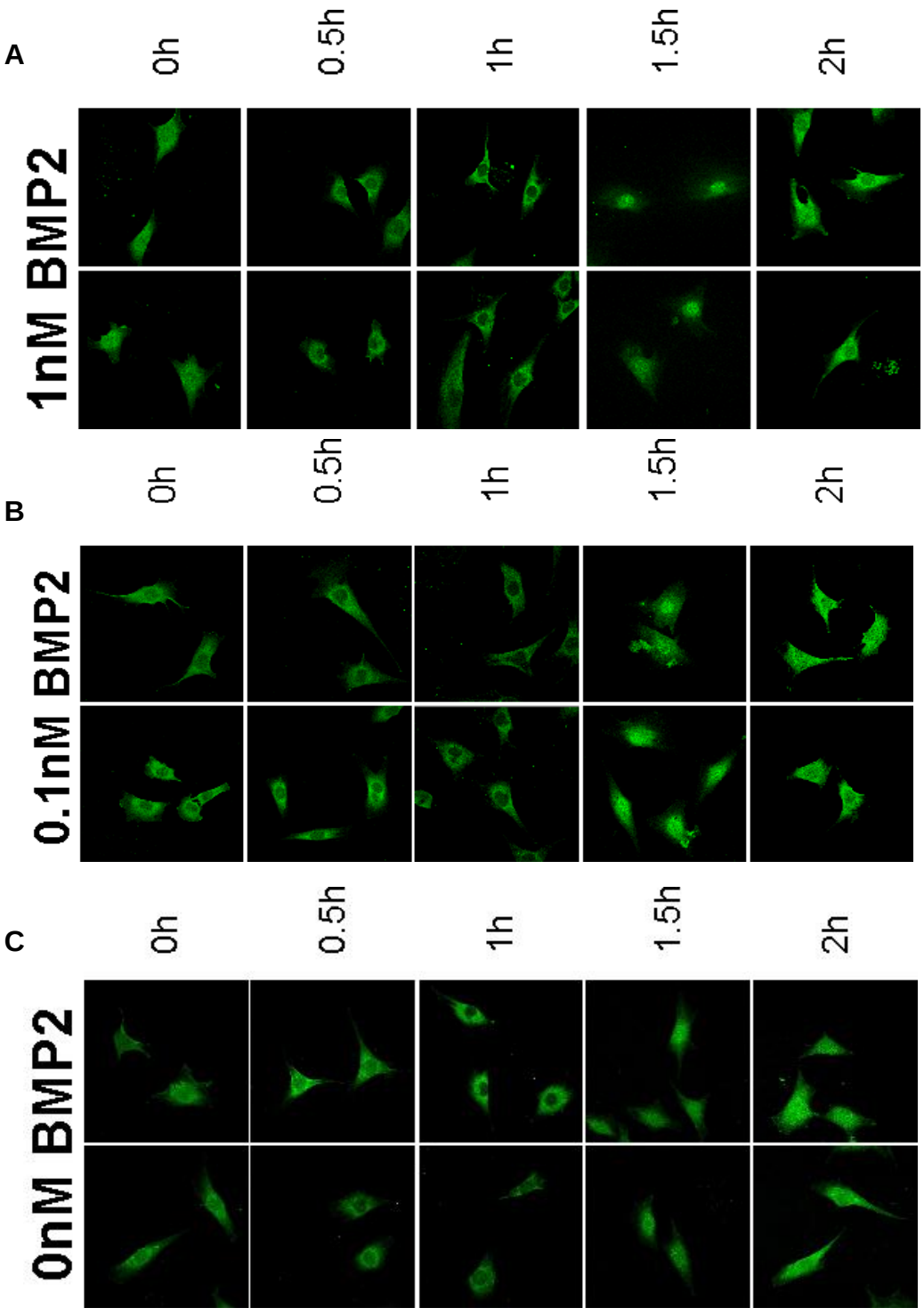

Fig. 5.14 Nucleocytoplasmic shuttling of Smad1. c2c12 wt cells were seeded out on glass cover slips and stimulated with (C) 0nM, (B) 0.1nM or (A) 1nM BMP2 for 0h, 0.5h, 1h, 1.5h or 2h. Then the cells were fixed, sampled with anti-Smad1 primary antibody and Alexa 488-secondary antibody and confocal images were acquired. (Figure modified from Schul et al. [172])

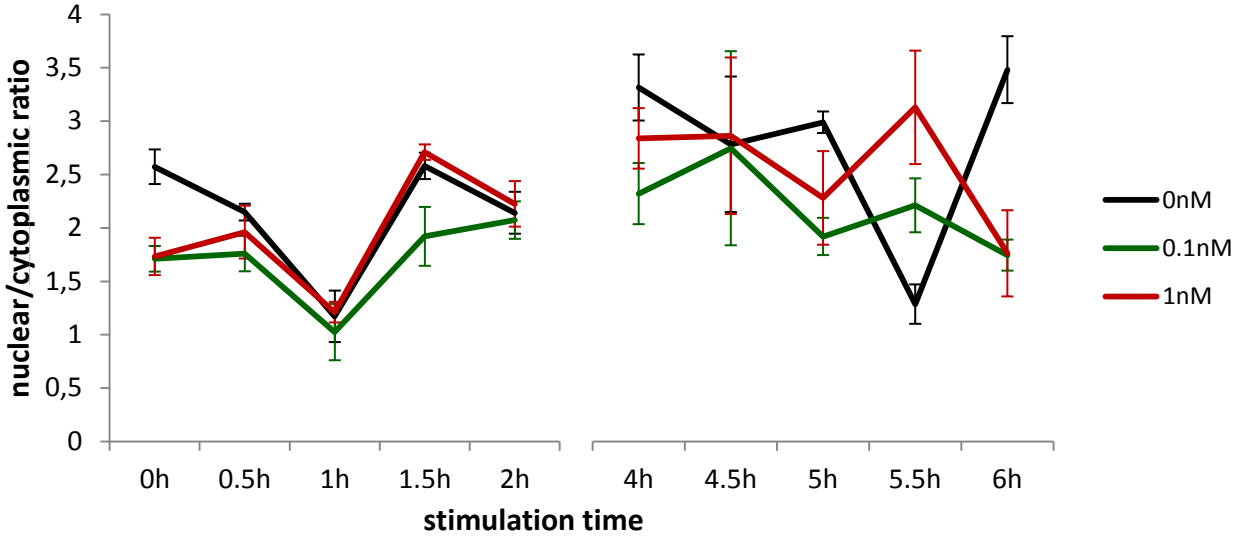

Fig. 5.15 Nucleo/cytoplasmic ratios of Smad1 after stimulation with BMP2. c2c12 wildtype cells were seeded out on cover slips and stimulated with 0nM (black), 0.1nM (green) or 1nM (red) BMP2 and fixed after the indicated time points. After that, immunofluorescent staining was conducted using an anti-Smad1 primary antibody, Alexa488 secondary antibody and specific membrane- as well as nuclear staining. 3D-Analysis of the stainings was processed using confocal stacks and the Volocity 3D image analysis software; the nuclear/cytoplasmic ratio was calculated and illustrated. The depicted values are the average of six cells for every time point and concentration. (Figure modified from Schul et al. [172])

5.6.2 Live observation of the Smad1 subcellular distribution

In order to verify the data from the immunofluorescence experiments, a GFP-Smad1 fusion construct was cloned and transiently cotransfected with a H2B-mCherry vector into c2c12 wild type cells. The H2B-mCherry vector was essential to identify the nuclei and determine their volumes. The transfected cells were then stimulated with either 0nM BMP2 or 1nM BMP2 incubated at 37°C and confocal stacks were taken every 20 minutes. The image colors were changed to rainbow pseudo colours, to clarify the potential nuclear accumulation.

Again, Figures 5.16 A and C show no nuclear accumulation of the GFP-Smad1 fusion protein for either treatment after 1h post stimulation start. In order to ensure that the fusion protein is functioning and able to visualize nuclear accumulation of Smad1, the nuclear-export-inhibitor Leptomycin B (LMB) was added additionally to the treated cells. Subsequently, GFP-Smad1 fusion proteins clearly accumulated in the nuclei of LMB treated cells over time, independent of previous BMP stimulation (Fig. 5.16 B and D). These findings confirmed the results from the previously described immunofluorescence experiments - Smad1 shuttles constantly between the nucleus and the cytoplasm. Furthermore, the subcellular localization of Smad1 due to this basal nucleo-cytoplasmic shuttling is not significantly influenced by stimulation with either 0.1nM or 1nM BMP2.

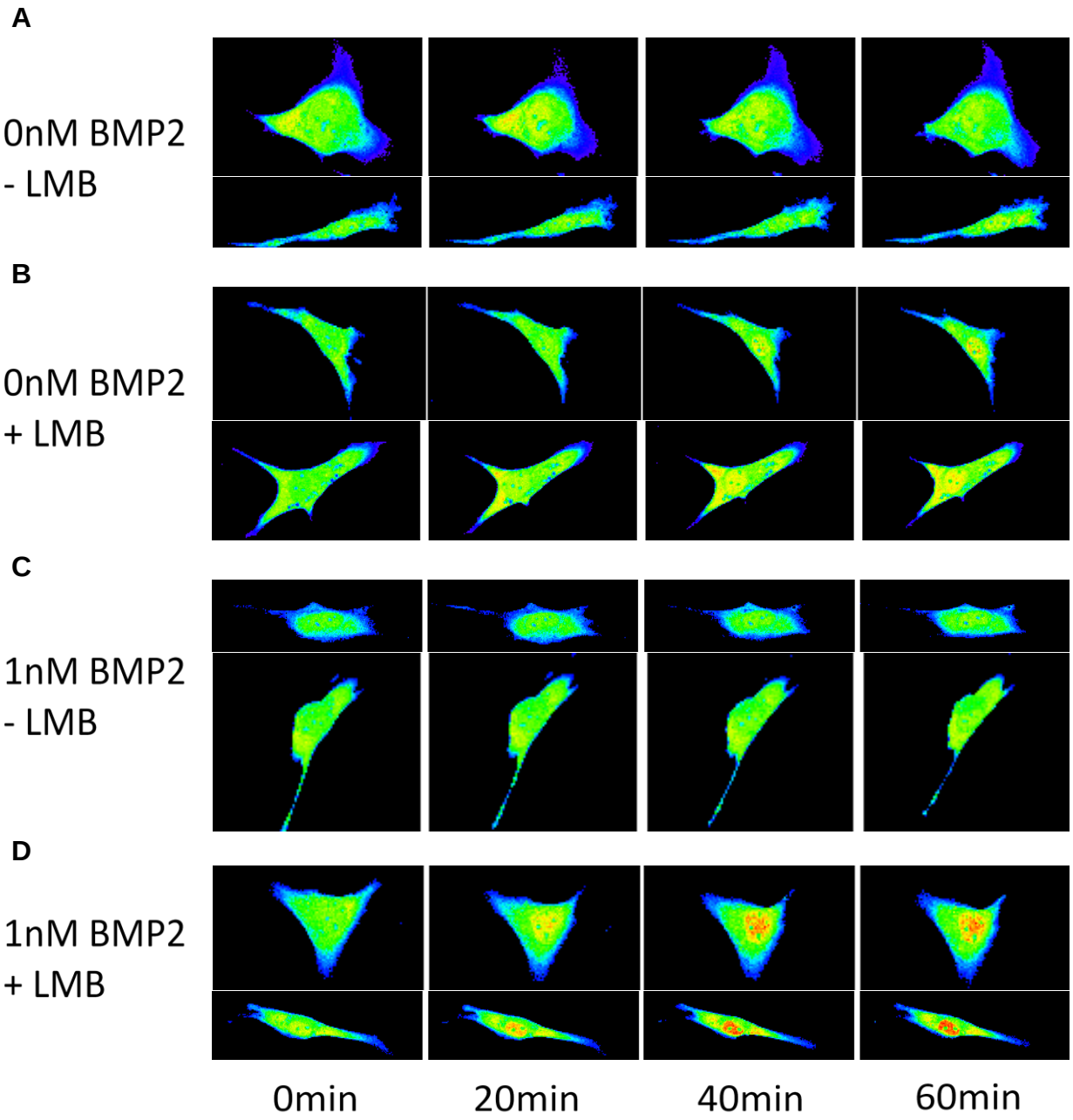

Fig. 5.16 Analysis of the Smad1-live shuttling using a GFP-Smad1 fusion. c2c12 wild type cells were transiently cotransfected with the GFP-Smad1 fusion-construct and a H2B-mCherry vector. The cells were starved over night and stimulated with either 0nM BMP2 or 1nM BMP alone or with additional adding of Leptomycin B. After that, the cells were incubated at 37°C while observing with the confocal microscope. The cells were imaged every 20 minutes until 1h after stimulation and the stacks were edited with the Volocity 3D Image Analysis Software. The pictures are illustrated in rainbow pseudo colors. (Figure modified from Schul et al. [172])

5.6.3 Phospho-Smad1 amount as a function of the ligand concentration

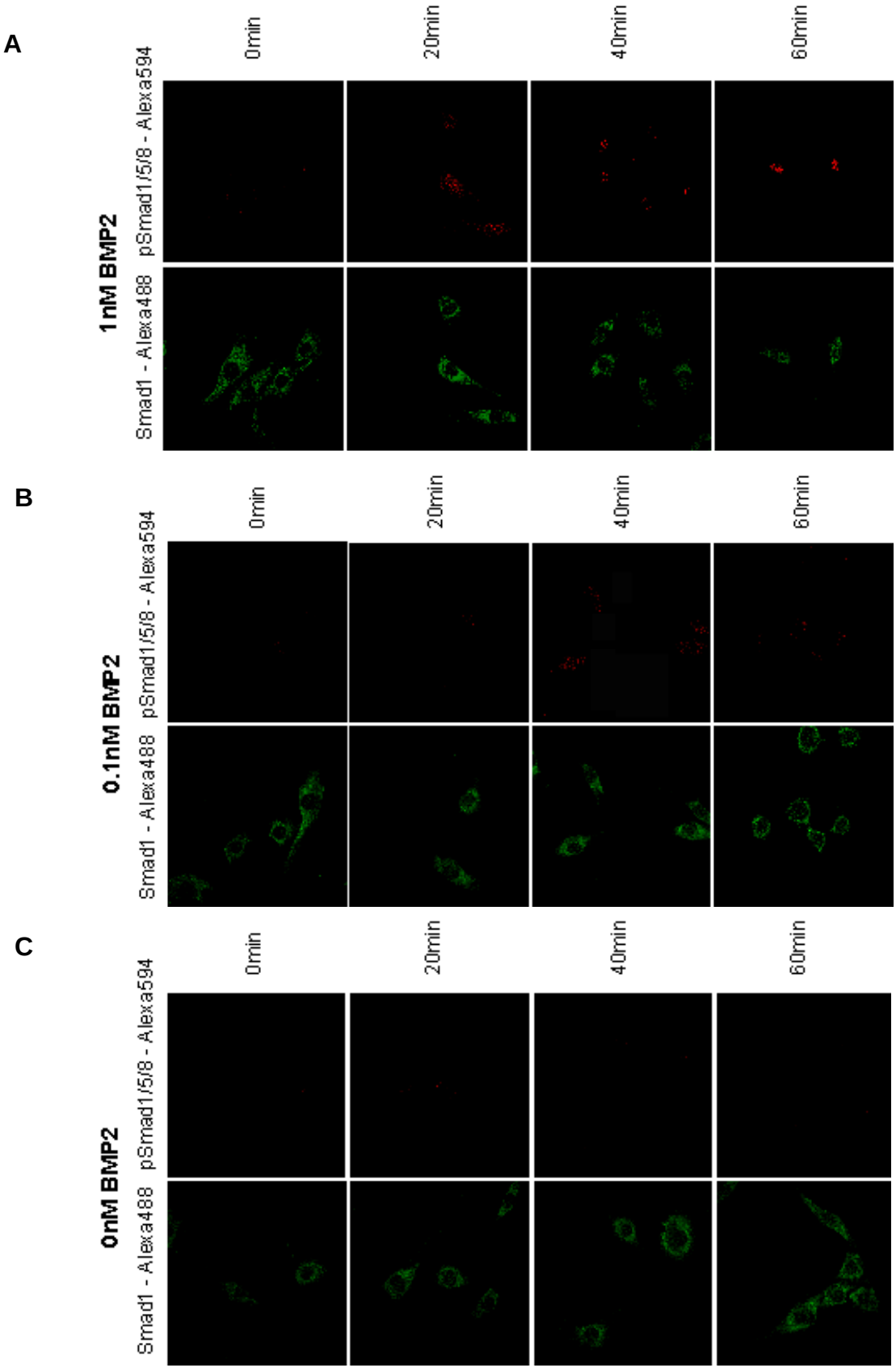

Fig. 5.17 Nuclear pSmad/total Smad1 ratio after stimulation with BMP2. c2c12 wildtype cells were seeded on glass cover slips and stimulated with 0nM, 0.1nM or 1nM BMP2 for 0min, 20min, 40min or 60min. After fixation with 4%PFA and methanol-permeabilization, the cells were sampled with a primary phospho-Smad1/5/8 and secondary Alexa594-secondary antibody. Further immunostaining was performed using an anti-Smad1 primary antibody and Alexa 488-secondary antibody; incubation with Hoechst was executed for nuclear staining. Then confocal stacks were taken and processed using Volocity 3D software. (Figure modified from Schul et al. [172])

The analyses of the subcellular Smad1 distribution after stimulation with 0nM, 0.1nM and 1nM BMP2 revealed no nuclear accumulation of Smad1, but that the Smad1 proteins shuttle constantly between the nucleus and the cytoplasm. The gene expression analyses illustrated that the target gene transcription is dependent from the stimulation concentration. Based on these results, the phospho-Smad1 amount was examined as a function of the BMP2 concentration.

c2c12 wild type cells were seeded and stimulated with 0nM, 0.1nM or 1nM BMP2. Then they were fixed after the indicated time points and sampled with anti-Smad1 and anti-phosphoSmad1/5/8 antibodies plus secondary Alexa488 or Alexa 594 antibodies, respectively.

Figure 5.17 depicts the confocal images from the double immunofluorescent stainings. Total Smad1 is colored in green and phospho-Smad1/5/8 is colored in red. For the non-stimulated cells the total Smad1 distribution is similar to that seen in Figure 5.14C; the major amount of Smad1 is located in the cytoplasm and only few phospho-Smad1/5/8 could be detected for every time point.

After stimulation with 0.1nM BMP2, again the total Smad1 subcellular localization was predominantely in the cytoplasm. But the phospho-Smad1/5/8 amount increased proportionally to the stimulation time. For 40 and 60 minutes, red fluorescence could be clearly detected in the nuclei and increased as against 0nM BMP2 (Figure 5.17B).

This result was more prominent for the stimulation with 1nM BMP2 (Figure 5.17A). The total Smad1 distribution was comparable to the 0nM and 0.1nM case. But the amount of the red fluorescence was strikingly increased for every time point, compared to the non-stimulated cells.

This experiment clearly illustrates, that the absolute phospho-Smad1/5/8 amount in the nucleus rises as a function of the stimulation concentration and the stimulation time.

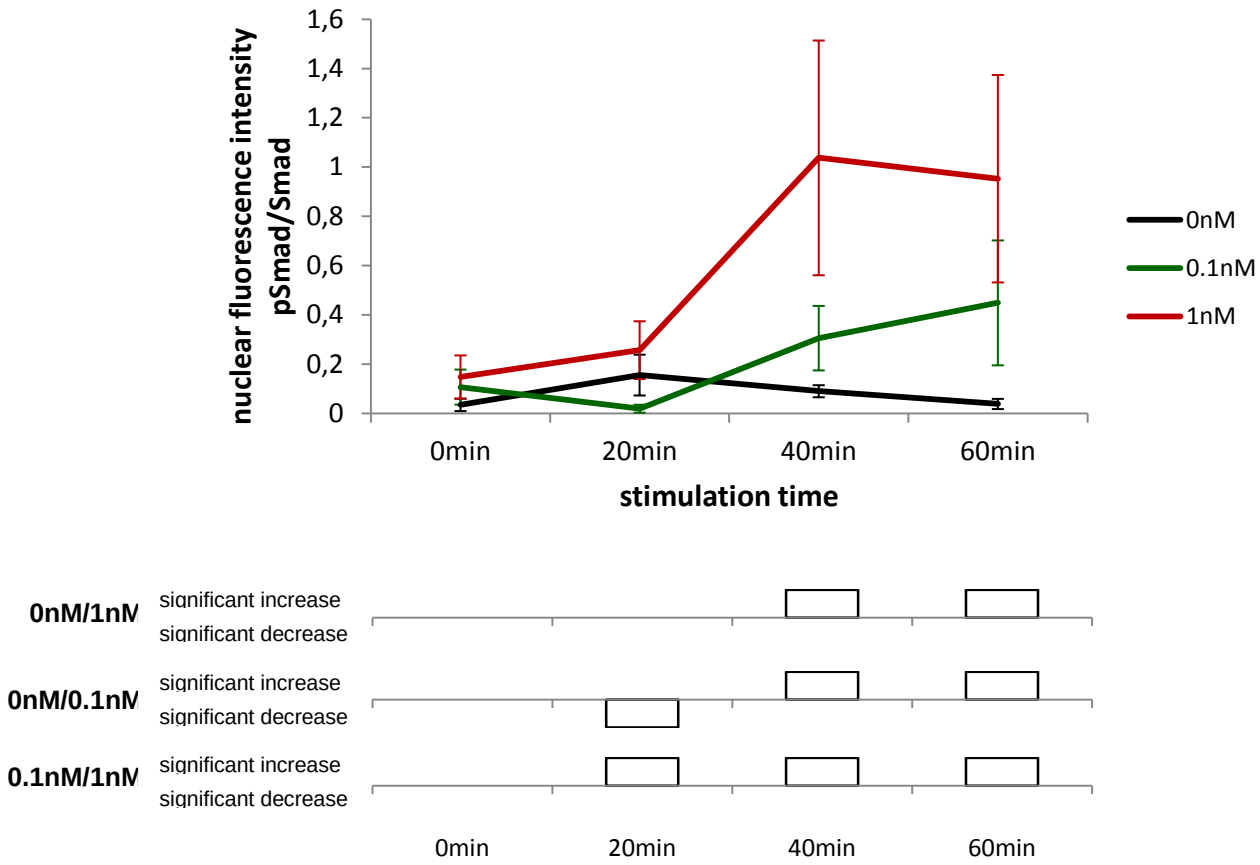

Fig. 5.18 Data evaluation for the double immunofluorescent stainings of c2c12 cells. The fluorescence intensities from Figure 3.16 were isolated with the Volocity 3D Software and used to calculate the phospho-Smad/Smad ratio. The non-stimulated case is depicted in black, stimulation with 0.1nM BMP2 in green and 1nM BMP2 in red. Below are the results of the significance tests. (Figure modified from Schul et al. [172])

For the statistical analysis, the fluorescence intensities of the nuclear total-Smad1 and the nuclear phospho-Smad1/5/8 were isolated and consulted to calculate the relative phospho-Smad1/5/8 amount in the nucleus. Figure 5.18 shows that the relative phospho-Smad1/5/8 amount is consistent for every time point for the non-stimulated situation (black line). For the stimulation with 0.1nM BMP2 (green line), the amount of the activated Smads in the nucleus significantly decreased after 20 minutes, but for 40 and 60 minutes it increased significantly compared to 0nM BMP2. The stimulation with 1nM BMP2 (red) led to a significant increase of the pSmad1/5/8 amount in the nucleus for 40 and 60 minutes compared to the non-stimulated control. Compared to the cells stimulated with 0.1nM BMP2, every time point shows a significant increase of the pSmad1/5/8 amount.

The data evaluation of the double immunofluorescent staining show that contrary to the total Smad1 amount, the phospho-Smad1/5/8 amount increases proportionally to the BMP2 concentration and the stimulation time.

6. Discussion

Cell-cell communication is the basis for efficient multicellular life. Cellular signaling pathways integrate extracellular signals and translate them into appropriate responses, for instance proliferation, differentiation or migration. How important a tightly controlled quantitative integration of ligand levels is for multicellular organisms, is best illustrated in embryonic development. For decoding cellular responses and gaining insight how extracellular signals from the environment are integrated and cellular decisions are regulated, a lot of work has been done on qualitative analyses of biological systems [166]. These experimentally derived data can be integrated into computational tools and processed into predictive mathematical models to decipher the quantitative nature of signaling pathways and to account for its complexity. The reliability of such model predictions depends on the amount of quantitative data with sufficient quality.

The critical features that lead to systemic cellular responses have been found to be the spatial distribution [167,168] and temporal dynamics [169,170] of signaling key proteins, as the current focus of research interests is the examination of protein connectivity, crosstalk and dynamics. These insights serve as inspiration to further investigate the emergent properties of signaling pathways and how they are quantitatively linked to decisions concerning cell fate [166].

A lot of work has been done on modeling different signaling pathways including the TGF-ß signaling. Since BMP and TGF-ß signaling have a related pathway and share several components like the co-Smad4, the inhibitory Smads 6 and 7 as well as one receptor subtype, one could assume that the models of the TGF-ß pathway are conferrable to the BMP-pathway. In this study, the dynamics of the BMP signaling pathway have been examined. My experiments clearly demonstrate, that strong distinctions exist compared to the TGF-ß signaling dynamics. The gene expression profiles vary strongly between these two pathways and the subcellular localization behaviour of the corresponding Smad proteins are different. In the present study I was able to quantitatively describe key parameters of BMP signaling (Fig. 6.1). I was able to link ligand concentration and exposure time to the spatio-temporal localization of the BMP key signal transducer Smad1, the resulting timelines of expression of typical target genes, as well as the half-life of active signal transduction. The results of this study were partially unexpected and the following section embeds my conclusions into the current state of knowledge.

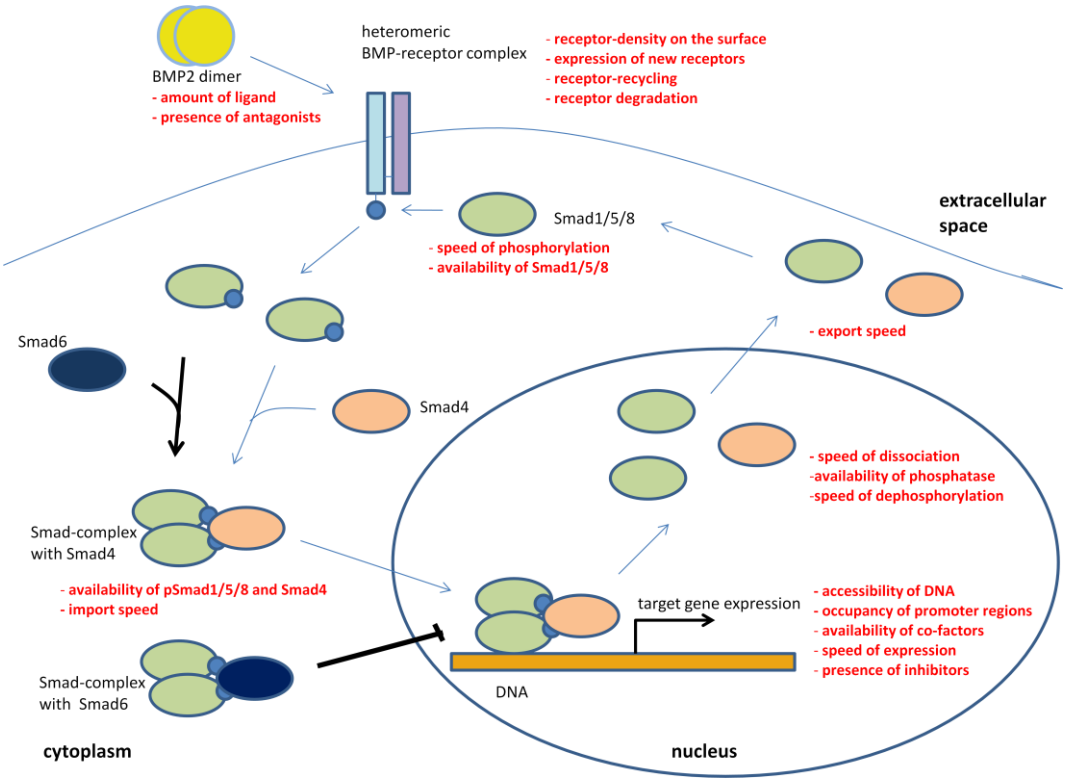

Fig. 6.1 BMP-signaling pathway scheme. The scheme depicts the process of the BMP signal transduction with its main components and potential modulators (written in red).

6.1 BMP target gene expression level is dose-dependent

The target gene expression induced by the stimulation with different concentrations of BMP2 was examined using two different experimental approaches: measurement of the expression levels of endogenous target genes as well as the activity of a stably transgenic Gaussia Luciferase under control of a BRE. Both analyses showed a dose-dependent behaviour of expression levels in c2c12 cells upon stimulation with BMP. The higher the stimulation intensity, the higher was the outcome for both independent read-outs. This observation was expected as cells respond to the absolute amount of available molecules. However, it is not clear if the proportionality of the BMP concentration and target gene transcription can be attributed to the higher gene expression level of every single cell or if it should be attributed to the activation of a higher cell number. For the NF-kB pathway it has been found, that the cells are activated in response to TNFα in a switch-like manner and that the activated cell fraction is proportional to the TNAα concentration [171]. Furthermore, the induction of early NF-kB target genes is independent of the stimulation concentration whereas later target genes are expressed only at higher stimulus levels. This phenomenon should be investigated in future experiments for the BMP signaling pathway [172].

BMPs are a subgroup of the TGF-ß superfamily, the signaling pathways are closely related and have common pathway components. On these grounds it seems reasonable to expect the signaling dynamics of these two pathways to be similar. Zi et al performed the quantitative analysis of TGF-ß signaling dynamics and this study suggests that long-term switch-like signaling responses might be critical for cell fate determination [165]. They found, that the cells show almost no signaling response when the stimulation dose is less than 10^2 molecules/cell. After stimulation with an intermediate concentration (lower than 10^5 molecules/cell) the cells show a transient signaling response with a peak after 45min of stimulation. When the TGF-ß level is higher than 10^5 molecules/cell, the cells switch to a sustained long-term signaling response [165]. In the current literature, there is no hint to the corresponding data of the BMP pathway. The BMP stimulation concentrations used during my study approximate 10^5 – 10^7 molecules/cell. Thus, the ligand concentration range for continuous pathway stimulation is the same for both signaling pathways. In summary, both pathways have in common that the overall cellular response is concentration dependent. For the TGF-ß pathway it has been shown, that each single cell responds to the absolute amount of available molecules [165], whereas for BMP signaling the possibility of a switch-like cellular activation is still conceivable. But when considering the function of BMPs during embryogenesis and the development of sharp organ borders, it seems most likely that every single cell responds to the absolute BMP concentration [172].

BMPs form morphogen gradients in developing embryos and it is well known that these proteins play an important role during organ specification. In the ectoderm, low BMP levels induce cell fates of the central nervous system, intermediate levels the neural crest, and high levels drive epidermal differentiation. In the mesoderm BMP gradients are responsible for the induction of the notochord, the somites, the lateral plate and blood island differentiation. But how the BMP gradient in developing embryos is transformed into cellular responses is still unknown. Furthermore, it is not clear why different BMP concentrations result in sharp borders. Tribulo et al claimed, that the border of the neural plate must be specified by a threshold concentration [173]. They found out that a precise and intermediate level of BMP is required to induce its direct target gene *msx* [173], which is essential for neural crest specification. This study is a hint, that the BMP gradient is not transformed into a generic graded target gene transcription. The reason for this precise threshold concentration of *msx* could also be the activation of *msx* repressors at higher BMP levels [173]. This observation seems to be the converse of the results of my study. My study demonstrated a direct dependence of *id1* and *smad6* to the stimulation concentration. Nonetheless, my study

and its results are based on a limited concentration range. However, it is possible that even these target genes possess a threshold concentration inducing further (maybe stronger) pathway modulators and therefore positive or negative feedback loops. These facts clearly demonstrate that more in depth studies are necessary to be able to completely unravel the signaling target gene expression profiles and corresponding cellular responses. These observations also suggest that the expression of every single target gene in each specific genomic setting probably needs to be studied specifically, as a generic model of quantitative control does not seem likely.

BMP signaling is not only involved in embryonic patterning but also in several pathogenic developments. Since BMPs are supposed to act as cell proliferation suppressors as well as inducers of cell cycle arrest and apoptosis [141], it is obvious that impaired BMP signaling is involved in many disorders. Besides some hereditary diseases [129,134,139,174], affected BMP signaling also causes different types of cancer [140,143,145,150,175,176]. Some mouse models for lung cancer have been published, that associate elevated BMP2 levels with increased malignancy, promoted lung tumor growth and stimulated angiogenesis in developing tumors [177]. The present study shows, that the BMP target gene transcription is dose-dependent. As BMP2 has been found to induce cell cycle regulators, this might be a reason for pathological cellular proliferation. These studies suggest on the one hand cancer promotion and on the other hand cancer inhibition. The role of BMP signaling in different cancer types starts to emerge and studies appear contradictory. Alarmo et al reviewed the bidirectional functions of BMP2/4 and 7 in breast cancer, as they have been shown to inhibit and promote breast cancer progression [176]. More detailed analysis on BMP signaling and its regulation in tumorigenesis is obviously needed to clarify the impact of BMPs in cancer [176]. Again, the genomic context seems to effectively determine the outcome of signal transduction.

The results out of my study clearly demonstrate that downregulation or termination of BMP target gene transcription may only be acquired by pathway inhibition via receptor kinase blockage. This fact may be very important for clinical applications and therapy of severe diseases like cancer or developmental defects. On the other hand, impaired BMP signaling could be compensated by the administration of BMP to the patients. As BMP2 has been shown to possess osteoinductive capacity and several BMP-subtypes have been shown to stimulate in vitro stem cell differentiation into osteoblasts, recombinant gene technology has been used to produce BMPs for clinical application in the treatment of cases in which fracture healing is compromised [178]. This is the first step towards the clinical and therapeutic use of BMPs.

6.2 Short-time receptor stimuli are sufficient to drive long-term target gene transcription

Besides the concentration dependency of BMP target gene transcription, this study demonstrated that the gene expression level of analyzed genes was independent of the stimulation duration for every stimulation concentration sampled. Short-term receptor stimuli were adequate to induce a gene expression profile comparable to long-term receptor stimuli. This phenomenon could be due to the half-life of BMP proteins. The half-life of BMP proteins in cell culture media and in vivo is rather short, as its concentration rapidly decreases within 1h to below 50% and after 10h only 10% of the original concentration remains in the medium [179]. This fact supports the results for the short time receptor stimulus. However, there are several layers of complexity added to the determination of the half-life of the signal mediated by BMP2, as ligand-bound receptor-complexes are internalized, continue to signal and are finally shut down only by specific degradation [172].

As one main function of the BMP pathway is cell fate determination during embyrogenesis, switch-like, ultrasensitive and rigid systems seem to be more likely. All-or-nothing responses are in general a feature of mitosis, apoptosis and cell differentiation. Critical characteristics for this kind of cellular response are positive or double negative feedback loops [180]. For the BMP signaling pathway no evidence in the current literature can be found that supports positive feedback loops. However, a double negative feedback loop has been found for BMP and Chordin in *Nematostella* [181]. Furthermore, several other mechanisms are involved in the patterning process during embryonic development. As the results of the present study were quired using cell culture experiments, they cannot be directly transferred to *in vivo* systems. Specific inhibitors are known to be responsible for interfering with BMP signaling during embryogenesis, e.g. Nodal, Noggin or Follistatin [182]. In 2012, Alborzinia et al. published that exogenous BMP ligands are internalized after receptor binding and accumulate in the center of the cell [183]. The authors could not observe a significant degradation of this intracellular BMP. Alborzinia's data are compatible with the notion that BMP2 could either be recycled to the cell surface at later time points or directly reactivate BMP type I receptor kinases within the cell. This could be an explanation for the oscillating target gene expression profiles of BMP2. Furthermore, it is well known that BMP ligands are morphogens. Some morphogens are known to be able to undergo transcytosis. Within this process the ligands are captured in vesicles, transported across the cell and ejected on the other side of the cell [172]. Thus, it is conceivable that BMP proteins also own this property.

For the TGF-ß pathway it has been published in 2011 that the Smad2 phosphorylation kinetics is very sensitive and correlates with both ligand concentration and duration [165]. Sustained stimulation can be imitated by periodic short pulses, but basically the pathway answers with short-term responses upon short-term stimulation. This is a robust system and easier to predict in mathematical models compared to the BMP system.

The reason for the similarity of the outcome between short-term and long-term stimulation is still unknown and several aspects serve as an explanation of this unexpected finding. Every dynamic system possesses a limiting factor that is responsible for the maximum value or outcome [184–187]. As in the present study short term stimulation shows the same cellular response as long-term stimulation, it is obvious that the limiting factor of BMP signaling is already utilized to capacity. The limiting factors for the BMP signaling pathway could be the total utilization of surface receptors, a lag phase between receptor inactivation and Smad dephosphorylation, the total occupancy rate of Smad-proteins (Smad1/5/8 or Smad4), the total utilization of Smad-dephosphorylation enzymes or the limitation of the import/export processes (Fig. 6.1). The identification of the restriction within the signaling pathway could be examinated by various experimental setups. Overexpression studies could be used to analyze the influence of the amount of BMP-receptors on the surface, the relevance of the amount of Smad1/5/8 or Smad4 or as well the importance of the amount of phosphatases for Smad-dephosphorylation dynamics. In addition, the nuclear import or export mechanisms could be blocked to get insight in the significance of this system to the overall signaling outcome (Fig. 4.1). If one or more of these factors appear as limiting factors during these studies, a shift or a completely different signal output pattern for the same ligand input would be expected. These shifts might occur as gene expression discrepancies per tissue, per cell type, embryonic area or dysregulation per tumor. Several publications outline the importance of such bottlenecks for healthy pathways [188–190].

When comparing the results of the short-term and long-term stimulation of the stable gLuc-cells in detail, it turns out that the expression patterns are similar but not equal. For the long-term stimulation situation at later time points after 15h, the peaks do not decrease to the relative fold change of 1 but rather start to increase again to the next peak at higher fold changes, single expression peaks get overlapped. The reason for this phenomenon could be the total stimulation and operating grade of the surface receptors with following creeping re-stimulation after receptor recycling or stimulation of newly expressed receptors.

6.3 Oscillating target gene expression is independent of the BMP concentration

The results of the current study indicate that BMP target gene expression oscillates with maximum peaks after approximately 1-2 hours. Expression waves persisted until 30 hours post-stimulation. The wave-like expression profiles as well as the waves's frequencies seem to be independent of the BMP level. However, the various target genes are activated differentially and could be grouped in subsets of immediate early, intermediate early and late early response genes [191]. I decided to investigate two target genes, *id1* as the best known target of BMP signaling, and *smad6* as an inhibitory pathway regulator. Furthermore, these two genes were previously found to be immediate early target genes [191]. The maximum peak of *smad6* expression was observed 2h after stimulation, one hour later compared to the *id1* peak. The delayed *smad6* expression was unexpected, but with regard to its function appears reasonable. Smad6 is a member of the inhibitory Smads and leads to the downregulation of the signaling pathway via negative feedback loop [96]. Smad6 competes with Smad4 for binding to the activated R-Smads and furthermore, acts as a nuclear BMP-induced repressor of transcription. Thus, the BMP induced target gene transcription is downregulated and decreases to the base level. Due to the temporal and functional differences between *id1* and *smad6* and the functional dependency of the expression time after stimulation, these genes should be classed into different subgroups. Such subclasses could be for example *id1* as immediate earliest target gene and *smad6* as immediate early target gene [172].

The long-term observation of *id1* and *smad6* in the current study described further expression peaks at approximately two hours intervals, with rapid subsequent decrease. This oscillatory behaviour was found for both genes, and for every stimulation concentration the same pattern occurred. Hence, the wave-like expression profile is independent of the ligand dose (once a minimal threshold is reached). This conclusion is supported by Yoshiura et al., as they published ultradian oscillations of *smad6* in response to serum 120' and 230' after serum stimulation [192]. In the same study phospho-Smad1/5/8 levels have been found to be oscillatory with peaks after approximately 1.5h and 3.5h, suggesting that Smad1/5/8 regulate *smad6* oscillation [192]. They also confirmed the negative feedback behaviour by continuously expressing Smad6, resulting in decreased phospho-Smad1 formation and abolished oscillations. Oscillating target gene transcription is also supported by the fact that *hes1* expression, which is controlled by BMP2, oscillates in embryonic stem cells.

Additionally, this oscillatory expression could be mimicked using a *hes1*-promoter driven Luciferase [193].

A further reason for the oscillating target gene expression could be endocrine BMP-like signals, which might induce the gene expression oscillations. But in the current literature no evidence could be found, that stimulation with BMP induces positive feedback loops. The contrary has been observed by Fei et al. in embryonic stem cells, where *bmp4* is downregulated after stimulation with BMP4 [194]. Furthermore, one would expect a delay or shift of target gene expression in the wash-away experiments, if the oscillations were an effect of endocrine BMP-like signals. However, Alborzinia et al. have found that exogenous BMP2 was rapidly bound to the cell surface and subsequently internalized and accumulated in the cell center without being significantly degraded [183]. Based on this observation, BMP2 could be recycled to the cell surface at later time points or reactivate BMP type I receptor kinase in the cytoplasm. This is an interesting fact and would be a very interesting topic to be studied in depth in future [172].

Another possibility to explain target gene oscillations could be that internalized BMP ligands might recycle back to the cell surface and reactivate receptors. Alborzinia et al. published in 2012, that exogenous BMP ligands are internalized after receptor binding and accumulate in endosomes in the cytoplasm [183]. The authors could not observe a significant degradation of this intracellular BMP. This study in addition to the current data suggests that BMP2 could be recycled to the cell surface at later time points or reactivate BMP type I receptor kinase in the cell. Furthermore, it is well known that BMP ligands are morphogens and thus are able to undergo transcytosis [195]. This could also be a hint for the recycling of internalized BMP ligands to the extracellular space [172].

For the TGF-ß/Smad pathway it has been demonstrated that upon sustained stimulation with TGF-ß the amount of phospho-Smad2 increases to a maximum peak and then decreases to a constant level over at least 8h [165]. This fact outlines a hint for a correlating target gene expression profile. This behavior is completely different from the oscillating response of the BMP signaling pathway.

Oscillating responses are commonly discovered in cellular behavior and cover a wide range of timescales, from seconds in calcium signaling to 24 hours in circadian rhythms. Furthermore, oscillations play key roles in several mechanisms like the immune system, cell growth or cell death and embryo development, respectively [196]. With ongoing research in the area of protein and signaling kinetics and dynamics, periodicity is more and more observed and accepted [196–199]. Benefits of oscillating responses could be reduced exposure to high levels of ligand through better energy

efficiency of the cell for the purpose of lower protein production or thresholding. However, these biological advantages implicate experimental complications like more precise measurements or higher error-proneness. Another advantage could be the possibility of transducing the oscillatory activity into another fluctuating process, like the circadian clock and the corresponding circadian rhythm [200]. Furthermore, transforming stimuli into oscillatory signals is more robust against noise in the input signal and signal propagation [201]. This claim is supported by Tostevin et al., who found last year that oscillating input of a transcription factor produces more constant protein levels than a constant input during transcriptional processes [202]. Thus, the authors suggest that oscillating signals may be used to minimize noise in gene regulation [202]. An oscillating signaling transduction mechanism is more capable of encoding a variety of information's compared to rigid transduction mechanisms. Wave-like patterns can code information in two components, in form of the amplitudes or in form of the frequency. These curves can also be more complicated, when multiple frequencies are overlayed on top of each other and thus create hidden waves, which can potentially be decoded by cells [203]. These oscillating progressions can be revealed mathematically using the fast Fourier transformation, which is commonly used for the identification of various clusters in biologic issues [204,205]. The current study revealed, that BMP signaling seems to encode the input via the height of the transcription levels and not via the frequencies of the transcription peaks, as the frequencies were highly similar for every stimulation concentration but the peak height increased in direct proportion to the ligand dose. However, higher transcription rates do not necessarily require higher mRNA levels. Several mRNA stabilizing processes represent an alternative or additional explanation, for instance better or different capping, mRNA stabilization in consequence of attaching to transcription complexes or higher multimerization during transcription due to higher input. Clarification could be obtained using a nuclear run-on assay or experiments to analyze the mRNA half-life.

6.4 Target gene expression oscillation is directly dependent on BMP receptor kinase

Comparison of kinase-inhibition with continuous ligand exposure and wash-away treatment demonstrated that the target gene oscillation is directly dependent on the phosphorylation-state of the receptor kinase. Furthermore, ligand-bound receptor complexes maintain target-gene stimulation for at least 8h and in oscillating patterns without receptor reactivation with newly administered ligand.

Treatment with Dorsomorphin (BMP type I receptor kinase inhibitor) leads to a discriminated signaling response. Shortly after stimulation with 1nM BMP2, the nuclear phospho-Smad1 level is considerably higher than the level with 0.1nM. Thus after stimulation with 1nM BMP2 and subsequent kinase-inhibitor treatment, the phospho-Smad1 level is sufficient to exclusively trigger expression of very early target genes. This might be attributed to the dose-dependency in combination with the inhibitor potency. Since phospho-Smad1 proteins are rapidly degraded by E3 ubiquitin ligases, expression of later target genes are not initiated. phospho-Smad1 levels after 15' stimulation with 0.1nM BMP2 consequently fall short of even driving at least immediate early target gene expression [172].

As discussed in the previous section, several advantages arise out of oscillating responses. However, currently the real reasons and causes for these oscillations remain unclear. Possible reasons for the sustained oscillating target gene expression after short-time Smad-activation could be (1) maintained kinase activity without further receptor activation and/or (2) prolonged Smad viability and activity.

In the current literature, no evidence can be found for kinase activity duration after stimulation. A logical statement would be the equalization of receptor stimulation and kinase activity or Smad activation, respectively. However, the activated BMP receptors are known to be internalized via clathrin-coated pits into endosomes [17]. Thus, the internalized receptors still signal right up to at least 30h after ligand stimulation. But endocytosis may have diverse effects on signal transduction. As it reduces the number of bio-available receptors on the cell surface and leads to receptor-degradation via the lysosomal pathway, receptor internalization influences the signaling outcome negatively. On the contrary, endocytosis in general has also a lot of positive roles for signal transduction as endosomes have can be important signaling tools as they increase the proximity of the two receptor subtypes and of the receptors and their substrates [206,207]. Furthermore, Heining et al. demonstrated that dynamin-dependent endocytosis is crucial for the spatial activation of the BMP signaling cascade [208]. This group also suggested, that the expression of the BMP/Smad target genes are diversely affected by inhibiting endocytosis arising from spatially segregated signaling pathways, the endocytosis path and an endocytosis-independent path [208]. Supporting the results of the present study, they found that *id1* is an endocytosis-dependent gene and therefore its sustained expression after ligand removal is almost certainly due to endocytic regulation of signaling. Furthermore, they claimed that early stages of differentiation are strongly dependent on the endocytotic route and that limited temporal ligand treatment is sufficient to promote osteoblast differentiation [208].

Some positive TGF-ß/BMP signaling regulators are known to be localized in endosomes. One group of these regulatory proteins contain the FYVE domain (Fab1, YOTB, Vac1, EEA1), which is a cysteine-rich and zinc-binding domain and binds to phosphatidylinositol 3-phosphate [209]. These lipids are enriched in early endosomes and can specifically recruit FYVE-domain containing proteins to early endosomes [210]. Furthermore, the FYVE-containing proteins have an increasing effect on the TGF-ß and BMP signaling outcome [211,212]. For the TGF-ß pathway has been observed, that the SARA and Hrs, containing the FYVE-domain, specifically interact with Smad2/3 and TGF-ß receptors, and thus promote Smad-phosphorylation and TGF-ß signaling result [213]. A third FYVE-domain containing protein, Endofin, has been found to stimulate BMP signaling by recruiting Smad1 to BMP receptors in endosomes [214]. But Endofin is also suggested to recruit protein phosphatase 1 to dephoshorylate BMP type I receptors and attenuate BMP signaling [214]. How these contradictory functions of Endofin are controlled remains unclear.

As the BMP target gene transcription could only be blocked by the BMP type I receptor inhibitor Dorsomorphin, I claim that the gene expression as well as the oscillating pattern is directly dependent on the receptor kinase. As the kinase gets constantly activated in endosomes, target gene expression and the negative feedback loop are maintained for at least 30h after stimulation without new BMP stimulation impulses, resulting in the observed wave-like expression pattern. When the receptor kinase becomes inhibited by Dorsomorphin or presumably any other kinase inhibitor or degradation, target gene transcription gets abolished after 1h. Thus, the half-life time of the BMP signaling pathway is 0.5h. Interestingly, after Dorsomorphin treatment gene expression is downregulated below the non-stimulated control level indicating a basal expression of the BMP target genes probably induced by a basal level of receptor activity [172].

The main reason for the oscillating target gene expression upon continuous kinase activity remains unexplored. However, the most probable cause is the negative feedback loop via inhibitory Smads or other pathway inhibitors or regulators. As the inhibitory Smad-proteins act downstream of the receptor complexes, they might form a subsequent and tighter second bottleneck and override the main choke point – the receptor activity (Fig. 6.2). This could be investigated in the future by knock-out experiments or genetic modification of the tertiary structure of the receptor.

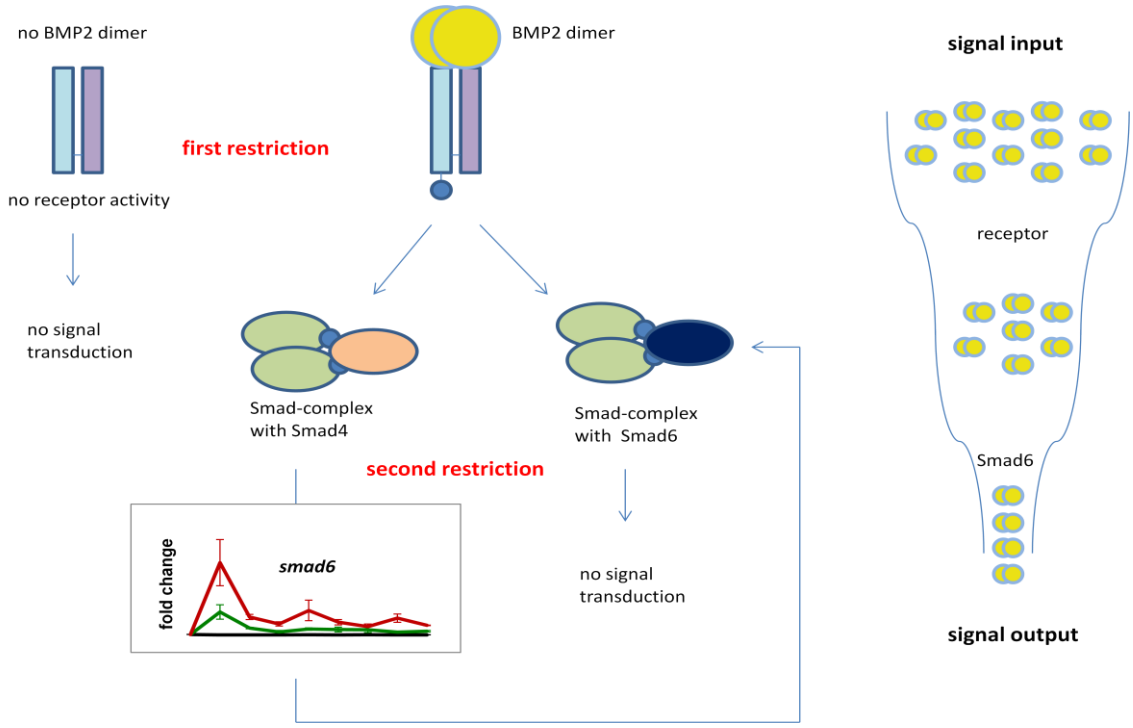

Fig. 6.2 Schematic description of the negative feedback loop via Smad6. The scheme depicts the two independent restriction points of the BMP signaling pathway resulting in the described bottlenecks and oscillating target gene expression with rapid subsequent decrease.

6.5 Crucial differences regarding the spatio-temporal intracellular localization of the R-Smad family members upon stimulation

For the TFGß-Smad2/3 pathway is well known that Smad2/3 strongly accumulate in the nucleus upon stimulation with very low TGF-ß concentrations in the picomolar range [64,67,172]. The data of the present study indicate that this reaction cannot be transferred to the BMP/Smad1 pathway in c2c12 cells. Instead, this study describes that the phospho-Smad1 level in the nuclei increases in proportion to the ligand-concentration, with 0.1nM and 1nM BMP, but not the overall Smad1 amount. A comparable observation has been described for Smad1 in a B-cell lymphoma cell line after stimulation with TGF-ß [215]. Furthermore, studies in Xenopus embryos also suggest that the pathway activity has little effect on the localization of total Smad1 [216]. Reasons for this discrepancy within members of the Smad family could be differences in the nuclear export/import signals. Several groups have extensively studied these sequences in the MH1- and MH2-domains of the R-Smad proteins [61,62,65,69]. Smad2 and 3 are imported into the nucleus via importins [65,217], NLS-based nuclear import and karyopherin-independent import mechanisms and the export is mediated by exportin 4 and Ran [67]. Smad1 bears a NLS in its MH1 domain[62] and

gets imported via importins 7 and 8[68]. In contrast to Smad2/3, Smad1 has two NES responsible for the protein export to the cytoplasm. NES1 is located in the MH2 domain. The second export signal (NES2) is located in the linker region adjacent to the MH1 domain and known to attend the exportin 1-mediated transport [69] and identical to the Smad4 nuclear export signal. Due to the NES2, Smad1 is sensitive to Leptomycin B treatment whereas Smad2 and Smad3 are not. These facts clearly state a highly dynamic system for the control of Smad localization and diverse shuttling mechanisms within the Smad-family members. The CRM-1 mediated export via NES2 of Smad1 and Smad4 could be the main reason for the discrepancy of the nuclear localization within the R-Smad family members. Compared to Smad2/3, more Smad1 molecules could be exported with this additional export mechanism in a specific timeframe, resulting in faster Smad1 nucleocytoplasmic turnover, re-phosphorylation and reactivation of transcription [172].

Furthermore, subcellular retention mechanisms/compartments could represent important players in terms of differences regarding nucleocytoplasmic shuttling dynamics. In the current literature, to my knowledge no studies exist for specific nuclear retention factors for Smad1. Certainly, for Smad2 several studies observed proteins controlling the resident time in the nucleus. The interaction with NUP, a protein localized in the nuclear periphery, as well as the cause of nuclear accumulation due to FoxH1 overexpression was described by Xu et al. [67]. Furthermore, Smad2/3 and 4 have been found to interplay with microtubules in several cell lines [218]. In contrast, SARA functions as a cytoplasmic retention factor for Smad2, as this protein contains a Smad-binding domain and is preferentially targeted to early endosomes [219]. For Smad1, MAPK-dependent Smurf1 inhibits the interaction with Nup214 and thus leads to cytoplasmic retention [220].

My results strongly suggest a constant, basal nucleocytoplasmic shuttling of Smad1, which is not significantly modulated by stimulation with up to 1nM BMP2. However, it has been shown that stimulation with 10nM BMP2 leads to a clear nuclear accumulation of Smad1 [221]. As a conclusion, Smad1-shuttling dynamics are dose-dependent with a threshold value between 1nM and 10nM. The Smad1 import-rate exceeds the export-rate and the proteins accumulate in the nucleus. Reasons for that might be lacking dephosphorylation, more phospho-Smad1 proteins per complex meaning longer resting time on DNA, or that export-proteins have poorer binding efficiency for phospho-Smad1 proteins; many possible, likely complementary explanations for the observed phenomenon have been suggested, but the real cause remains unexplored and has to be examined in the future.

Generally, nucleocytoplasmic shuttling provides a very sensitive and sophisticated system to continuously transduce receptor activity to the cell. Thus, the Smad-proteins should plausibly monitor the signal input and enable the cell to immediately react to changes in the signal intensities. The results of the present study indicate that one has to distinguish strictly between nucleocytoplasmic shuttling of Smad1 or nucleocytoplasmic shuttling of phospho-Smad1, as Smad1 nucleocytoplasmic shuttling is not dependent on the BMP dose. The reason for this mechanism could be a faster and less stressful acclimation of the cell to the sudden stimulus, as the cellular condition stays in a steady-state with the basal shuttling mechanism. On the other hand, the Smad1 nucleocytoplasmic shuttling mechanism might be irrelevant and not regulated during the BMP signaling pathway (Fig. 6.3 A). The nuclear import/export mechanisms could simplistically act as restricting lower and upper limits and do not act as sensor or regulator. Thus, an explanation might be a higher relative amount of imported (active) Smad-complexes or a change in the affinity of the Smad-complex for the DNA with altered input concentrations. The binding affinity could be in direct proportion to the amount of phospho-Smad1 in the multimer-complex (Fig 6.3 B).

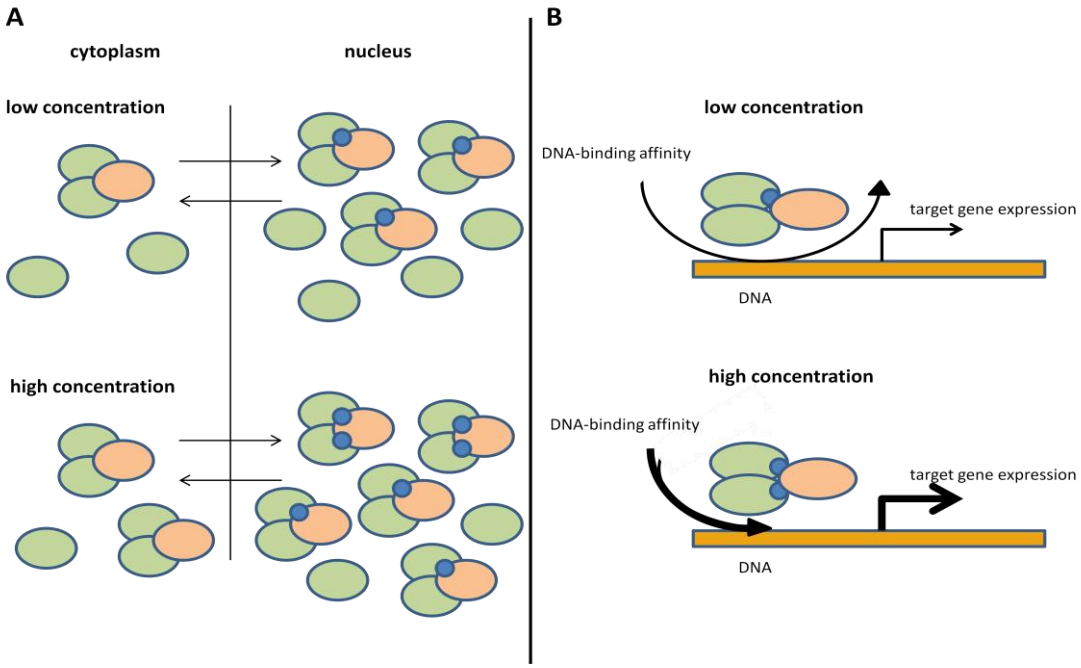

Fig. 6.3 Nucleocytoplasmic shuttling and DNA-binding affinity of the Smad-proteins. (A) The scheme illustrates a not regulated import and export mechanism (uniform arrows) with the same amount of transported particles for both concentrations. The critical factor is the percentage of Smad-complexes within all transported particles. (B) Another crucial regulatory aspect could be a higher DNA-binding affinity of the Smad-complexes due to a higher amount of phospho-Smad within the single multimers.

During embryogenesis, body patterning and axis formation are determined by morphogen gradients and different cell fates result from distinct gene expression profiles. Furthermore, BMPs are used as therapeutics in the clinic. My data on signal half-life, the influence of BMP2 concentration, exposure time and receptor inhibition on the temporal course of target-gene-expression create a basis for a novel mathematical model for the BMP signaling pathway that could be used to improve the drug compositions, amounts and administration patterns for the patients benefit and the compensation of side effects, e.g. developmental defects. In addition to the biological significance, the outcomes of the current study highlight the importance of single-cell data in understanding and modeling biological systems.

Curriculum vitae

Affidavit

I hereby confirm that my thesis entitled “Spatio-temporal investigation and quantitative analysis of the BMP signaling pathway” is the result of my own work. I did not receive any help or support from commercial consultants. All sources and / or materials applied are listed and specified in the thesis.

Furthermore, I confirm that this thesis has not yet been submitted as part of another examination process neither in identical nor in similar form.

Place, Date Signature

Eidesstattliche Erklärung

Hiermit erkläre ich an Eides statt, die Dissertation „ Raum-Zeitliche Untersuchung und quantitative Analyse des BMP-Signaltransduktionsweges“ eigenständig, d.h. insbesondere selbstständig und ohne Hilfe eines kommerziellen Promotionsberaters, angefertigt und keine anderen als die von mir angegebenen Quellen und Hilfsmittel verwendet zu haben.

Ich erkläre außerdem, dass die Dissertation weder in gleicher noch in ähnlicher Form bereits in einem anderen Prüfungsverfahren vorgelegen hat.

Ort, Datum Unterschrift

Bibliography

1. Urist MR (2002) Bone: formation by autoinduction. 1965. Clinical orthopaedics and related research: 4–10. Available: http://www.ncbi.nlm.nih.gov/pubmed/11937861.

2. Reddi a H (2005) BMPs: from bone morphogenetic proteins to body morphogenetic proteins. Cytokine & growth factor reviews 16: 249–250. Available: http://www.ncbi.nlm.nih.gov/pubmed/15949967. Accessed 13 January 2012.

3. Kessler E, Takahara K, Biniaminov L, Brusel M, Greenspan DS (1996) Bone morphogenetic protein-1: the type I procollagen C-proteinase. Science (New York, NY) 271: 360–362. Available: http://www.ncbi.nlm.nih.gov/pubmed/8553073.

4. Vitt U a, Hsu SY, Hsueh a J (2001) Evolution and classification of cystine knot-containing hormones and related extracellular signaling molecules. Molecular endocrinology (Baltimore, Md) 15: 681–694. Available: http://www.ncbi.nlm.nih.gov/pubmed/11328851.

5. Wang E a, Rosen V, D'Alessandro JS, Bauduy M, Cordes P, et al. (1990) Recombinant human bone morphogenetic protein induces bone formation. Proceedings of the National Academy of Sciences of the United States of America 87: 2220–2224. Available: http://www.pubmedcentral.nih.gov/articlerender.fcgi?artid=53658&tool=pmcentrez&rendertype=abstract.

6. Aono A, Hazama M, Notoya K, Taketomi S, Yamasaki H, et al. (1995) Potent ectopic bone-inducing activity of bone morphogenetic protein-4/7 heterodimer. Biochem Biophys Res Commun 210: 670–677.

7. Kishigami S, Mishina Y (2005) BMP signaling and early embryonic patterning. Cytokine & growth factor reviews 16: 265–278. Available: http://www.ncbi.nlm.nih.gov/pubmed/15871922. Accessed 3 August 2011.

8. Hino J, Kangawa K, Matsuo H, Nohno T, Nishimatsu S (2004) Bone morphogenetic protein-3 family members and their biological functions. Front Biosci 1: 1520–1529.

9. Simic P, Vukicevic S (2005) Bone morphogenetic proteins in development and homeostasis of kidney. Cytokine & growth factor reviews 16: 299–308. Available: http://www.ncbi.nlm.nih.gov/pubmed/15923134. Accessed 22 November 2011.

10. Callis TE, Cao D, Wang D-Z (2005) Bone morphogenetic protein signaling modulates myocardin transactivation of cardiac genes. Circulation research 97: 992–1000. Available: http://www.pubmedcentral.nih.gov/articlerender.fcgi?artid=2930260&tool=pmcentrez&rendertype=abstract. Accessed 3 August 2011.

11. Shimasaki S (2004) The Bone Morphogenetic Protein System In Mammalian Reproduction. Endocrine Reviews 25: 72–101. Available: http://edrv.endojournals.org/cgi/doi/10.1210/er.2003-0007. Accessed 15 July 2011.

12. Kawamura C, Kizaki M, Ikeda Y (2002) Bone morphogenetic protein (BMP)-2 induces apoptosis in human myeloma cells. Leukemia & lymphoma 43: 635–639. Available: http://www.ncbi.nlm.nih.gov/pubmed/12002771. Accessed 13 January 2012.

13. Miyazono K, Maeda S, Imamura T (2005) BMP receptor signaling: transcriptional targets, regulation of signals, and signaling cross-talk. Cytokine & growth factor reviews 16: 251–263. Available: http://www.ncbi.nlm.nih.gov/pubmed/15871923. Accessed 25 August 2011.

14. Rosenzweig BL, Imamura T, Okadome T, Cox GN, Yamashita H, et al. (1995) Cloning and characterization of a human type II receptor for bone morphogenetic proteins. Proceedings of the National Academy of Sciences of the United States of America 92: 7632–7636. Available: http://www.pubmedcentral.nih.gov/articlerender.fcgi?artid=41199&tool=pmcentrez&rendertype=abstract.

15. Liu F, Ventura F, Doody J, Massagué J (1995) Human type II receptor for bone morphogenic proteins (BMPs): extension of the two-kinase receptor model to the BMPs. Molecular and cellular biology 15: 3479–3486. Available: http://www.pubmedcentral.nih.gov/articlerender.fcgi?artid=230584&tool=pmcentrez&rendertype=abstract.

16. Foletta VC, Lim MA, Soosairajah J, Kelly AP, Stanley EG, et al. (2003) Direct signaling by the BMP type II receptor via the cytoskeletal regulator LIMK1. The Journal of cell biology 162: 1089–1098. Available: http://www.pubmedcentral.nih.gov/articlerender.fcgi?artid=2172847&tool=pmcentrez&rendertype=abstract. Accessed 21 July 2011.

17. Sieber C, Kopf J, Hiepen C, Knaus P (2009) Recent advances in BMP receptor signaling. Cytokine & growth factor reviews 20: 343–355. Available: http://www.ncbi.nlm.nih.gov/pubmed/19897402. Accessed 21 June 2011.

18. Wieser R, Wrana JL, Massagué J (1995) GS domain mutations that constitutively activate T beta R-I, the downstream signaling component in the TGF-beta receptor complex. The EMBO journal 14: 2199–2208. Available: http://www.pubmedcentral.nih.gov/articlerender.fcgi?artid=398326&tool=pmcentrez&rendertype=abstract.

19. Shi Y, Massagué J (2003) Mechanisms of TGF-beta signaling from cell membrane to the nucleus. Cell 113: 685–700. Available: http://www.ncbi.nlm.nih.gov/pubmed/12809600.

20. Huse M, Chen Y (1999) Crystal Structure of the Cytoplasmic Domain of the Type I TGF ␤ Receptor in Complex with FKBP12 * Laboratories of Molecular Biophysics. Receptor 96: 425–436.

21. Feng X, Derynck R (1997) A kinase subdomain of transforming growth factor-β (TGF-β) type I receptor determines the TGF-β intracellular signaling specificity. 16: 3912–3923.

22. Kirsch T, Sebald W, Dreyer MK (2000) letters Crystal structure of the BMP-2 – BRIA ectodomain complex. America 7: 492–496.

23. Kirsch T, Nickel J, Sebald W (2000) BMP-2 antagonists emerge from alterations in the low-affinity binding epitope for receptor BMPR-II. The EMBO journal 19: 3314–3324. Available: http://www.pubmedcentral.nih.gov/articlerender.fcgi?artid=313944&tool=pmcentrez&rendertype=abstract.

24. Allendorph GP, Vale WW, Choe S (2006) Structure of the ternary signaling complex of a TGF-beta superfamily member. Proceedings of the National Academy of Sciences of the United States of America 103: 7643–7648. Available: http://www.pubmedcentral.nih.gov/articlerender.fcgi?artid=1456805&tool=pmcentrez&rendertype=abstract.

25. Keller S, Nickel J, Zhang J-L, Sebald W, Mueller TD (2004) Molecular recognition of BMP-2 and BMP receptor IA. Nature structural & molecular biology 11: 481–488. Available: http://www.ncbi.nlm.nih.gov/pubmed/15064755. Accessed 21 July 2011.

26. Gilboa L, Nohe a, Geissendörfer T, Sebald W, Henis YI, et al. (2000) Bone morphogenetic protein receptor complexes on the surface of live cells: a new oligomerization mode for serine/threonine kinase receptors. Molecular biology of the cell 11: 1023–1035. Available: http://www.pubmedcentral.nih.gov/articlerender.fcgi?artid=14828&tool=pmcentrez&rendertype=abstract.

27. Nohe A, Hassel S, Ehrlich M, Neubauer F, Sebald W, et al. (2002) The mode of bone morphogenetic protein (BMP) receptor oligomerization determines different BMP-2 signaling pathways. The Journal of biological chemistry 277: 5330–5338. Available: http://www.ncbi.nlm.nih.gov/pubmed/11714695. Accessed 21 July 2011.

28. Yu PB, Hong CC, Sachidanandan C, Babitt JL, Deng DY, et al. (2008) Dorsomorphin inhibits BMP signals required for embryogenesis and iron metabolism. Nature chemical biology 4: 33–41. Available:

http://www.pubmedcentral.nih.gov/articlerender.fcgi?artid=2727650&tool=pmcentrez&rendertype=abstract. Accessed 13 June 2011.

29. Wrighton KH, Lin X, Yu PB, Feng X-H (2009) Transforming Growth Factor {beta} Can Stimulate Smad1 Phosphorylation Independently of Bone Morphogenic Protein Receptors. The Journal of biological chemistry 284: 9755–9763. Available: http://www.pubmedcentral.nih.gov/articlerender.fcgi?artid=2665096&tool=pmcentrez&rendertype=abstract. Accessed 7 October 2011.

30. Yu PB, Deng DY, Lai CS, Hong CC, Cuny GD, et al. (2008) BMP type I receptor inhibition reduces heterotopic [corrected] ossification. Nature medicine 14: 1363–1369. Available: http://www.pubmedcentral.nih.gov/articlerender.fcgi?artid=2846458&tool=pmcentrez&rendertype=abstract. Accessed 4 July 2011.

31. Hao J, Daleo M a, Murphy CK, Yu PB, Ho JN, et al. (2008) Dorsomorphin, a selective small molecule inhibitor of BMP signaling, promotes cardiomyogenesis in embryonic stem cells. PloS one 3: e2904. Available: http://www.pubmedcentral.nih.gov/articlerender.fcgi?artid=2483414&tool=pmcentrez&rendertype=abstract. Accessed 21 July 2011.

32. Heldin CH, Miyazono K, Ten Dijke P (1997) TGF-beta signalling from cell membrane to nucleus through SMAD proteins. Nature 390: 465–471. Available: http://www.ncbi.nlm.nih.gov/pubmed/9393997.

33. Yamamoto N, Akiyama S, Katagiri T, Namiki M, Kurokawa T, et al. (1997) Smad1 and smad5 act downstream of intracellular signalings of BMP-2 that inhibits myogenic differentiation and induces osteoblast differentiation in C2C12 myoblasts. Biochemical and biophysical research communications 238: 574–580. Available: http://www.ncbi.nlm.nih.gov/pubmed/9299554.

34. Shi Y, Wang YF, Jayaraman L, Yang H, Massagué J, et al. (1998) Crystal structure of a Smad MH1 domain bound to DNA: insights on DNA binding in TGF-beta signaling. Cell 94: 585–594. Available: http://www.ncbi.nlm.nih.gov/pubmed/9741623.

35. Lo RS, Chen YG, Shi Y, Pavletich NP, Massagué J (1998) The L3 loop: a structural motif determining specific interactions between SMAD proteins and TGF-beta receptors. The EMBO journal 17: 996–1005. Available: http://www.pubmedcentral.nih.gov/articlerender.fcgi?artid=1170449&tool=pmcentrez&rendertype=abstract.

36. Chen Y-G, Hata a., Lo RS, Wotton D, Shi Y, et al. (1998) Determinants of specificity in TGF-beta signal transduction. Genes & Development 12: 2144–2152. Available: http://www.genesdev.org/cgi/doi/10.1101/gad.12.14.2144. Accessed 27 January 2012.

37. Qin BY, Chacko BM, Lam SS, De Caestecker MP, Correia JJ, et al. (2001) Structural basis of Smad1 activation by receptor kinase phosphorylation. Molecular cell 8: 1303–1312. Available: http://www.ncbi.nlm.nih.gov/pubmed/11779505.

38. Wu JW, Fairman R, Penry J, Shi Y (2001) Formation of a stable heterodimer between Smad2 and Smad4. The Journal of biological chemistry 276: 20688–20694. Available: http://www.ncbi.nlm.nih.gov/pubmed/11274206. Accessed 26 September 2011.

39. Wu JW, Hu M, Chai J, Seoane J, Huse M, et al. (2001) Crystal structure of a phosphorylated Smad2. Recognition of phosphoserine by the MH2 domain and insights on Smad function in TGF-beta signaling. Molecular cell 8: 1277–1289. Available: http://www.ncbi.nlm.nih.gov/pubmed/11779503.

40. Chacko BM, Qin BY, Tiwari A, Shi G, Lam S, et al. (2004) Structural basis of heteromeric smad protein assembly in TGF-beta signaling. Molecular cell 15: 813–823. Available: http://www.ncbi.nlm.nih.gov/pubmed/15350224.

41. Kawabata M, Inoue H, Hanyu a, Imamura T, Miyazono K (1998) Smad proteins exist as monomers in vivo and undergo homo- and hetero-oligomerization upon activation by serine/threonine kinase receptors. The EMBO journal 17: 4056–4065. Available:

http://www.pubmedcentral.nih.gov/articlerender.fcgi?artid=1170738&tool=pmcentrez&rendertype=abstract.

42. Feng X-H, Derynck R (2005) Specificity and versatility in tgf-beta signaling through Smads. Annual review of cell and developmental biology 21: 659–693. Available: http://www.ncbi.nlm.nih.gov/pubmed/16212511. Accessed 14 June 2011.

43. Inman GJ, Hill CS (2002) Stoichiometry of active smad-transcription factor complexes on DNA. The Journal of biological chemistry 277: 51008–51016. Available: http://www.ncbi.nlm.nih.gov/pubmed/12374795. Accessed 26 September 2011.

44. Hata a, Lo RS, Wotton D, Lagna G, Massagué J (1997) Mutations increasing autoinhibition inactivate tumour suppressors Smad2 and Smad4. Nature 388: 82–87. Available: http://www.ncbi.nlm.nih.gov/pubmed/9214507.

45. Kaivo-oja N, Jeffery L a, Ritvos O, Mottershead DG (2006) Smad signalling in the ovary. Reproductive biology and endocrinology : RB&E 4: 21. Available: http://www.pubmedcentral.nih.gov/articlerender.fcgi?artid=1459162&tool=pmcentrez&rendertype=abstract. Accessed 27 June 2011.

46. Zhu H, Kavsak P, Abdollah S (1999) A SMAD ubiquitin ligase targets the BMP pathway and affects embryonic pattern formation sequence identity and are most closely related to Pub1 , a ubiquitin. Molecular Biology 400: 687–693.

47. Zhang Y, Musci T, Derynck R (1997) The tumor suppressor Smad4/DPC 4 as a central mediator of Smad function. Current biology 7: 270–276. Available: http://www.ncbi.nlm.nih.gov/pubmed/9094310.

48. Derynck R, Zhang YE (2003) Smad-dependent and Smad-independent pathways in TGF-. October 4.

49. De Caestecker MP, Hemmati P, Larisch-Bloch S, Ajmera R, Roberts a B, et al. (1997) Characterization of functional domains within Smad4/DPC4. The Journal of biological chemistry 272: 13690–13696. Available: http://www.ncbi.nlm.nih.gov/pubmed/9153220.

50. Qin B, Lam SS, Lin K (1999) Crystal structure of a transcriptionally active Smad4 fragment. Structure (London, England : 1993) 7: 1493–1503. Available: http://www.ncbi.nlm.nih.gov/pubmed/10647180.

51. Morén A, Imamura T, Miyazono K, Heldin C-H, Moustakas A (2005) Degradation of the tumor suppressor Smad4 by WW and HECT domain ubiquitin ligases. The Journal of biological chemistry 280: 22115–22123. Available: http://www.ncbi.nlm.nih.gov/pubmed/15817471. Accessed 14 October 2011.

52. Morén A, Hellman U, Inada Y, Imamura T, Heldin C-H, et al. (2003) Differential ubiquitination defines the functional status of the tumor suppressor Smad4. The Journal of biological chemistry 278: 33571–33582. Available: http://www.ncbi.nlm.nih.gov/pubmed/12794086. Accessed 27 January 2012.

53. Xu J, Attisano L (2000) Mutations in the tumor suppressors Smad2 and Smad4 inactivate transforming growth factor beta signaling by targeting Smads to the ubiquitin-proteasome pathway. Proceedings of the National Academy of Sciences of the United States of America 97: 4820–4825. Available: http://www.pubmedcentral.nih.gov/articlerender.fcgi?artid=18316&tool=pmcentrez&rendertype=abstract.

54. Lee PSW, Chang C, Liu D, Derynck R (2003) Sumoylation of Smad4, the common Smad mediator of transforming growth factor-beta family signaling. The Journal of biological chemistry 278: 27853–27863. Available: http://www.ncbi.nlm.nih.gov/pubmed/12740389. Accessed 4 August 2011.

55. Ishida W, Hamamoto T, Kusanagi K, Yagi K, Kawabata M, et al. (2000) Smad6 Is a Smad1 / 5-induced Smad Inhibitor. Biochemistry 275: 6075–6079.

56. Afrakhte M, Morén a, Jossan S, Itoh S, Sampath K, et al. (1998) Induction of inhibitory Smad6 and Smad7 mRNA by TGF-beta family members. Biochemical and biophysical research communications 249: 505–511. Available: http://www.ncbi.nlm.nih.gov/pubmed/9712726.

57. Hanyu a, Ishidou Y, Ebisawa T, Shimanuki T, Imamura T, et al. (2001) The N domain of Smad7 is essential for specific inhibition of transforming growth factor-beta signaling. The Journal of cell biology 155: 1017–1027. Available: http://www.pubmedcentral.nih.gov/articlerender.fcgi?artid=2150897&tool=pmcentrez&rendertype=abstract. Accessed 6 July 2011.

58. Fornerod M, Ohno M, Yoshida M, Mattaj IW (1997) CRM1 Is an Export Receptor for Leucine-Rich. Cell 90: 1051–1060.

59. Pierreux CE, Nicolás FJ, Caroline S, Hill CS (2000) Transforming Growth Factor β -Independent Shuttling of Smad4 between the Cytoplasm and Nucleus Transforming Growth Factor β -Independent Shuttling of Smad4 between the Cytoplasm and Nucleus. Society. doi:10.1128/MCB.20.23.9041-9054.2000.Updated.

60. Dirk G, Kutay U (1999) T b c n c. Transport.

61. Nicolás FJ, De Bosscher K, Schmierer B, Hill CS (2004) Analysis of Smad nucleocytoplasmic shuttling in living cells. Journal of cell science 117: 4113–4125. Available: http://www.ncbi.nlm.nih.gov/pubmed/15280432. Accessed 15 August 2011.

62. Xiao Z, Watson N, Rodriguez C, Lodish HF (2001) Nucleocytoplasmic shuttling of Smad1 conferred by its nuclear localization and nuclear export signals. The Journal of biological chemistry 276: 39404–39410. Available: http://www.ncbi.nlm.nih.gov/pubmed/11509558. Accessed 3 August 2011.

63. Schmierer B, Hill CS (2005) Kinetic Analysis of Smad Nucleocytoplasmic Shuttling Reveals a Mechanism for Transforming Growth Factor ß-Dependent Nuclear Accumulation of Smads. Molecular and cellular biology 25: 9845–9858. doi:10.1128/MCB.25.22.9845.

64. Inman GJ, Nicolás FJ, Hill CS (2002) Nucleocytoplasmic shuttling of Smads 2, 3, and 4 permits sensing of TGF-beta receptor activity. Molecular cell 10: 283–294. Available: http://www.ncbi.nlm.nih.gov/pubmed/12191474.

65. Xiao Z, Liu X, Lodish HF (2000) Importin beta mediates nuclear translocation of Smad 3. The Journal of biological chemistry 275: 23425–23428. Available: http://www.ncbi.nlm.nih.gov/pubmed/10846168. Accessed 28 September 2011.

66. Kurisaki a, Kose S, Yoneda Y, Heldin CH, Moustakas a (2001) Transforming growth factor-beta induces nuclear import of Smad3 in an importin-beta1 and Ran-dependent manner. Molecular biology of the cell 12: 1079–1091. Available: http://www.pubmedcentral.nih.gov/articlerender.fcgi?artid=32288&tool=pmcentrez&rendertype=abstract.

67. Xu L, Kang Y, Cöl S, Massagué J (2002) Smad2 nucleocytoplasmic shuttling by nucleoporins CAN/Nup214 and Nup153 feeds TGFbeta signaling complexes in the cytoplasm and nucleus. Molecular cell 10: 271–282. Available: http://www.ncbi.nlm.nih.gov/pubmed/12191473.

68. Chen X, Xu L (2010) Specific nucleoporin requirement for Smad nuclear translocation. Molecular and cellular biology 30: 4022–4034. Available: http://www.pubmedcentral.nih.gov/articlerender.fcgi?artid=2916443&tool=pmcentrez&rendertype=abstract. Accessed 20 October 2011.

69. Xiao Z, Brownawell AM, Macara IG, Lodish HF (2003) A novel nuclear export signal in Smad1 is essential for its signaling activity. The Journal of biological chemistry 278: 34245–34252. Available: http://www.ncbi.nlm.nih.gov/pubmed/12821673. Accessed 26 December 2011.

70. Itóh S, Landström M, Hermansson a, Itoh F, Heldin CH, et al. (1998) Transforming growth factor beta1 induces nuclear export of inhibitory Smad7. The Journal of biological chemistry 273: 29195–29201. Available: http://www.ncbi.nlm.nih.gov/pubmed/9786930.

71. Hanyu a, Ishidou Y, Ebisawa T, Shimanuki T, Imamura T, et al. (2001) The N domain of Smad7 is essential for specific inhibition of transforming growth factor-beta signaling. The Journal of cell biology 155: 1017–1027. Available: http://www.pubmedcentral.nih.gov/articlerender.fcgi?artid=2150897&tool=pmcentrez&rendertype=abstract. Accessed 6 July 2011.

72. Ebisawa T, Fukuchi M, Murakami G, Chiba T, Tanaka K, et al. (2001) Smurf1 interacts with transforming growth factor-beta type I receptor through Smad7 and induces receptor degradation. The Journal of biological chemistry 276: 12477–12480. Available: http://www.ncbi.nlm.nih.gov/pubmed/11278251. Accessed 3 August 2011.

73. Kavsak P, Rasmussen RK, Causing CG, Bonni S, Zhu H, et al. (2000) Smad7 Binds to Smurf2 to Form an E3 Ubiquitin Ligase that Targets the TGF Receptor for Degradation State University of New York at Stony Brook. 6: 1365–1375.

74. López-Rovira T, Chalaux E, Massagué J, Rosa JL, Ventura F (2002) Direct binding of Smad1 and Smad4 to two distinct motifs mediates bone morphogenetic protein-specific transcriptional activation of Id1 gene. The Journal of biological chemistry 277: 3176–3185. Available: http://www.ncbi.nlm.nih.gov/pubmed/11700304. Accessed 14 June 2011.

75. Takase M, Imamura T, Sampath TK, Takeda K, Ichijo H, et al. (1998) Induction of Smad6 mRNA by bone morphogenetic proteins. Biochemical and biophysical research communications 244: 26–29. Available: http://www.ncbi.nlm.nih.gov/pubmed/9514869.

76. Tang SJ, Hoodless P a, Lu Z, Breitman ML, McInnes RR, et al. (1998) The Tlx-2 homeobox gene is a downstream target of BMP signalling and is required for mouse mesoderm development. Development (Cambridge, England) 125: 1877–1887. Available: http://www.ncbi.nlm.nih.gov/pubmed/9550720.

77. Paulsen M, Legewie S, Eils R, Karaulanov E, Niehrs C (2011) Negative feedback in the bone morphogenetic protein 4 (BMP4) synexpression group governs its dynamic signaling range and canalizes development. PNAS 4: 1–6. doi:10.1073/pnas.1100179108/-/DCSupplemental.www.pnas.org/cgi/doi/10.1073/pnas.1100179108.

78. Vindevoghel L, Lechleider RJ, Kon a, De Caestecker MP, Uitto J, et al. (1998) SMAD3/4-dependent transcriptional activation of the human type VII collagen gene (COL7A1) promoter by transforming growth factor beta. Proceedings of the National Academy of Sciences of the United States of America 95: 14769–14774. Available: http://www.pubmedcentral.nih.gov/articlerender.fcgi?artid=24524&tool=pmcentrez&rendertype=abstract.

79. Hata a, Seoane J, Lagna G, Montalvo E, Hemmati-Brivanlou a, et al. (2000) OAZ uses distinct DNA- and protein-binding zinc fingers in separate BMP-Smad and Olf signaling pathways. Cell 100: 229–240. Available: http://www.ncbi.nlm.nih.gov/pubmed/10660046.

80. Zawel L, Dai JL, Buckhaults P, Zhou S, Kinzler KW, et al. (1998) Human Smad3 and Smad4 are sequence-specific transcription activators. Molecular cell 1: 611–617. Available: http://www.ncbi.nlm.nih.gov/pubmed/9660945.

81. Korchynskyi O, Ten Dijke P (2002) Identification and functional characterization of distinct critically important bone morphogenetic protein-specific response elements in the Id1 promoter. The Journal of biological chemistry 277: 4883–4891. Available: http://www.ncbi.nlm.nih.gov/pubmed/11729207. Accessed 18 July 2011.

82. Gazzerro E, Canalis E (2006) Bone morphogenetic proteins and their antagonists. Reviews in endocrine & metabolic disorders 7: 51–65. Available: http://www.ncbi.nlm.nih.gov/pubmed/17029022. Accessed 17 June 2011.

83. Zimmerman LB, De Jesús-Escobar JM, Harland RM (1996) The Spemann organizer signal noggin binds and inactivates bone morphogenetic protein 4. Cell 86: 599–606. Available: http://www.ncbi.nlm.nih.gov/pubmed/8752214.

84. Groppe J, Greenwald J, Wiater E, Rodriguez-Leon J, Economides AN, et al. (2002) Structural basis of BMP signalling inhibition by the cystine knot protein Noggin. Nature 420: 636–642. Available: http://www.ncbi.nlm.nih.gov/pubmed/12478285.

85. Samad T a, Rebbapragada A, Bell E, Zhang Y, Sidis Y, et al. (2005) DRAGON, a bone morphogenetic protein co-receptor. The Journal of biological chemistry 280: 14122–14129. Available: http://www.ncbi.nlm.nih.gov/pubmed/15671031. Accessed 20 July 2011.

86. Babitt JL, Zhang Y, Samad T a, Xia Y, Tang J, et al. (2005) Repulsive guidance molecule (RGMa), a DRAGON homologue, is a bone morphogenetic protein co-receptor. The Journal of biological chemistry 280: 29820–29827. Available: http://www.ncbi.nlm.nih.gov/pubmed/15975920. Accessed 8 October 2011.

87. Halbrooks PJ, Ding R, Wozney JM, Bain G (2007) Role of RGM coreceptors in bone morphogenetic protein signaling. Journal of molecular signaling 2: 4. Available: http://www.pubmedcentral.nih.gov/articlerender.fcgi?artid=1933414&tool=pmcentrez&rendertype=abstract. Accessed 29 July 2011.

88. Scherner O, Meurer SK, Tihaa L, Gressner AM, Weiskirchen R (2007) Endoglin differentially modulates antagonistic transforming growth factor-beta1 and BMP-7 signaling. The Journal of biological chemistry 282: 13934–13943. Available: http://www.ncbi.nlm.nih.gov/pubmed/17376778. Accessed 22 July 2011.

89. Kirkbride KC, Townsend T a, Bruinsma MW, Barnett J V, Blobe GC (2008) Bone morphogenetic proteins signal through the transforming growth factor-beta type III receptor. The Journal of biological chemistry 283: 7628–7637. Available: http://www.ncbi.nlm.nih.gov/pubmed/18184661. Accessed 3 October 2011.

90. Onichtchouk D, Chen YG, Dosch R, Gawantka V, Delius H, et al. (1999) Silencing of TGF-beta signalling by the pseudoreceptor BAMBI. Nature 401: 480–485. Available: http://www.ncbi.nlm.nih.gov/pubmed/10519551.

91. Sammar M, Stricker S, Schwabe GC, Sieber C, Hartung A, et al. (2004) Modulation of GDF5/BRI-b signalling through interaction with the tyrosine kinase receptor Ror2. Genes to cells : devoted to molecular & cellular mechanisms 9: 1227–1238. Available: http://www.ncbi.nlm.nih.gov/pubmed/15569154. Accessed 14 December 2011.

92. Jin W, Yun C, Kim H-S, Kim S-J (2007) TrkC binds to the bone morphogenetic protein type II receptor to suppress bone morphogenetic protein signaling. Cancer research 67: 9869–9877. Available: http://www.ncbi.nlm.nih.gov/pubmed/17942918. Accessed 10 February 2012.

93. Hata a, Lagna G, Massagué J, Hemmati-Brivanlou a (1998) Smad6 inhibits BMP/Smad1 signaling by specifically competing with the Smad4 tumor suppressor. Genes & development 12: 186–197. Available: http://www.ncbi.nlm.nih.gov/pubmed/21540640.

94. Murakami G, Watabe T, Takaoka K, Miyazono K, Imamura T (2003) Cooperative Inhibition of Bone Morphogenetic Protein Signaling by Smurf1 and Inhibitory Smads. Molecular Biology of the Cell 14: 2809 –2817. doi:10.1091/mbc.E02.

95. Lin X, Liang Y, Sun B, Liang M, Brunicardi FC, et al. (2003) Smad6 Recruits Transcription Corepressor CtBP To Repress Bone Morphogenetic Protein-Induced Transcription Smad6 Recruits Transcription Corepressor CtBP To Repress Bone Morphogenetic Protein-Induced Transcription. Society. doi:10.1128/MCB.23.24.9081.

96. Bai S, Shi X, Yang X, Cao X (2000) Smad6 as a transcriptional corepressor. The Journal of biological chemistry 275: 8267–8270. Available: http://www.ncbi.nlm.nih.gov/pubmed/10722652.

97. Nakao A, Afrakhte M, More A, Nakayama T, Christian JL, et al. (1997) Identification of Smad7 , a TGF ℓ -inducible antagonist of TGF- ℓ signalling. Nature 389.

98. Koinuma D, Shinozaki M, Komuro A, Goto K, Saitoh M, et al. (2003) Arkadia ampli ® es TGF-b superfamily signalling through degradation of Smad7. EMBO Journal 22: 6458–6470.

99. Takeda M, Mizuide M, Oka M, Watabe T, Inoue H, et al. (2004) Interaction with Smad4 Is Indispensable for Suppression of BMP Signaling by c-Ski. Molecular Biology of the Cell 15: 963–972. doi:10.1091/mbc.E03.

100. Suzuki H, Yagi K, Kondo M, Kato M, Miyazono K, et al. (2004) c-Ski inhibits the TGF-beta signaling pathway through stabilization of inactive Smad complexes on Smad-binding elements. Oncogene 23: 5068–5076. Available: http://www.ncbi.nlm.nih.gov/pubmed/15107821. Accessed 10 February 2012.

101. Yoshida Y, Tanaka S, Umemori H, Minowa O, Usui M, et al. (2000) of BMP / Smad Signaling by Tob in Osteoblasts. 103: 1085–1097.

102. Yoshida Y, Von Bubnoff A, Ikematsu N, Blitz IL, Tsuzuku JK, et al. (2003) Tob proteins enhance inhibitory Smad-receptor interactions to repress BMP signaling. Mechanisms of Development 120: 629–637. Available: http://linkinghub.elsevier.com/retrieve/pii/S0925477303000200. Accessed 10 February 2012.

103. Zhang Y, Chang C, Gehling DJ, Hemmati-Brivanlou a, Derynck R (2001) Regulation of Smad degradation and activity by Smurf2, an E3 ubiquitin ligase. Proceedings of the National Academy of Sciences of the United States of America 98: 974–979. Available: http://www.pubmedcentral.nih.gov/articlerender.fcgi?artid=14694&tool=pmcentrez&rendertype=abstract.

104. Ying Y, Qi X, Zhao GQ (2001) Induction of primordial germ cells from murine epiblasts by synergistic action of BMP4 and BMP8B signaling pathways. Proceedings of the National Academy of Sciences of the United States of America 98: 7858–7862. Available: http://www.pubmedcentral.nih.gov/articlerender.fcgi?artid=35432&tool=pmcentrez&rendertype=abstract.

105. Chang H, Huylebroeck D, Verschueren K, Guo Q, Matzuk MM, et al. (1999) Smad5 knockout mice die at mid-gestation due to multiple embryonic and extraembryonic defects. Development (Cambridge, England) 126: 1631–1642. Available: http://www.ncbi.nlm.nih.gov/pubmed/10079226.

106. Tremblay KD, Dunn NR, Robertson EJ (2001) Mouse embryos lacking Smad1 signals display defects in extra-embryonic tissues and germ cell formation. Development (Cambridge, England) 128: 3609–3621. Available: http://www.ncbi.nlm.nih.gov/pubmed/11566864.

107. Mishina Y, Suzuki a, Ueno N, Behringer RR (1995) Bmpr encodes a type I bone morphogenetic protein receptor that is essential for gastrulation during mouse embryogenesis. Genes & Development 9: 3027–3037. Available: http://www.genesdev.org/cgi/doi/10.1101/gad.9.24.3027. Accessed 18 November 2011.

108. Beppu H, Kawabata M, Hamamoto T, Chytil a, Minowa O, et al. (2000) BMP type II receptor is required for gastrulation and early development of mouse embryos. Developmental biology 221: 249–258. Available: http://www.ncbi.nlm.nih.gov/pubmed/10772805. Accessed 13 February 2012.

109. Hamada H, Meno C, Watanabe D, Saijoh Y (2002) Establishment of vertebrate left-right asymmetry. Nature reviews Genetics 3: 103–113. Available: http://www.ncbi.nlm.nih.gov/pubmed/11836504. Accessed 16 July 2011.

110. Chang H, Zwijsen a, Vogel H, Huylebroeck D, Matzuk MM (2000) Smad5 is essential for left-right asymmetry in mice. Developmental biology 219: 71–78. Available: http://www.ncbi.nlm.nih.gov/pubmed/10677256. Accessed 12 November 2011.

111. Fujiwara T, Dehart DB, Sulik KK, Hogan BLM (2002) Distinct requirements for extra-embryonic and embryonic bone morphogenetic protein 4 in the formation of the node and primitive streak and

coordination of left-right asymmetry in the mouse. Development (Cambridge, England) 129: 4685–4696. Available: http://www.ncbi.nlm.nih.gov/pubmed/12361961.

112. Baker JC, Beddington RSP, Harland RM (1999) activates neural development Wnt signaling in Xenopus embryos inhibits Bmp4 expression and activates neural development. Genes & Development: 3149–3159.

113. Zhang K, Li L, Huang C, Shen C, Tan F, et al. (2010) Distinct functions of BMP4 during different stages of mouse ES cell neural commitment. Development (Cambridge, England) 137: 2095–2105. Available: http://www.ncbi.nlm.nih.gov/pubmed/20504958. Accessed 23 August 2011.

114. Furuta Y, Hogan BLM (1998) BMP4 is essential for lens induction in the mouse embryo. Genes & Development 12: 3764–3775. Available: http://www.genesdev.org/cgi/doi/10.1101/gad.12.23.3764. Accessed 13 February 2012.

115. Luo G, Hofmann C, Bronckers a L, Sohocki M, Bradley a, et al. (1995) BMP-7 is an inducer of nephrogenesis, and is also required for eye development and skeletal patterning. Genes & Development 9: 2808–2820. Available: http://www.genesdev.org/cgi/doi/10.1101/gad.9.22.2808. Accessed 16 August 2011.

116. Daluiski a, Engstrand T, Bahamonde ME, Gamer LW, Agius E, et al. (2001) Bone morphogenetic protein-3 is a negative regulator of bone density. Nature genetics 27: 84–88. Available: http://www.ncbi.nlm.nih.gov/pubmed/11138004.

117. Kim RY, Robertson EJ, Solloway MJ (2001) Bmp6 and Bmp7 are required for cushion formation and septation in the developing mouse heart. Developmental biology 235: 449–466. Available: http://www.ncbi.nlm.nih.gov/pubmed/11437450. Accessed 3 August 2011.

118. Lawson K a, Dunn NR, Roelen B a, Zeinstra LM, Davis a M, et al. (1999) Bmp4 is required for the generation of primordial germ cells in the mouse embryo. Genes & development 13: 424–436. Available: http://www.pubmedcentral.nih.gov/articlerender.fcgi?artid=316469&tool=pmcentrez&rendertype=abstract.

119. Ying Y, Liu XM, Marble a, Lawson K a, Zhao GQ (2000) Requirement of Bmp8b for the generation of primordial germ cells in the mouse. Molecular endocrinology (Baltimore, Md) 14: 1053–1063. Available: http://www.ncbi.nlm.nih.gov/pubmed/10894154.

120. Zhao GQ, Garbers DL (2002) Male germ cell specification and differentiation. Developmental cell 2: 537–547. Available: http://www.ncbi.nlm.nih.gov/pubmed/17631837.

121. Juengel JL (2002) Growth Differentiation Factor 9 and Bone Morphogenetic Protein 15 Are Essential for Ovarian Follicular Development in Sheep. Biology of Reproduction 67: 1777–1789. Available: http://www.biolreprod.org/cgi/doi/10.1095/biolreprod.102.007146. Accessed 20 February 2012.

122. Connor JM, Evans D a (1982) Genetic aspects of fibrodysplasia ossificans progressiva. Journal of medical genetics 19: 35–39. Available: http://www.pubmedcentral.nih.gov/articlerender.fcgi?artid=3253727&tool=pmcentrez&rendertype=abstract.

123. Shore EM, Xu M, Feldman GJ, Fenstermacher D a, Cho T-J, et al. (2006) A recurrent mutation in the BMP type I receptor ACVR1 causes inherited and sporadic fibrodysplasia ossificans progressiva. Nature genetics 38: 525–527. Available: http://www.ncbi.nlm.nih.gov/pubmed/16642017. Accessed 11 September 2011.

124. Sémonin O, Fontaine K, Daviaud C, Ayuso C, Lucotte G (2001) Identification of Three Novel Mutations of the Noggin Gene in Patients With Fibrodysplasia Ossificans Progressiva. American Journal of Medical Genetics 102: 314–317.

125. Lucotte G, Sémonin O, Lutz P (1999) A de novo heterozygous deletion of 42 base-pairs in the noggin gene of a fibrodysplasia ossificans progressiva patient. Clinical Genetics 56: 469–470.

126. Puri A, McGoon MD, Kushwaha SS (2007) Pulmonary arterial hypertension: current therapeutic strategies. Nature clinical practice Cardiovascular medicine 4: 319–329. Available: http://www.ncbi.nlm.nih.gov/pubmed/17522721. Accessed 1 March 2012.

127. Atkinson C, Stewand S, Upton PD, Machado R, Thomson JR, et al. (2002) Primary Pulmonary Hypertension Is Associated With Reduced Pulmonary Vascular Expression of Type II Bone Morphogenetic Protein Receptor. Circulation 105: 1672–1678. Available: http://circ.ahajournals.org/cgi/doi/10.1161/01.CIR.0000012754.72951.3D. Accessed 6 March 2012.

128. Lane KB, Machado RD, Pauciulo MW, Thomson JR, Phillips J a, et al. (2000) Heterozygous germline mutations in BMPR2, encoding a TGF-beta receptor, cause familial primary pulmonary hypertension. Nature genetics 26: 81–84. Available: http://www.ncbi.nlm.nih.gov/pubmed/10973254.

129. Deng Z, Morse JH, Slager SL, Cuervo N, Moore KJ, et al. (2000) Familial primary pulmonary hypertension (gene PPH1) is caused by mutations in the bone morphogenetic protein receptor-II gene. American journal of human genetics 67: 737–744. Available: http://www.pubmedcentral.nih.gov/articlerender.fcgi?artid=1287532&tool=pmcentrez&rendertype=abstract.

130. Thomson JR, Machado RD, Pauciulo MW, Morgan N V, Humbert M, et al. (2000) Sporadic primary pulmonary hypertension is associated with germline mutations of the gene encoding BMPR-II, a receptor member of the TGF-beta family. Journal of medical genetics 37: 741–745. Available: http://www.pubmedcentral.nih.gov/articlerender.fcgi?artid=1757155&tool=pmcentrez&rendertype=abstract.

131. West J, Fagan K, Steudel W, Fouty B, Lane K, et al. (2004) Pulmonary hypertension in transgenic mice expressing a dominant-negative BMPRII gene in smooth muscle. Circulation research 94: 1109–1114. Available: http://www.ncbi.nlm.nih.gov/pubmed/15031260. Accessed 9 April 2012.

132. Nasim MT, Ogo T, Chowdhury HM, Zhao L, Chen C -n., et al. (2012) BMPR-II deficiency elicits pro-proliferative and anti-apoptotic responses through the activation of TGF -TAK1-MAPK pathways in PAH. Human Molecular Genetics 21: 2548–2558. Available: http://www.hmg.oxfordjournals.org/cgi/doi/10.1093/hmg/dds073. Accessed 7 May 2012.

133. McDonald J, Pyeritz RE (n.d.) Hereditary Hemorrhagic Telangiectasia. GeneReviews.

134. Dupuis-Girod S, Bailly S, Plauchu H (2010) Hereditary hemorrhagic telangiectasia: from molecular biology to patient care. Journal of thrombosis and haemostasis : JTH 8: 1447–1456. Available: http://www.ncbi.nlm.nih.gov/pubmed/20345718. Accessed 6 April 2012.

135. Govani FS, Shovlin CL (2009) Hereditary haemorrhagic telangiectasia: a clinical and scientific review. European journal of human genetics : EJHG 17: 860–871. Available: http://www.pubmedcentral.nih.gov/articlerender.fcgi?artid=2986493&tool=pmcentrez&rendertype=abstract. Accessed 23 March 2012.

136. Osier R-, Ii T, Hht A (1995) A third locus for hereditary haemorrhagic telangiectasia maps to chromosome 12q. Human Molecular Genetics 4: 945–949.

137. Johnson DW, Berg JN, Gallione CJ, McAllister K a, Warner JP, et al. (1995) A second locus for hereditary hemorrhagic telangiectasia maps to chromosome 12. Genome Research 5: 21–28. Available: http://www.genome.org/cgi/doi/10.1101/gr.5.1.21. Accessed 16 May 2012.

138. Shovlin CL, Hughes JMB, Tuddenham EGD, Temperley I, Perembelon YFN, et al. (1994) A gene for hereditary haemorrhagic telangiectasia maps to chromosome 9q3. Nature genetics 6.

139. Gallione CJ, Repetto GM, Legius E, Rustgi AK, Schelley SL, et al. (2004) Mechanisms of disease A combined syndrome of juvenile polyposis and hereditary haemorrhagic telangiectasia associated with mutations in MADH4 (SMAD4). The Lancet 363: 852–859.

140. Waite K a, Eng C (2003) From developmental disorder to heritable cancer: it's all in the BMP/TGF-beta family. Nature reviews Genetics 4: 763–773. Available: http://www.ncbi.nlm.nih.gov/pubmed/14526373. Accessed 21 March 2012.

141. Klein PS (2004) Interactions between BMP and Wnt Signaling Pathways nd es Bio sci en No t D ist r ibu Hui-Chuan Huang. 3: 676–678.

142. Gobbi G, Sangiorgi L, Lenzi L, Casadei R, Canaider S, et al. (2002) Seven BMPs and all their receptors are simultaneously expressed in osteosarcoma cells. International Journal of Oncology 20: 143–147.

143. Arnold SF, Tims E, Mcgrath BE (1999) Identification of bone morphogenetic proteins and their receptors in human breast cancer cell lines: importance of BMP2. Cytokine 11: 1031–1037. Available: http://www.ncbi.nlm.nih.gov/pubmed/10623428.

144. Kodach LL, Bleuming S a, Musler AR, Peppelenbosch MP, Hommes DW, et al. (2008) The bone morphogenetic protein pathway is active in human colon adenomas and inactivated in colorectal cancer. Cancer 112: 300–306. Available: http://www.ncbi.nlm.nih.gov/pubmed/18008360. Accessed 24 May 2012.

145. Beck SE, Jung BH, Fiorino A, Gomez J, Rosario E Del, et al. (2006) Bone morphogenetic protein signaling and growth suppression in colon cancer. American journal of physiology Gastrointestinal and liver physiology 291: G135–45. Available: http://www.ncbi.nlm.nih.gov/pubmed/16769811. Accessed 25 April 2012.

146. Wen X-Z, Akiyama Y, Baylin SB, Yuasa Y (2006) Frequent epigenetic silencing of the bone morphogenetic protein 2 gene through methylation in gastric carcinomas. Oncogene 25: 2666–2673. Available: http://www.ncbi.nlm.nih.gov/pubmed/16314833. Accessed 24 May 2012.

147. Yamada N, Kato M, Ten Dijke P, Yamashita H, Sampath TK, et al. (1996) Bone morphogenetic protein type IB receptor is progressively expressed in malignant glioma tumours. British journal of cancer 73: 624–629. Available: http://www.pubmedcentral.nih.gov/articlerender.fcgi?artid=2074358&tool=pmcentrez&rendertype=abstract.

148. Ming Kwan K, Li AG, Wang X-J, Wurst W, Behringer RR (2004) Essential roles of BMPR-IA signaling in differentiation and growth of hair follicles and in skin tumorigenesis. Genesis (New York, NY : 2000) 39: 10–25. Available: http://www.ncbi.nlm.nih.gov/pubmed/15124223. Accessed 24 May 2012.

149. Hallahan AR, Pritchard JI, Chandraratna R a S, Ellenbogen RG, Geyer JR, et al. (2003) BMP-2 mediates retinoid-induced apoptosis in medulloblastoma cells through a paracrine effect. Nature medicine 9: 1033–1038. Available: http://www.ncbi.nlm.nih.gov/pubmed/12872164.

150. Miyazaki H, Watabe T, Kitamura T, Miyazono K (2004) BMP signals inhibit proliferation and in vivo tumor growth of androgen-insensitive prostate carcinoma cells. Oncogene 23: 9326–9335. Available: http://www.ncbi.nlm.nih.gov/pubmed/15531927. Accessed 4 April 2012.

151. Chromosome H, Hahn SA, Schutte M, Hoque ATMS, Moskaluk CA, et al. (1994) DPC4 , A Candidate Tumor Suppressor Gene at. 107247: 21–24.

152. Qiao W, Li a G, Owens P, Xu X, Wang X-J, et al. (2006) Hair follicle defects and squamous cell carcinoma formation in Smad4 conditional knockout mouse skin. Oncogene 25: 207–217. Available: http://www.ncbi.nlm.nih.gov/pubmed/16170355. Accessed 24 May 2012.

153. Gautschi OP, Frey SP, Zellweger R (2007) Bone Morphogenetic Proteins in Clinical Applications. ANZ Journal of Surgery 77: 626–631. Available: http://www.blackwell-synergy.com/doi/abs/10.1111/j.1445-2197.2007.04175.x. Accessed 26 March 2012.

154. Kang Q, Sun MH, Cheng H, Peng Y, Montag a G, et al. (2004) Characterization of the distinct orthotopic bone-forming activity of 14 BMPs using recombinant adenovirus-mediated gene delivery. Gene Therapy 11: 1312–1320. Available: http://www.nature.com/doifinder/10.1038/sj.gt.3302298. Accessed 5 May 2012.

155. Seeherman H, Li R, Wozney J (2003) A review of preclinical program development for evaluating injectable carriers for osteogenic factors. The Journal of bone and joint surgery American volume 85-A Suppl: 96–108. Available: http://www.ncbi.nlm.nih.gov/pubmed/12925616.

156. Bessa PC, Casal M, Reis RL (2008) Bone morphogenetic proteins in tissue engineering : the road from the laboratory to the clinic , part I (basic concepts): 1–13. doi:10.1002/term.

157. Kanakaris NK, Mallina R, Calori GM, Kontakis G, Giannoudis P V (2009) Use of bone morphogenetic proteins in arthrodesis: clinical results. Injury 40 Suppl 3: S62–6. Available: http://www.ncbi.nlm.nih.gov/pubmed/20082794. Accessed 25 May 2012.

158. Zeisberg M, Kalluri R (2008) Reversal of experimental renal fibrosis by BMP7 provides insights into novel therapeutic strategies for chronic kidney disease. Pediatric nephrology (Berlin, Germany) 23: 1395–1398. Available: http://www.ncbi.nlm.nih.gov/pubmed/18446379. Accessed 24 April 2012.

159. Zouani OF, Chollet C, Guillotin B, Durrieu M-C (2010) Differentiation of pre-osteoblast cells on poly(ethylene terephthalate) grafted with RGD and/or BMPs mimetic peptides. Biomaterials 31: 8245–8253. Available: http://www.ncbi.nlm.nih.gov/pubmed/20667411. Accessed 15 May 2012.

160. Yaffe D, Saxel O (1977) Serial passaging and differentiation of myogenic cells isolated from dystrophic mouse muscle. Nature 270: 725–727.

161. Kawakami K, Noda T (2004) Transposition of the Tol2 Element, an Ac-Like Element From the Japanese Medaka Fish Oryzias latipes, in Mouse Embryonic Stem Cells. Genetics 166: 895–899.

162. Fan F, Wood K (2007) Bioluminescent assays for high-throughput screening. Assay Drug Dev Technol 5: 127–136.

163. Monteiro RM, De Sousa Lopes SMC, Korchynskyi O, Ten Dijke P, Mummery CL (2004) Spatio-temporal activation of Smad1 and Smad5 in vivo: monitoring transcriptional activity of Smad proteins. Journal of cell science 117: 4653–4663. Available: http://www.ncbi.nlm.nih.gov/pubmed/15331632. Accessed 28 September 2011.

164. Ruecker O, Zillner K, Groebner-Ferreira R, Heitzer M (2008) Gaussia-luciferase as a sensitive reporter gene for monitoring promoter activity in the nucleus of the green alga Chlamydomonas reinhardtii. Molecular genetics and genomics 280: 153–162. Available: http://www.ncbi.nlm.nih.gov/pubmed/18516621. Accessed 23 September 2011.

165. Zi Z, Feng Z, Chapnick D a, Dahl M, Deng D, et al. (2011) Quantitative analysis of transient and sustained transforming growth factor-β signaling dynamics. Molecular systems biology 7. Available: http://www.pubmedcentral.nih.gov/articlerender.fcgi?artid=3130555&tool=pmcentrez&rendertype=abstract. Accessed 22 March 2012.

166. Bachmann J, Raue a, Schilling M, Becker V, Timmer J, et al. (2012) Predictive mathematical models of cancer signalling pathways. Journal of internal medicine 271: 155–165. Available: http://www.ncbi.nlm.nih.gov/pubmed/22142263. Accessed 5 March 2012.

167. Niethammer P, Bastiaens P, Karsenti E (2004) Stathmin-tubulin interaction gradients in motile and mitotic cells. Science (New York, NY) 303: 1862–1866. Available: http://www.ncbi.nlm.nih.gov/pubmed/15031504. Accessed 15 March 2012.

168. Kholodenko BN, Hancock JF, Kolch W (2010) Signalling ballet in space and time. Nature reviews Molecular cell biology 11: 414–426. Available: http://www.pubmedcentral.nih.gov/articlerender.fcgi?artid=2977972&tool=pmcentrez&rendertype=abstract. Accessed 8 March 2012.

169. Marshall CJ (1995) Specificity of receptor tyrosine kinase signaling: transient versus sustained extracellular signal-regulated kinase activation. Cell 80: 179–185. Available: http://www.ncbi.nlm.nih.gov/pubmed/7834738.

170. Batchelor E, Loewer A, Mock C, Lahav G (2011) Stimulus-dependent dynamics of p53 in single cells. Molecular systems biology 7: 488. Available: http://www.pubmedcentral.nih.gov/articlerender.fcgi?artid=3130553&tool=pmcentrez&rendertype=abstract. Accessed 1 March 2012.

171. Covert MW (2011) NIH Public Access. 466: 267–271. doi:10.1038/nature09145.Single-cell.

172. Schul D, Schmitt A, Regneri J, Schartl M, Wagner TU (2013) Bursted BMP triggered receptor kinase activity drives Smad1 mediated long-term target gene oscillation in c2c12 cells. PloS one 8: e59442. Available: http://www.pubmedcentral.nih.gov/articlerender.fcgi?artid=3613406&tool=pmcentrez&rendertype=abstract. Accessed 26 May 2013.

173. Tribulo C, Aybar MJ, Nguyen VH, Mullins MC, Mayor R (2003) Regulation of Msx genes by a Bmp gradient is essential for neural crest specification. Development (Cambridge, England) 130: 6441–6452. Available: http://www.ncbi.nlm.nih.gov/pubmed/14627721. Accessed 17 March 2013.

174. Massagué J, Blain SW, Lo RS (2000) TGFbeta signaling in growth control, cancer, and heritable disorders. Cell 103: 295–309. Available: http://www.ncbi.nlm.nih.gov/pubmed/11057902.

175. Park Y, Kim JW, Kim DS, Kim EB, Park SJ, et al. (2008) The Bone Morphogenesis Protein-2 (BMP-2) is associated with progression to metastatic disease in gastric cancer. Cancer research and treatment : official journal of Korean Cancer Association 40: 127–132. Available: http://www.pubmedcentral.nih.gov/articlerender.fcgi?artid=2697466&tool=pmcentrez&rendertype=abstract.

176. Alarmo E-L, Kallioniemi A (2010) Bone morphogenetic proteins in breast cancer: dual role in tumourigenesis? Endocrine-related cancer 17: R123–39. Available: http://www.ncbi.nlm.nih.gov/pubmed/20335308. Accessed 26 March 2012.

177. Jiang S, Fritz DT, Rogers MB (2010) A conserved post-transcriptional BMP2 switch in lung cells. Journal of cellular biochemistry 110: 509–521. Available: http://www.ncbi.nlm.nih.gov/pubmed/20432245. Accessed 2 June 2012.

178. Zheng Y, Wu G, Liu T, Liu Y, Wismeijer D, et al. (2013) A Novel BMP2-Coprecipitated, Layer-by-Layer Assembled Biomimetic Calcium Phosphate Particle: A Biodegradable and Highly Efficient Osteoinducer. Clinical implant dentistry and related research: 1–12. Available: http://www.ncbi.nlm.nih.gov/pubmed/23458515. Accessed 29 March 2013.

179. Zhao B, Katagiri T, Toyoda H, Takada T, Yanai T, et al. (2006) Heparin potentiates the in vivo ectopic bone formation induced by bone morphogenetic protein-2. The Journal of biological chemistry 281: 23246–23253. Available: http://www.ncbi.nlm.nih.gov/pubmed/16754660. Accessed 10 April 2012.

180. Ferrell JE (n.d.) Feedback regulation of opposing enzymes generates bistable responses. 18: 244–245.

181. Niehrs C (2010) On growth and form: a Cartesian coordinate system of Wnt and BMP signaling specifies bilaterian body axes. Development (Cambridge, England) 137: 845–857. Available: http://www.ncbi.nlm.nih.gov/pubmed/20179091. Accessed 29 March 2013.

182. Aybar MJ, Mayor R (2002) Early induction of neural crest cells: lessons learned from frog, fish and chick. Current opinion in genetics & development 12: 452–458. Available: http://www.ncbi.nlm.nih.gov/pubmed/12100892.

183. Alborzinia H, Schmidt-glenewinkel H, Ilkavets I, Breitkopf- K, Feld IN, et al. (2012) Quantitative kinetic analysis of BMP2 uptake into cells and its modulation by BMP-antagonists. Journal of cell.

184. Teves SS, Henikoff S (2013) The heat shock response: A case study of chromatin dynamics in gene regulation. Biochemistry and Cell Biology 91: 42–48.

185. Más J, Gerritsen I, Hahmann C, Jiménez-Cervantes C, García-Borrón J (2003) Rate limiting factors in melanocortin 1 receptor signalling through the cAMP pathway. Pigment Cell Res 16: 540–547.

186. Barkley LR, Hong HK, Kingsbury SR, James M, Stoeber K, et al. (2007) Cdc6 is a rate-limiting factor for proliferative capacity during HL60 cell differentiation. Experimental cell research 313: 3789–3799. Available: http://www.ncbi.nlm.nih.gov/pubmed/17689530. Accessed 26 May 2013.

187. Ghorpade DS, Kaveri S V, Bayry J, Balaji KN (2011) Cooperative regulation of NOTCH1 protein-phosphatidylinositol 3-kinase (PI3K) signaling by NOD1, NOD2, and TLR2 receptors renders enhanced refractoriness to transforming growth factor-beta (TGF-beta)- or cytotoxic T-lymphocyte antigen 4 (CTLA-4)-mediated . The Journal of biological chemistry 286: 31347–31360. Available: http://www.pubmedcentral.nih.gov/articlerender.fcgi?artid=3173143&tool=pmcentrez&rendertype=abstract. Accessed 26 May 2013.

188. Enderling H, Hahnfeldt P (2011) Cancer stem cells in solid tumors: is “evading apoptosis” a hallmark of cancer? Progress in biophysics and molecular biology 106: 391–399. Available: http://www.ncbi.nlm.nih.gov/pubmed/21473880. Accessed 1 June 2013.

189. Israël M, Schwartz L (2011) The metabolic advantage of tumor cells. Molecular cancer 10: 70. Available: http://www.pubmedcentral.nih.gov/articlerender.fcgi?artid=3118193&tool=pmcentrez&rendertype=abstract. Accessed 31 May 2013.

190. Haeusgen W, Herdegen T, Waetzig V (2011) The bottleneck of JNK signaling: molecular and functional characteristics of MKK4 and MKK7. European journal of cell biology 90: 536–544. Available: http://www.ncbi.nlm.nih.gov/pubmed/21333379. Accessed 30 May 2013.

191. De Jong DS, Vaes BLT, Dechering KJ, Feijen A, Hendriks JM a, et al. (2004) Identification of novel regulators associated with early-phase osteoblast differentiation. Journal of bone and mineral research : the official journal of the American Society for Bone and Mineral Research 19: 947–958. Available: http://www.ncbi.nlm.nih.gov/pubmed/15125793. Accessed 13 June 2011.

192. Yoshiura S, Ohtsuka T, Takenaka Y, Nagahara H, Yoshikawa K, et al. (2007) Ultradian oscillations of Stat, Smad and Hes1 expression in response to serum. PNAS 104: 11292–11297.

193. Kobayashi T, Mizuno H, Imayoshi I, Furusawa C, Shirahige K, et al. (2009) The cyclic gene Hes1 contributes to diverse differentiation responses of embryonic stem cells. Genes & Development 23: 1870–1875. doi:10.1101/gad.1823109.1870.

194. Fei T, Xia K, Li Z, Zhou B, Zhu S, et al. (2010) Genome-wide mapping of SMAD target genes reveals the role of BMP signaling in embryonic stem cell fate determination. Genome research 20: 36–44. Available: http://www.pubmedcentral.nih.gov/articlerender.fcgi?artid=2798829&tool=pmcentrez&rendertype=abstract. Accessed 25 December 2012.

195. Umulis D, O’Connor MB, Blair SS (2009) The extracellular regulation of bone morphogenetic protein signaling. Development (Cambridge, England) 136: 3715–3728. Available: http://www.pubmedcentral.nih.gov/articlerender.fcgi?artid=2766339&tool=pmcentrez&rendertype=abstract. Accessed 10 March 2013.

196. Mengel B, Hunziker A, Pedersen L, Trusina A, Jensen MH, et al. (2010) Modeling oscillatory control in NF-κB, p53 and Wnt signaling. Current opinion in genetics & development 20: 656–664. Available: http://www.ncbi.nlm.nih.gov/pubmed/20934871. Accessed 20 March 2013.

197. Plikus M V., Widelitz RB, Maxson R, Chuong C-M (2009) Analyses of regenerative wave patterns in adult hair follicle populations reveal macro-environmental regulation of stem cell activity. October 53: 857–868. doi:10.1387/ijdb.072564mp.Analyses.

198. Shankaran H, Ippolito DL, Chrisler WB, Resat H, Bollinger N, et al. (2009) Rapid and sustained nuclear-cytoplasmic ERK oscillations induced by epidermal growth factor. Molecular systems biology 5: 332. Available:

http://www.pubmedcentral.nih.gov/articlerender.fcgi?artid=2824491&tool=pmcentrez&rendertype=abstract. Accessed 3 August 2011.

199. Purvis JE, Karhohs KW, Mock C, Batchelor E, Loewer a., et al. (2012) p53 Dynamics Control Cell Fate. Science 336: 1440–1444. Available: http://www.sciencemag.org/cgi/doi/10.1126/science.1218351. Accessed 14 June 2012.

200. circadian clock.pdf (n.d.).

201. Rapp PE, Mees a I, Sparrow CT (1981) Frequency encoded biochemical regulation is more accurate than amplitude dependent control. Journal of theoretical biology 90: 531–544. Available: http://www.ncbi.nlm.nih.gov/pubmed/6272030.

202. Tostevin F, De Ronde W, Ten Wolde P (2012) Reliability of Frequency and Amplitude Decoding in Gene Regulation. Physical Review Letters 108: 1–5. Available: http://link.aps.org/doi/10.1103/PhysRevLett.108.108104. Accessed 25 July 2012.

203. Cheong R, Levchenko A (2010) Oscillatory signaling processes: the how, the why and the where. Current opinion in genetics & development 20: 665–669. Available: http://www.ncbi.nlm.nih.gov/pubmed/20971631. Accessed 7 March 2013.

204. Benson DC (1990) Fourier methods for biosequence analysis. Nucleic acids research 18: 6305–6310. Available: http://www.pubmedcentral.nih.gov/articlerender.fcgi?artid=332496&tool=pmcentrez&rendertype=abstract.

205. Harris CM (1998) The Fourier analysis of biological transients. Journal of neuroscience methods 83: 15–34. Available: http://www.ncbi.nlm.nih.gov/pubmed/9765048.

206. Von Zastrow M, Sorkin A (2007) Signaling on the endocytic pathway. Current opinion in cell biology 19: 436–445. Available: http://www.pubmedcentral.nih.gov/articlerender.fcgi?artid=1992519&tool=pmcentrez&rendertype=abstract. Accessed 10 March 2013.

207. González-Gaitán M (2003) Signal dispersal and transduction through the endocytic pathway. Nature reviews Molecular cell biology 4: 213–224. Available: http://www.ncbi.nlm.nih.gov/pubmed/12612640. Accessed 23 March 2013.

208. Heining E, Bhushan R, Paarmann P, Henis YI, Knaus P (2011) Spatial Segregation of BMP/Smad Signaling Affects Osteoblast Differentiation in C2C12 Cells. PloS one 6: e25163. Available: http://www.ncbi.nlm.nih.gov/pubmed/21998639. Accessed 17 October 2011.

209. Gillooly DJ, Simonsen A, Stenmark H (2001) FYVE domain proteins. 258: 249–258.

210. Chen Y-G (2009) Endocytic regulation of TGF-beta signaling. Cell research 19: 58–70. Available: http://www.ncbi.nlm.nih.gov/pubmed/19050695. Accessed 10 March 2013.

211. Panopoulou E, Gillooly DJ, Wrana JL, Zerial M, Stenmark H, et al. (2002) Early endosomal regulation of Smad-dependent signaling in endothelial cells. The Journal of biological chemistry 277: 18046–18052. Available: http://www.ncbi.nlm.nih.gov/pubmed/11877415. Accessed 21 March 2013.

212. Chen Y-G, Wang Z, Ma J, Zhang L, Lu Z (2007) Endofin, a FYVE domain protein, interacts with Smad4 and facilitates transforming growth factor-beta signaling. The Journal of biological chemistry 282: 9688–9695. Available: http://www.ncbi.nlm.nih.gov/pubmed/17272273. Accessed 14 March 2013.

213. Tsukazaki T, Chiang T a, Davison a F, Attisano L, Wrana JL (1998) SARA, a FYVE domain protein that recruits Smad2 to the TGFbeta receptor. Cell 95: 779–791. Available: http://www.ncbi.nlm.nih.gov/pubmed/9865696.

214. Shi W, Chang C, Nie S, Xie S, Wan M, et al. (2007) Endofin acts as a Smad anchor for receptor activation in BMP signaling. Journal of cell science 120: 1216–1224. Available: http://www.ncbi.nlm.nih.gov/pubmed/17356069. Accessed 18 March 2013.

215. Munoz O, Fend F, De Beaumont R, Husson H, Astier A, et al. (2004) TGFbeta-mediated activation of Smad1 in B-cell non-Hodgkin's lymphoma and effect on cell proliferation. Leukemia 18: 2015–2025. Available: http://www.ncbi.nlm.nih.gov/pubmed/15470494. Accessed 5 April 2012.

216. Warmflash A, Zhang Q, Sorre B, Vonica A, Siggia ED, et al. (2012) Dynamics of TGF-β signaling reveal adaptive and pulsatile behaviors reflected in the nuclear localization of transcription factor Smad4. Proceedings of the National Academy of Sciences of the United States of America: 1–10. Available: http://www.ncbi.nlm.nih.gov/pubmed/22689943. Accessed 13 June 2012.

217. Kurisaki A, Kurisaki K, Kowanetz M, Yoneda Y, Heldin C, et al. (2006) The Mechanism of Nuclear Export of Smad3 Involves Exportin 4 and Ran. Molecular and cellular biology 26: 1318–1332. doi:10.1128/MCB.26.4.1318.

218. MT.pdf (n.d.).

219. Di Guglielmo GM, Le Roy C, Goodfellow AF, Wrana JL (2003) Distinct endocytic pathways regulate TGF-beta receptor signalling and turnover. Nature cell biology 5: 410–421. Available: http://www.ncbi.nlm.nih.gov/pubmed/12717440. Accessed 28 May 2013.

220. Sapkota G, Alarcón C, Spagnoli FM, Brivanlou AH, Massagué J (2007) Balancing BMP signaling through integrated inputs into the Smad1 linker. Molecular cell 25: 441–454. Available: http://www.ncbi.nlm.nih.gov/pubmed/17289590. Accessed 28 May 2013.

221. Schwappacher R, Weiske J, Heining E, Ezerski V, Marom B, et al. (2009) Novel crosstalk to BMP signalling: cGMP-dependent kinase I modulates BMP receptor and Smad activity. The EMBO journal 28: 1537–1550. doi:10.1038/emboj.2009.103.

Acknowledgements

I would like to express my deepest appreciation to Prof. Manfred Schartl for the great support and scientific advice during the last 5 years. Without his guidance and persistent help this dissertation would not have been possible.

Toni, to you also applies special thanks for the research project and not to forget your invaluable encouragement, suggestions and comments. With your personality you continually and convincingly conveyed the joy of research.

I also would like to thank my former lab members Isa, Eva and Michi for the unique lab time with regard to the inquisitive conversations as well as the fun times in the evening with cold beers.

Alex and Janine, I really enjoyed the scientific and non-scientific discussions during working hours as well as leisure time and I really appreciated the roof over my head when the days were long. Furthermore, I have to especially thank you for your support with revising the paper.

The members of the whole PCI have contributed immensely to my personal and professional time in Würzburg. I thank you all for the nice atmosphere, useful discussions and invaluable friendly assistance during my time in the lab.

Finally, and most importantly, I would like to thank Basti. His support, encouragement, quiet patience and unwavering love were undeniably the bedrock upon which the past 5 years of my life have been built. His tolerance of my moods is a testament in itself of his unyielding devotion and love. I thank my parents Rainer and Ute as well as my brother Marc for their faith in me and allowing me to be as ambitious as I wanted. It was under their watchful eye that I gained so much drive and an ability to tackle challenges head on.

Publications

Bursted BMP Triggered Receptor Kinase Activity Drives Smad1 Mediated Long-Term Target Gene Oscillation in c2c12 Cells

Daniela Schul, Alexandra Schmitt, Janine Regneri, Manfred Schartl, Toni Ulrich Wagner

Physiological Chemistry I, University of Wuerzburg, Wuerzburg, Germany.

PLoS One. 2013;8(4):e59442. doi: 10.1371/journal.pone.0059442. Epub 2013 Apr 1.